



# Introduction to Land Retrieval from PolSAR

ESA–MOST Dragon 4 Cooperation

**ADVANCED LAND REMOTE SENSING  
INTERNATIONAL TRAINING COURSE**

**“龙计划4” 高级陆地遥感国际培训班**

20–25 November 2017 | Yunnan Normal University  
Kunming, Yunnan Province, P.R. China

**Chen Erxue**

[chenerx@caf.ac.cn](mailto:chenerx@caf.ac.cn)

Institute of Forest Resources Information Technique  
Chinese Academy of Forestry

Thursday, 23 November 2017, 8:30-10:00

2017年11月20日—11月25日

云南师范大学, 中国, 昆明

# Topics

**Remote sensing applications can be generally categorized into two groups:**

- Qualitative application: land use/land cover classification**
- Quantitative applications: geophysical/biophysical parameters inversion/estimation**

**I. Applying PolSAR/PolInSAR to forest classification**

**II. Applying PolSAR/PolInSAR to forest vertical structure information retrievals**

**III. Current limitation and developing trends**

# I. Applying PolSAR/PolInSAR to forest classification

# Outlines

## 1. Introduction

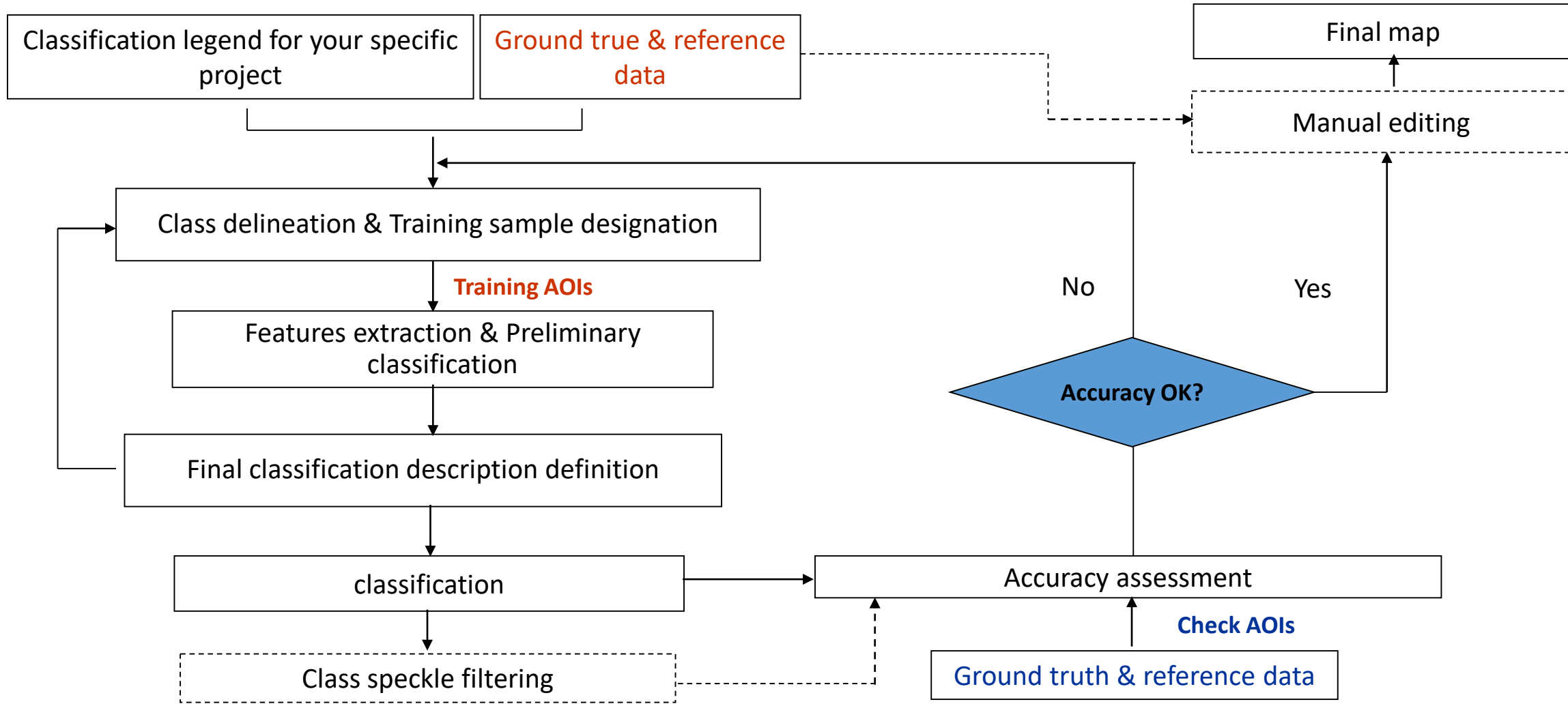
- 1.1 General technique framework for remote sensing image classification
- 1.2 Classification system and legend defining
- 1.3 Classification method introduction through PolSARPro
- 1.4 Feature selection and transformation
- 1.5 Classifier and its training and testing

## 2. Some case studies on PolSAR forest classification

- 2.1 Forest scar mapping using PolSAR data
- 2.2 Forest land type classification using multi-temporal ALOS PALSAR Dual-polarization data
- 2.3 Forest types classification using high resolution airborne PolSAR data



## 1.1 General technique framework for remote sensing image classification



## 1.2 Classification system and legend defining

### Classification system

- It is an abstract representation of the situation in the field using well defined diagnostic criteria
- One define it as: “The ordering or arrangement of objects into groups or sets on the basis of their relationships”

### A classification system is

- **Scale independent:** the classes should be applicable at any scale or level of detail;
- **Source independent:** independent of the means used to collect information, whether it be through satellite imagery, aerial photography, field survey or using a combination of sources.

### Remote sensing classification legend

- It is the application of a classification system in a specific area using a defined mapping scale and specific data set

### legend is

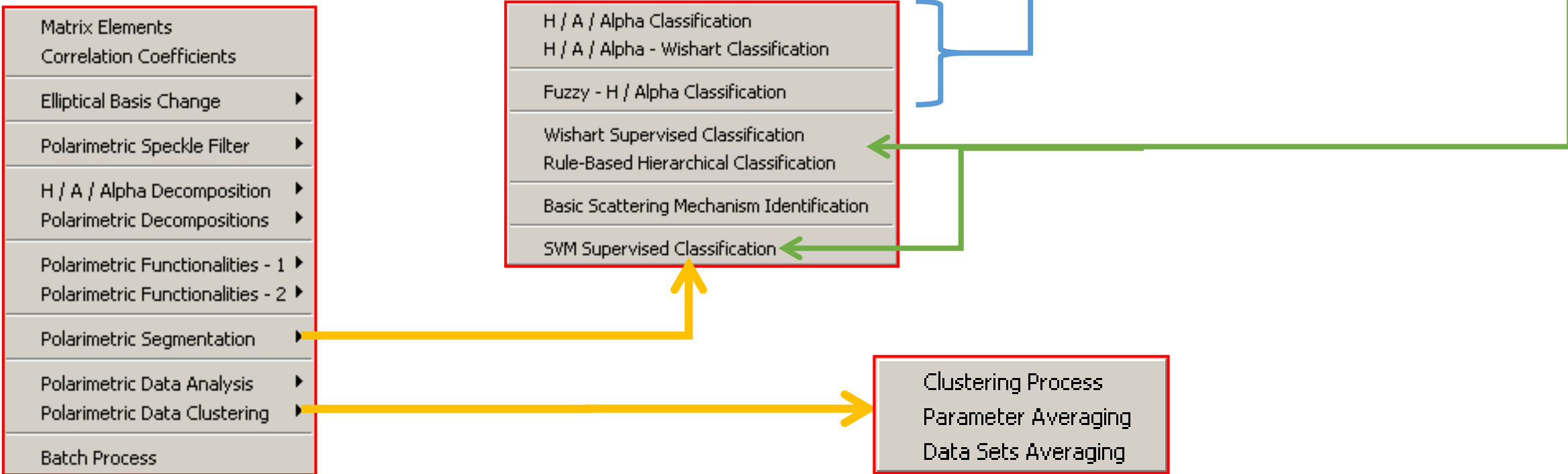
- Scale and cartographic representation dependent;
- Data and mapping methodology dependent.

## 1.3 Classification methods introduction through PolSARPro

Pixel based  $\leftrightarrow$  Object based

-Currently only pixel based classifier

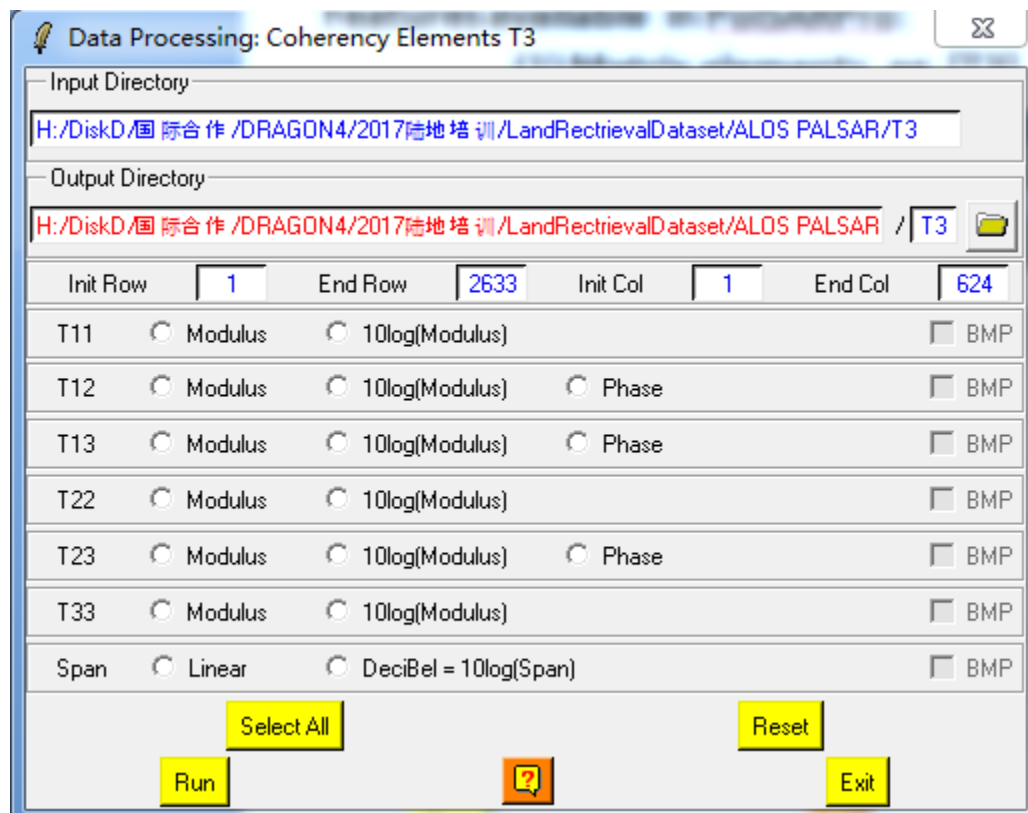
Unsupervised  $\leftrightarrow$  Supervised



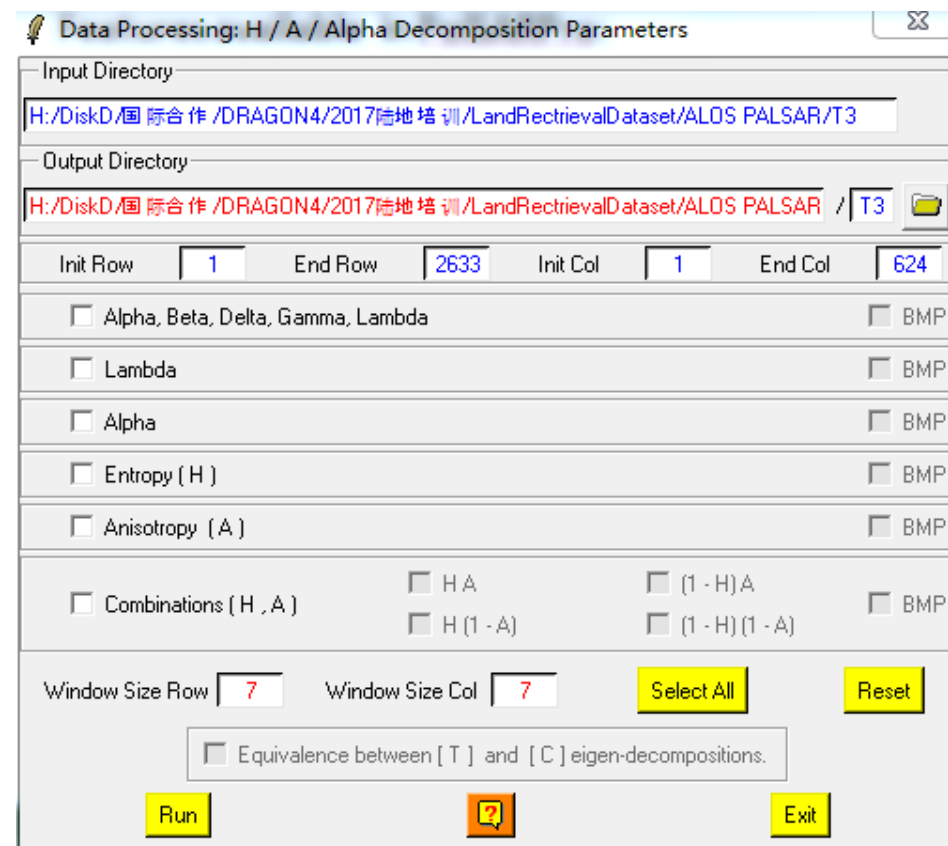
## 1.4 Feature selection and transformation

Features available in PolSARPro:

### (1) Matrix elements, eg. [T3]



### (2) Polarimetric decomposition features eg. H/Alpha/A decomposition

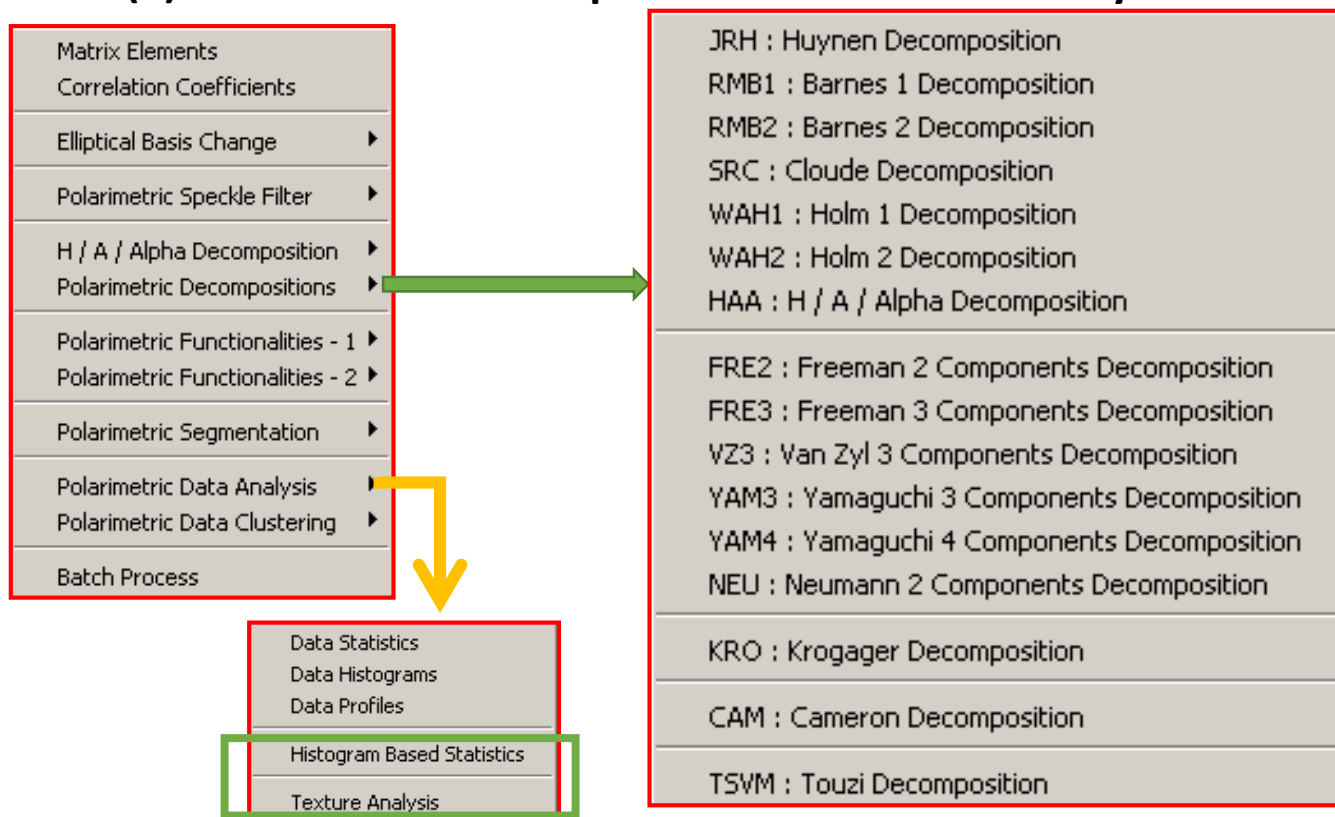




## 1.4 Feature selection and transformation

Features available in PolSARPro:

### (2) Polarimetric decomposition features and many others



**But it does not mean the more the better for classification:**

**Dimension disaster problem**

- With fixed training samples, accuracy increases with dim to one maximum acc., then decreases
- The key reason is the correlation between features , and more feature needs more training samples to solve the classification model.

**PorSARPro solution:**

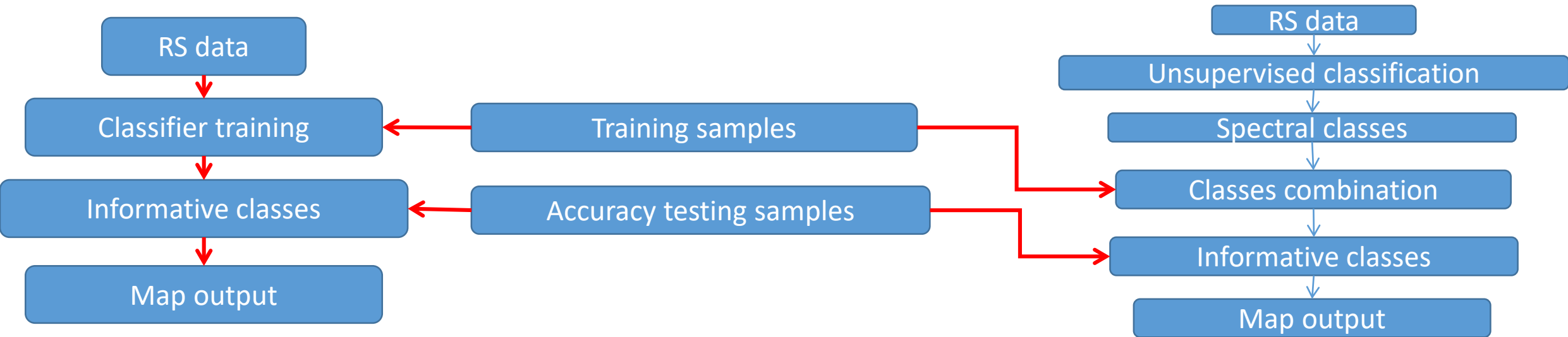
- SVM supervised classification, lets you to choose features.

## 1.5 Classifier training and testing

- Fully understanding the difference between “spectral classes “ and “informative classes”
  - Classes can be Spectrally separated, optical remote sensing
  - Classes can be separated by polarimetric mechanism or PolSAR data itself

But,

- Without training you can not get informative classes, both for supervised and unsupervised classification



### 2.1 Forest scar mapping using PolSAR data

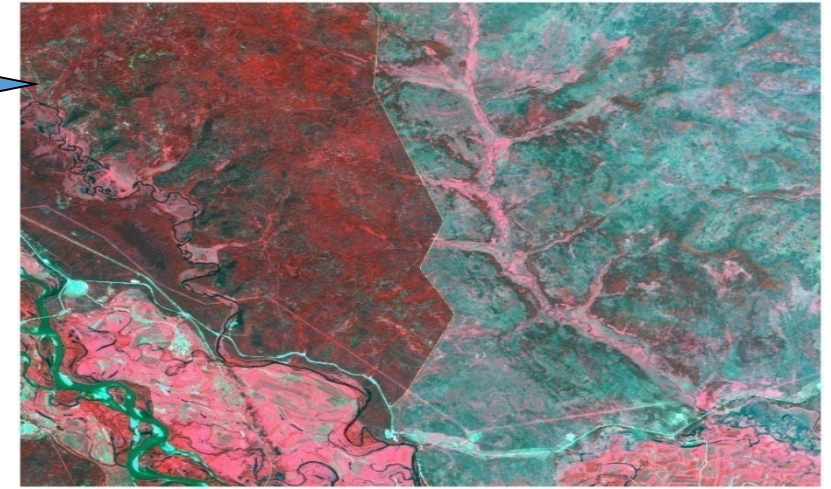
### 2.2 Forest land type classification using multi-temporal ALOS PALSAR Dual-polarization data

### 2.3 Forest types classification using high resolution airborne PolSAR data

### 2.1 Forest scar mapping using PolSAR data



# TEST SITE & DATA



Test site center:  $52^{\circ} 26'N$ ,  $125^{\circ} 32'E$

In Tahe County, Heilongjiang Province, China

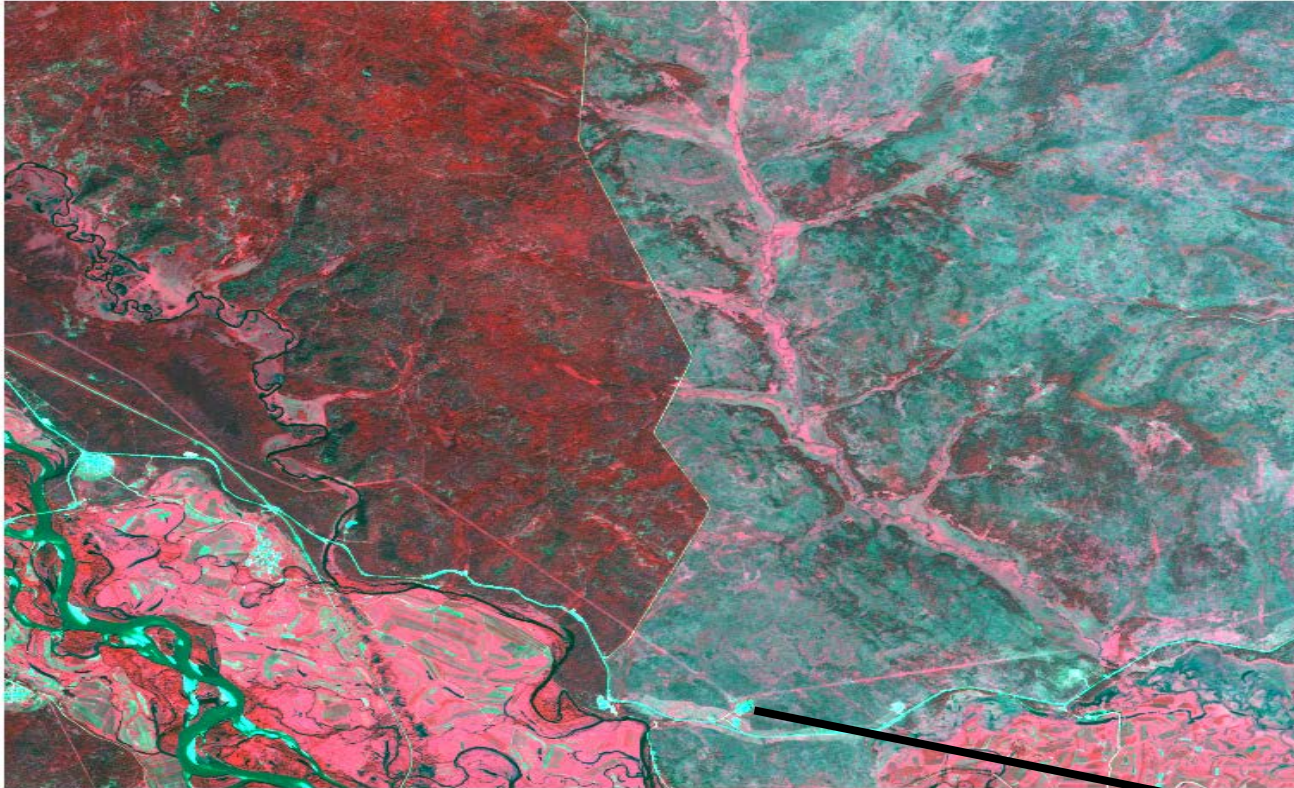
Climate Zone: Cold temperate zone.

Relatively flat with an average elevation  $\sim 330$  m, slope less than  $15^{\circ}$ .

Key dominate tree species: Larch and White Birch.



One forest fire occurred in May 17, 2003



SPOT5 multi-spectral image (R: NIR;G: Red; B:Green)

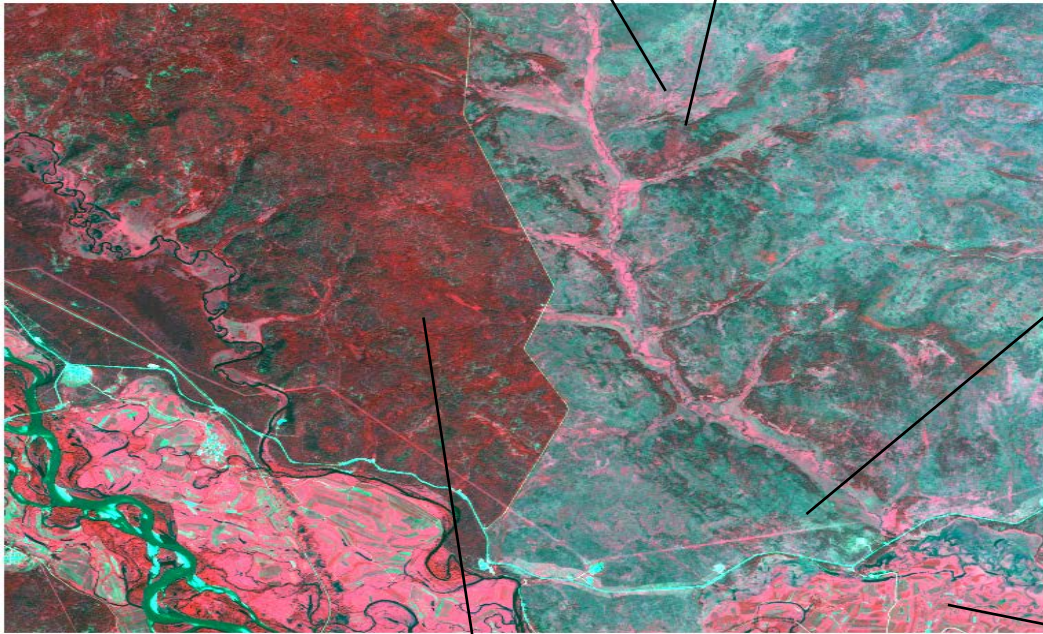
Imaging date: July 27, 2006



Sparse forest / shrub vegetation



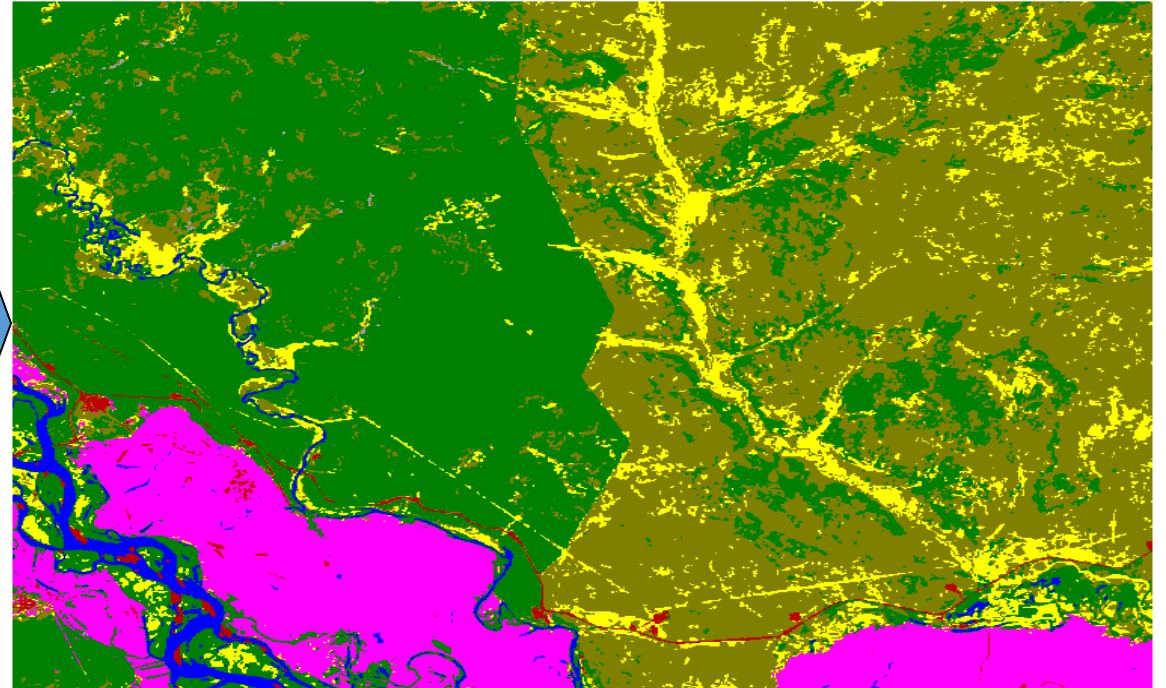
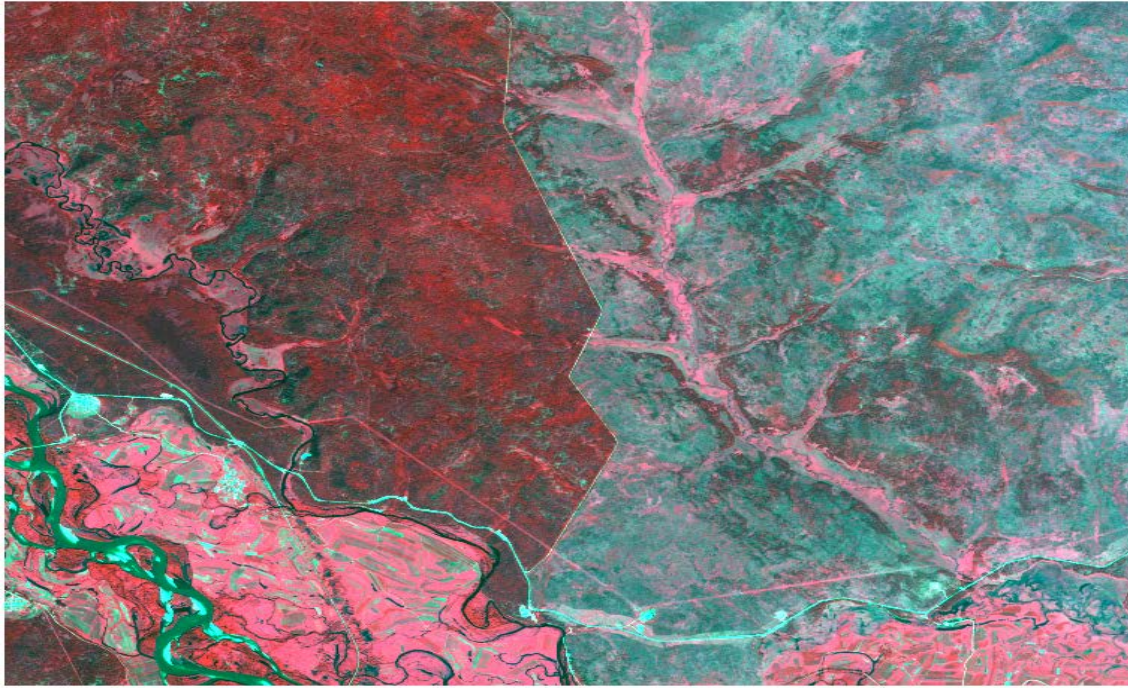
Manual stimulated regeneration



Soybean








**SPOT 5 10m multi-spectral (R: NIR; G: R; B:G)**

Imaging date: July 27, 2006

**Land cover map from SPOT5 images**

-  Forest
-  Grass
-  Agriculture field
-  Shrub
-  River
-  Urban, road, bare
-  Others

The forest grows rate is very low, so we can use the image as reference for the understanding of PolSAR data

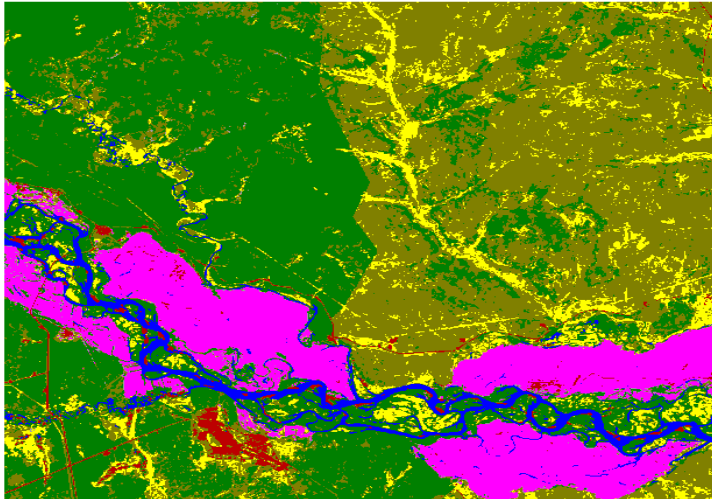


# SAR data

Data Types	Polarization	Imaging Date (y m d)	Incidence Angle (deg)	Orbit direction
PALSAR	Quad-pol	20080907	23.9	Descending
Radarsat-2	Quad-pol	20090714	38.4	Descending
Radarsat-2	Quad-pol	20091018	38.4	Descending

## ➤ The Effect of Imaging Season to Forest Scar Mapping

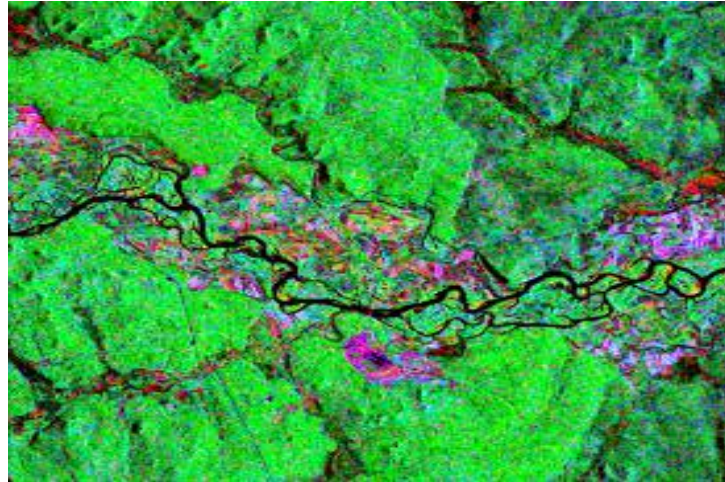
Land cover map



Imaging date: 20060727

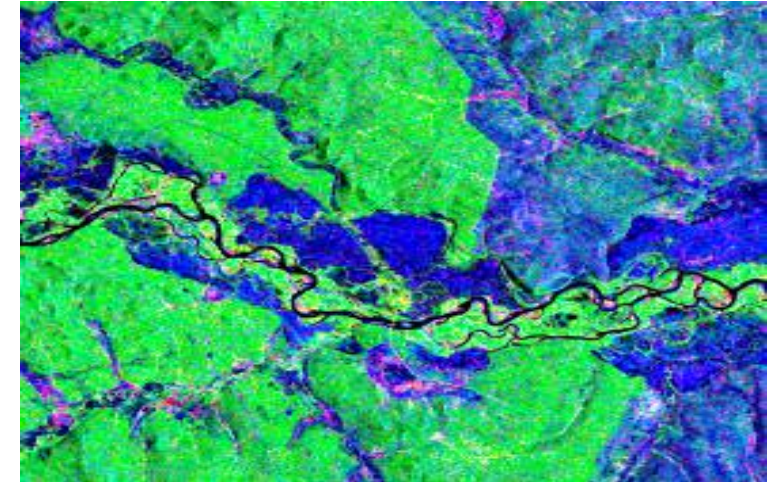
Wet, Summer Season

Radarsat-2 data: Freeman decomposition results



Imaging date: 20090714

Wet, Summer Season



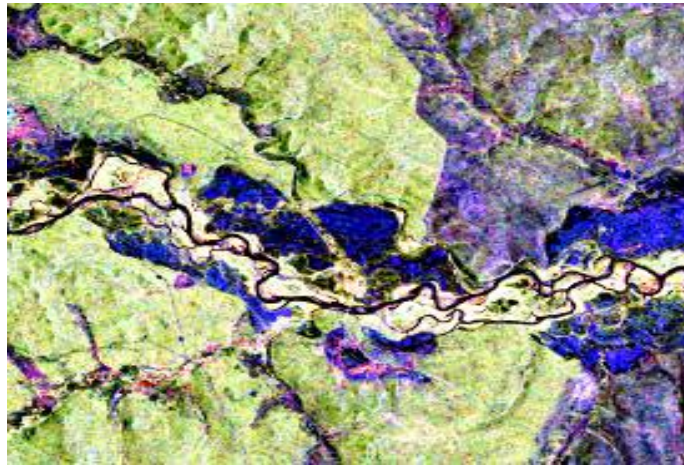
Imaging date: 20091018

Dry, Fall Season

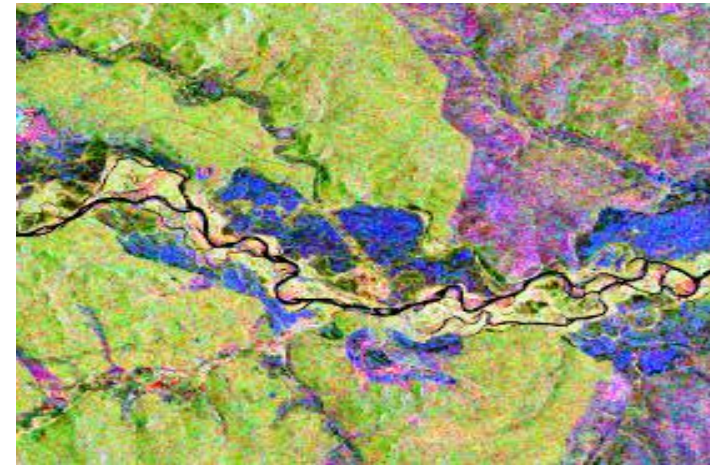


## ➤ The Effect of Wavelength to Forest Scar Mapping

Pauli-decomposition



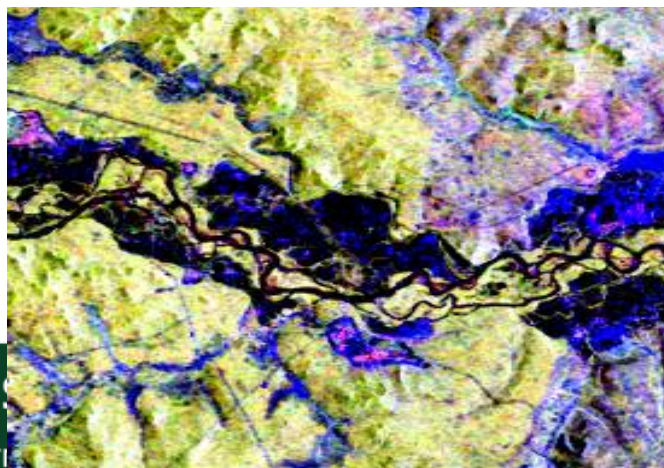
H-Alpha-A decomposition



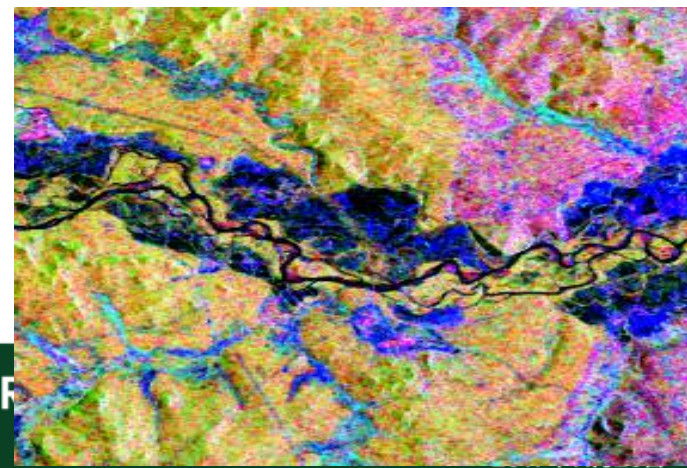
Radarsat-2 imaged  
in 20091018

Inc: 38 deg

Pauli-decomposition



H-Alpha-A decomposition



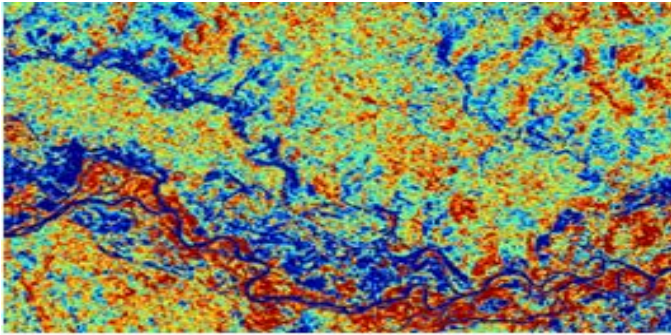
ALOS PALSAR imaged  
in 20080907

Inc: 24 deg

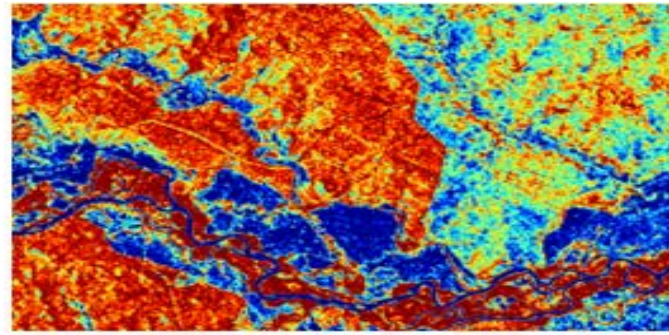




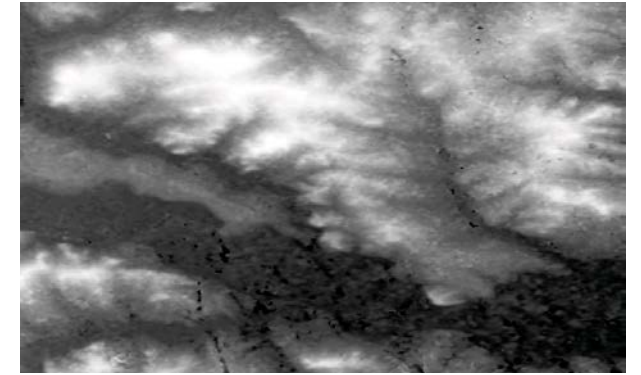
# Eigen values and relevant parameters from Radarsat-2 data(20091018)



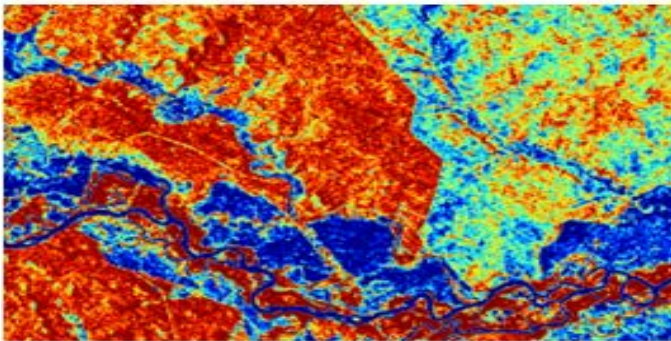
(a)  $\lambda_1$



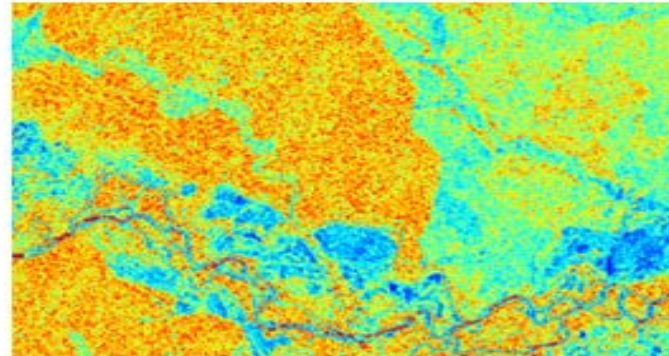
(b)  $\lambda_2$



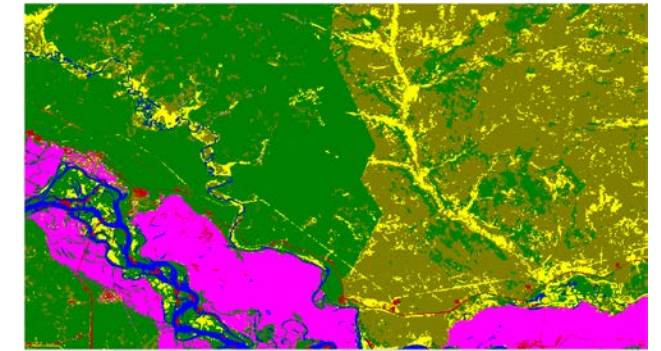
DEM



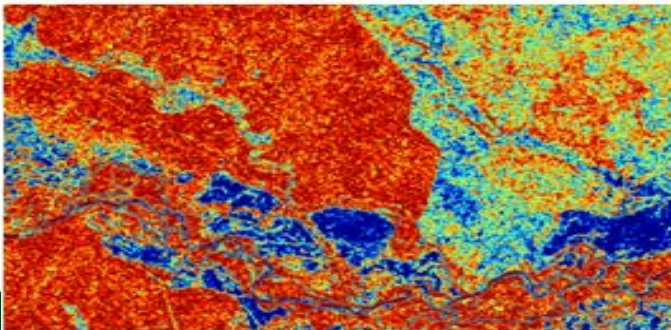
(c)  $\lambda_3$



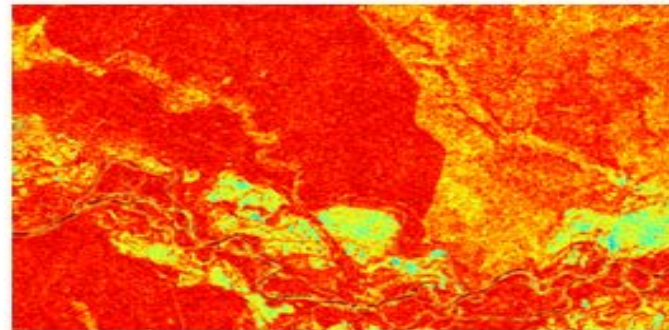
(d) *RVI*



Land cover map



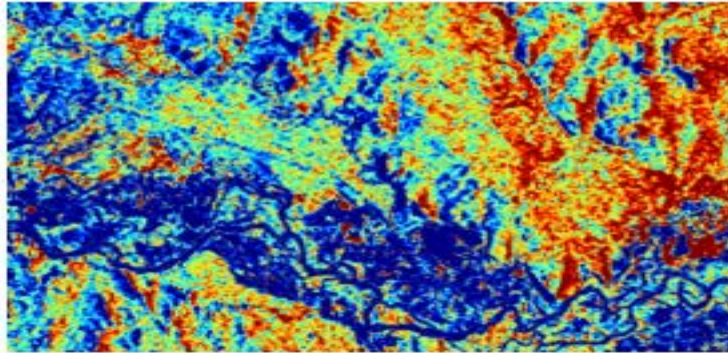
(e) *SEP*



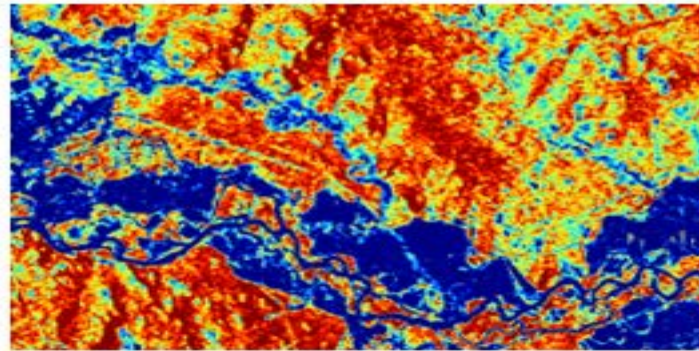
(f) *H*



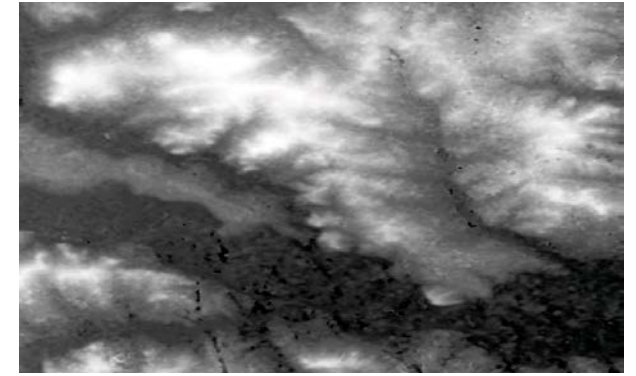
# Eigen values and relevant parameters from ALOS PALSAR data (20080907)



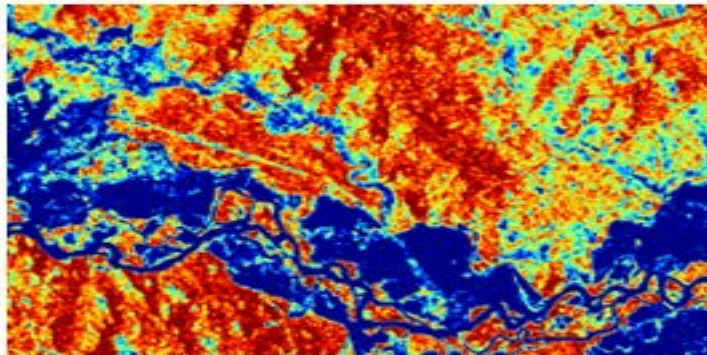
(a)  $\lambda_1$



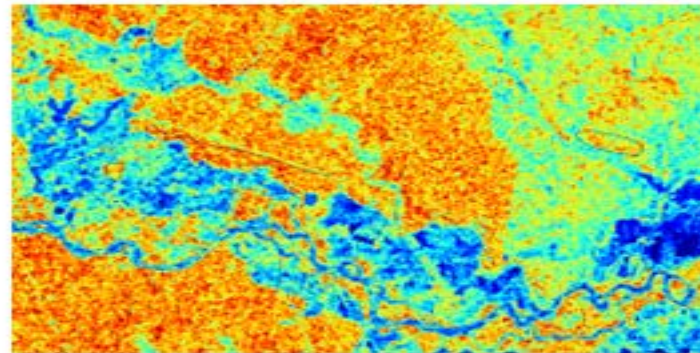
(b)  $\lambda_2$



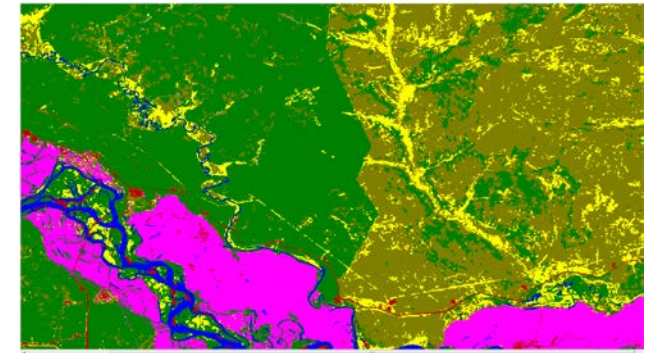
DEM



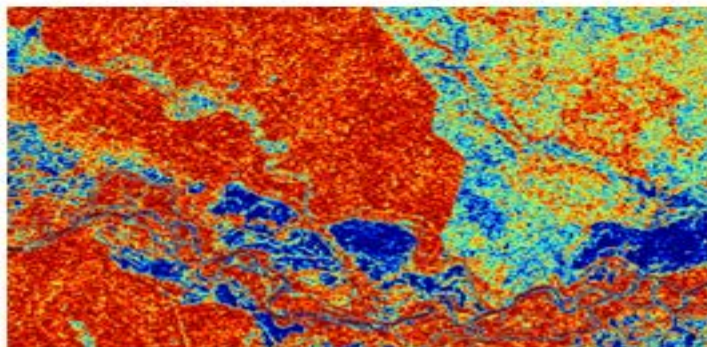
(c)  $\lambda_3$



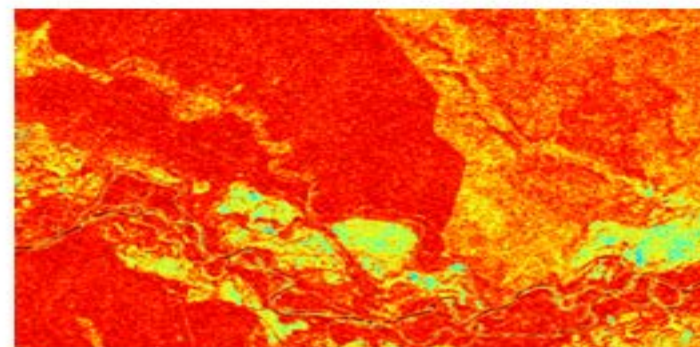
(d) *RVI*



Land cover map



(e) *SEP*



(f) *H*



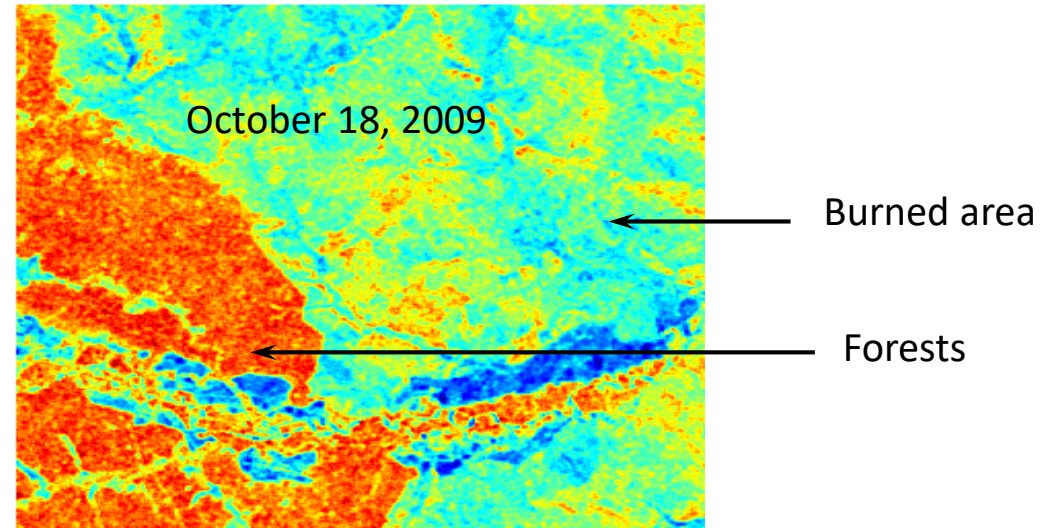
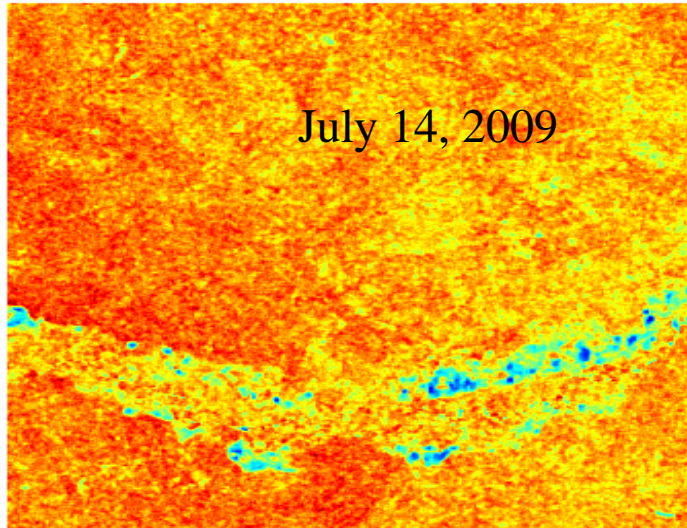
# Forest scar mapping with new polarimetric parameters

- RVI describes the size of cylinders

$$RVI = 4\lambda_3 / (\lambda_1 + \lambda_2 + \lambda_3)$$

Developed by Prof. Wen Hong's team

- Radarsat-2 RVI images



# Eigen Decomposition Parameters

- Entropy-alpha decomposition

$$T = \sum_{i=1}^3 \lambda_i u_i \cdot u_i^{*T} \quad u_i = [u_{1i}, u_{2i}, u_{3i}]^{*T} = e^{j\phi_i} \left[ \cos \alpha_i, \sin \alpha_i \cos \beta_i e^{j\delta_i}, \sin \alpha_i \sin \beta_i e^{j\gamma_i} \right]^{*T}$$

$$P_i = \frac{\lambda_i}{\sum_{k=1}^3 \lambda_k} \quad \text{with:} \quad \sum_{k=1}^3 P_k = 1$$

$$H = -\sum_{k=1}^3 P_k \log_3(P_k)$$

Polarimetric scattering entropy: randomness

$$\bar{\alpha} = \sum_{k=1}^3 P_k \alpha_k$$

Average  $\alpha$  angle: Scattering type

$$A = \frac{\lambda_2 - \lambda_3}{\lambda_2 + \lambda_3}$$

Polarimetric scattering anisotropy: complementary to  $H$

\*S. R. Cloude, and E. Pottier, "An entropy based classification scheme for land applications of polarimetric SAR", Transactions on Geoscience and Remote Sensing, vol. 35, no. 1, pp. 68-78, Jan. 1997.

# New parameters $\mu_1$ and $\mu_2$

- Correlation term from 1<sup>st</sup> eigenvector

$$\mu_1 = \text{real}(\langle u_{21} \cdot u_{11}^* \rangle / \langle |u_{21}| \cdot |u_{11}| \rangle) < 0$$

$\mu_1 < 0 \rightarrow$  Forested areas

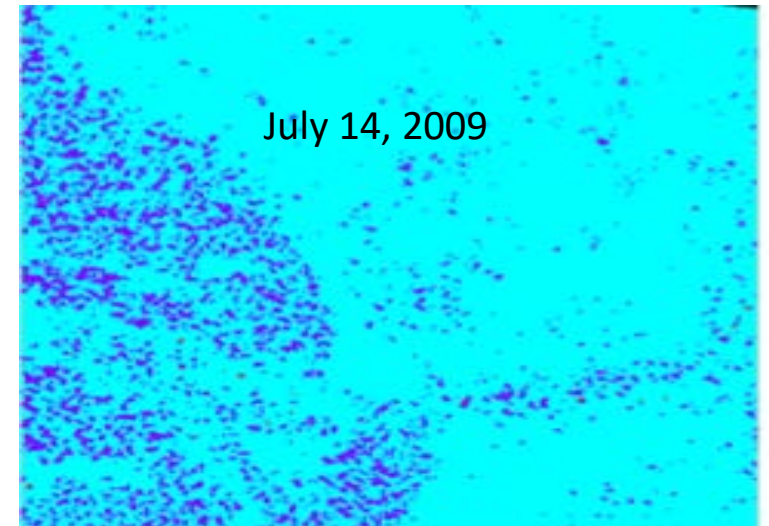
- Correlation term from 2<sup>nd</sup> eigenvector

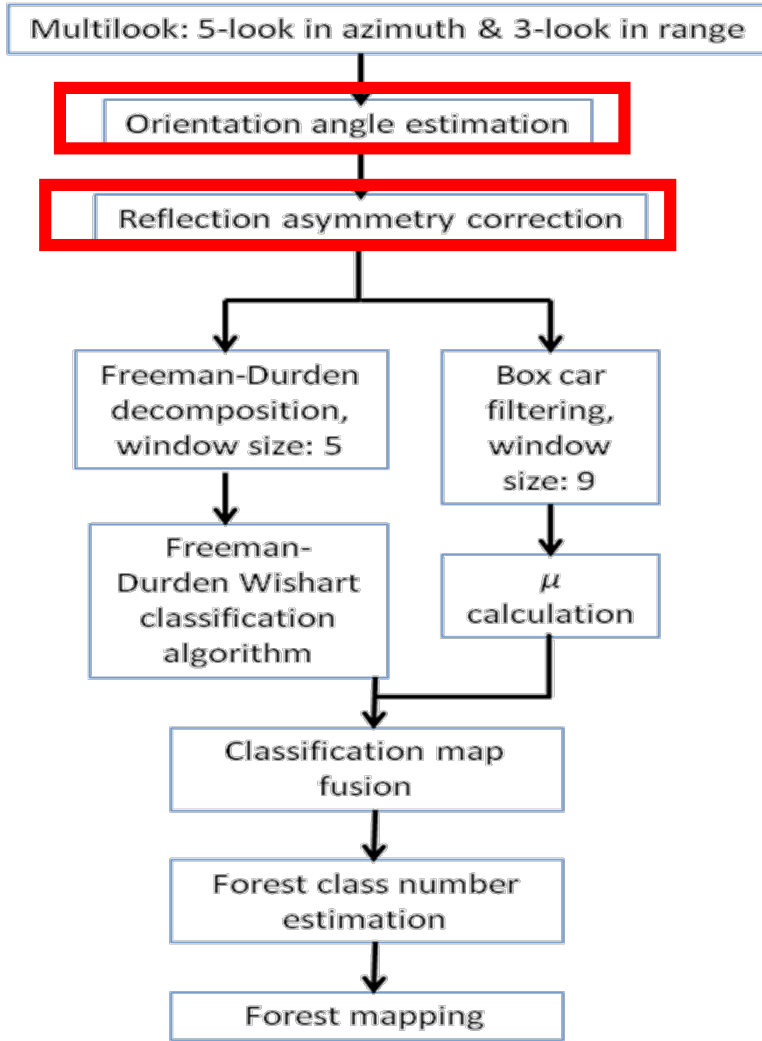
$$\mu_2 = \text{real}(\langle u_{22} \cdot u_{12}^* \rangle / \langle |u_{22}| \cdot |u_{12}| \rangle) > 0$$

Use  $\mu_2$  and  $A \rightarrow$  Water pixels

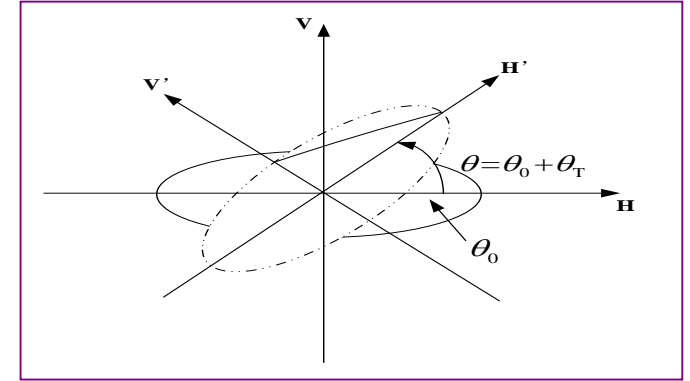
- Freeman-Durden Wishart classification with  $\mu$ -based labels.

$\mu$  map





- Introduced by orientation of terrain and vegetation.



Polarization ellipse rotation  
 $\theta$  - Polarization Orientation Angle (POA)

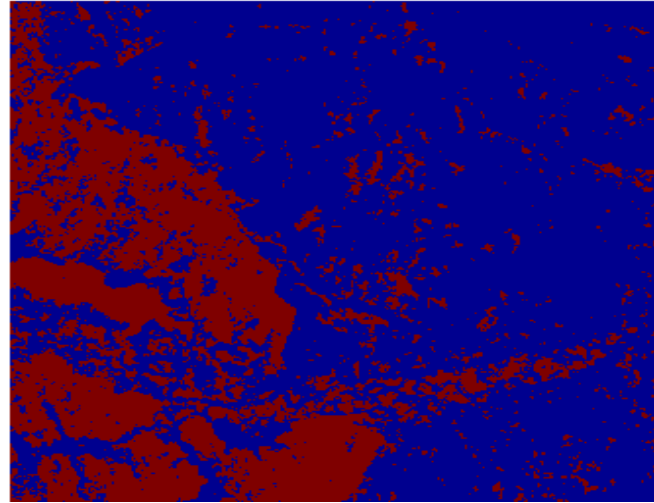
- Estimate it and do the compensation\*

$$\eta = \frac{1}{4} \left[ \tan^{-1} \left( \frac{-4 \operatorname{Re}(\langle \tilde{S}_{HH} - \tilde{S}_{VV} \rangle \tilde{S}_{HV}^*)}{-|\tilde{S}_{HH} - \tilde{S}_{VV}|^2 + 4|\tilde{S}_{HV}|^2} \right) + \pi \right]$$

$$\theta = \begin{cases} \eta, & \text{if } \eta \leq \pi/4 \\ \eta - \pi/2, & \text{if } \eta > \pi/4 \end{cases}$$

$$T^{new} = UTU^T, U = \begin{bmatrix} 1 & 0 & 0 \\ 0 & \cos 2\theta & \sin 2\theta \\ 0 & -\sin 2\theta & \cos 2\theta \end{bmatrix}$$

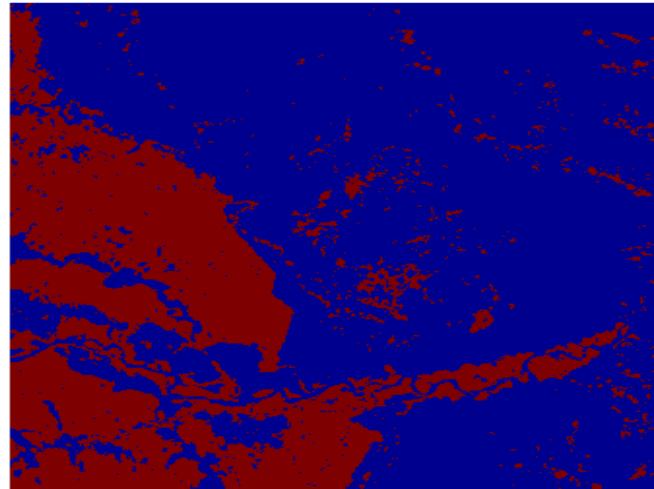
## The performance with the new parameter: validation results



Red: forested areas

July 14, 2009

**71.0% agreement with SPOT5**



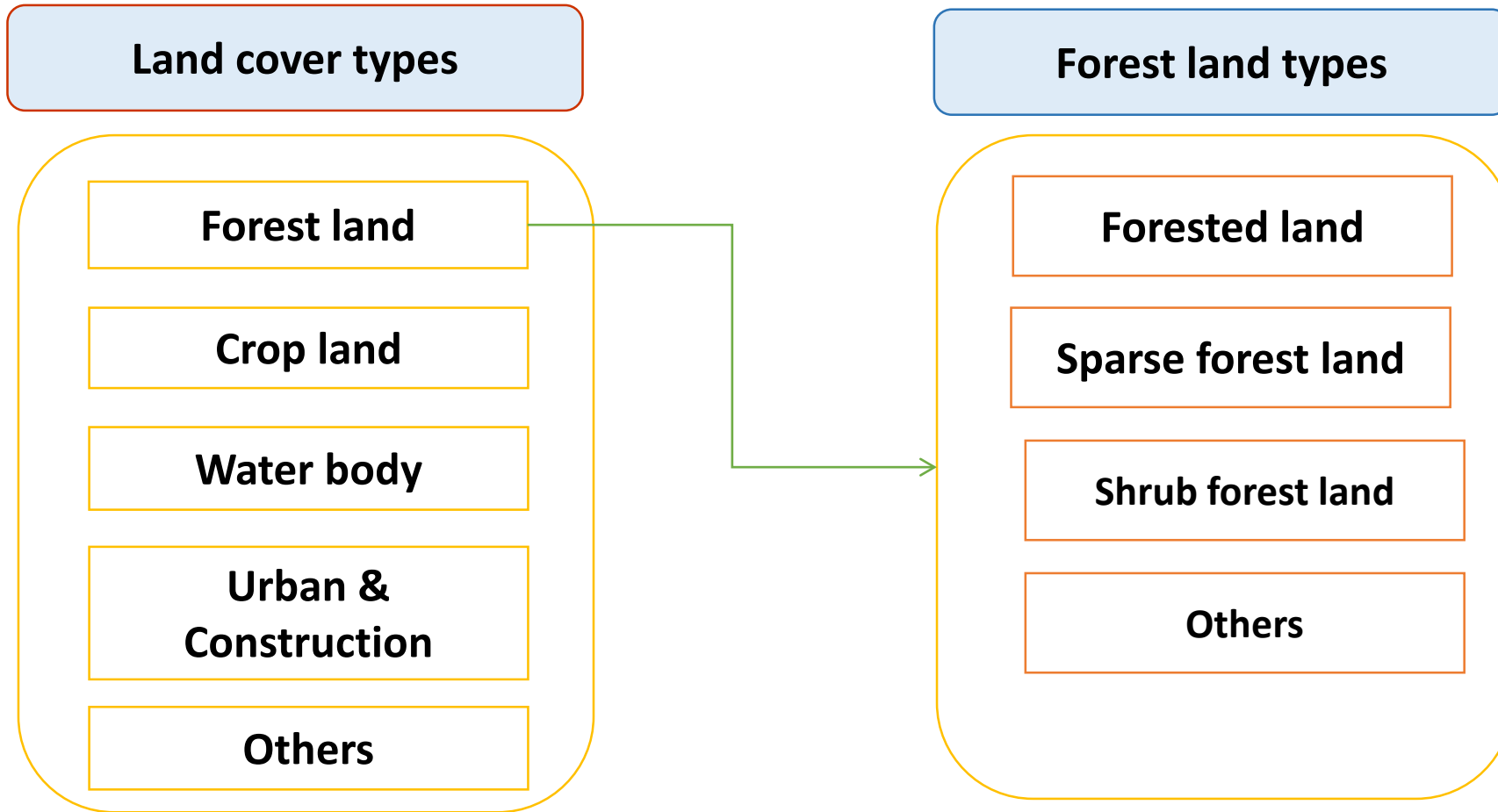
October 18, 2009

**81.4% agreement with SPOT5**



# 2.2 Forest land type classification using multi-temporal ALOS PALSAR Dual-polarization data

Classification system:



# 2.2 Forest land type classification using multi-temporal ALOS PALSAR Dual-polarization data

## Test site: Xunke, Heilongjiang Province

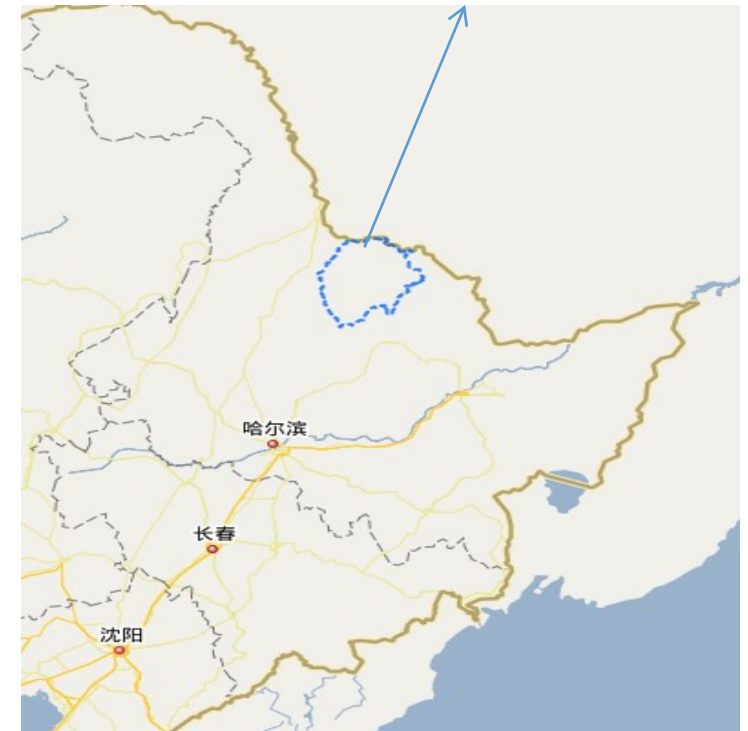
- Location: North-East of China
- Coverage: 127° 24' —129° 17' E  
47° 58' —49° 36' N  
(17344 km<sup>2</sup>)

■ SAR data :

ALOS PALSAR L1.1 SLC (L-band, 46 days temporal baseline)

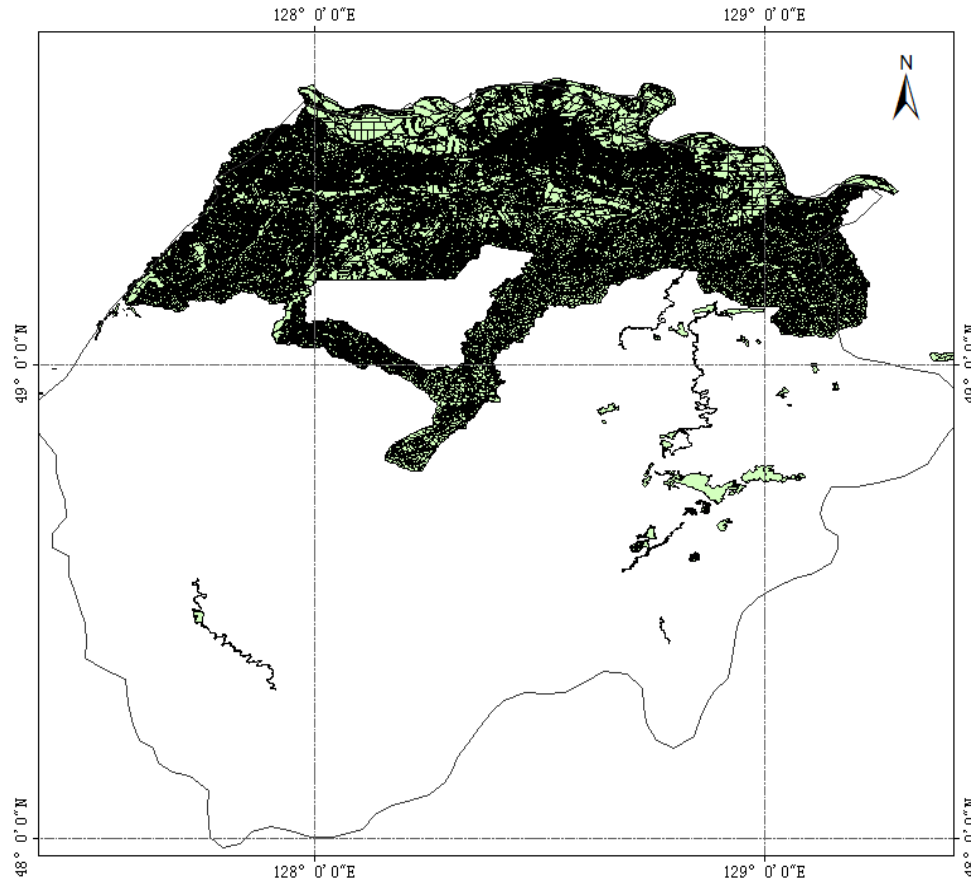
Polarization	Inc. angle	Date
HH/HV	34.3°	2007/06/22
HH/HV	34.3°	2007/08/07
HH/HV	34.3°	2007/09/22

Xunke test site

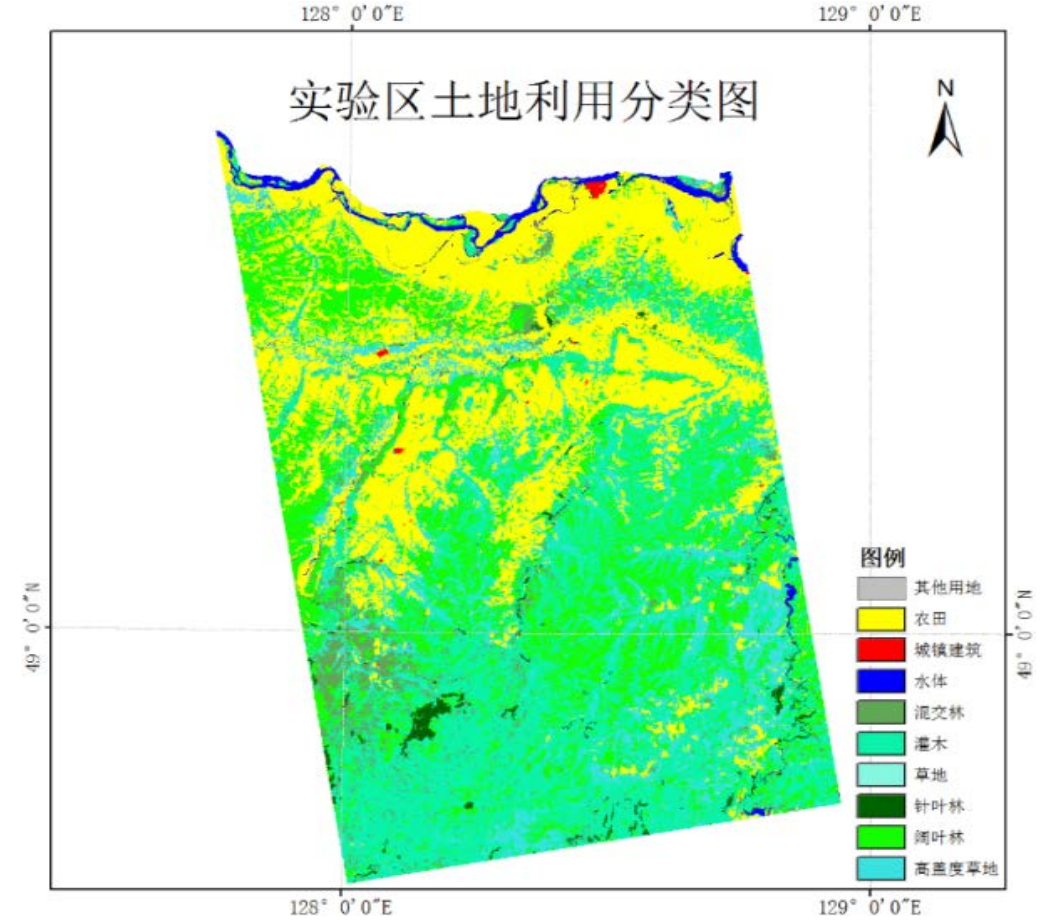


# 2.2 Forest land type classification using multi-temporal ALOS PALSAR Dual-polarization data

## Ground reference data



Forest resource inventory data of Xunke county

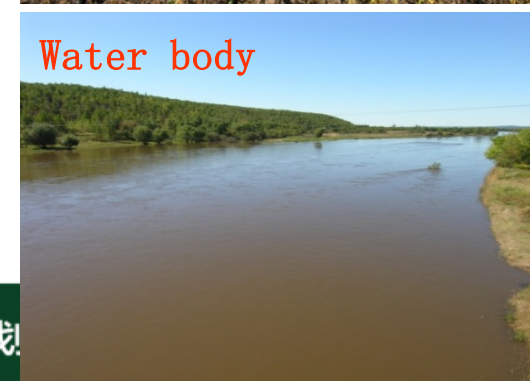
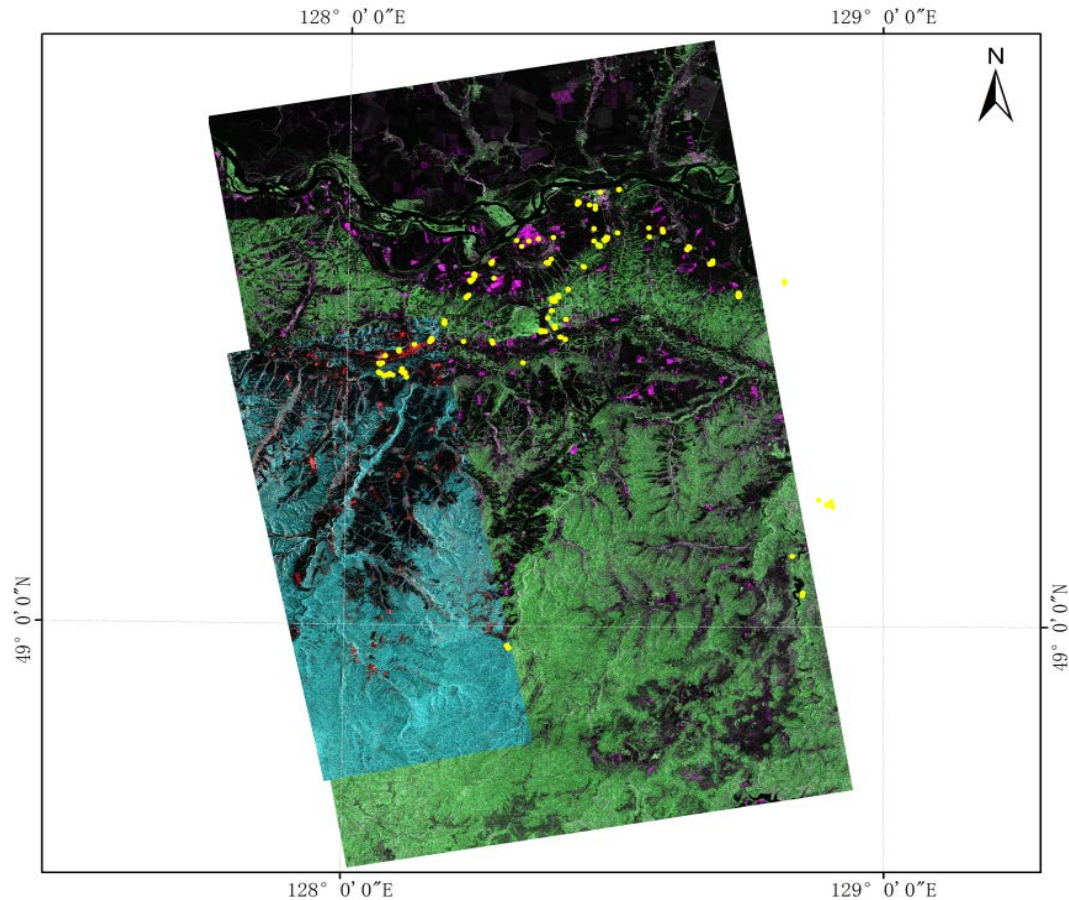


Land cover/use map generated from Landsat TM



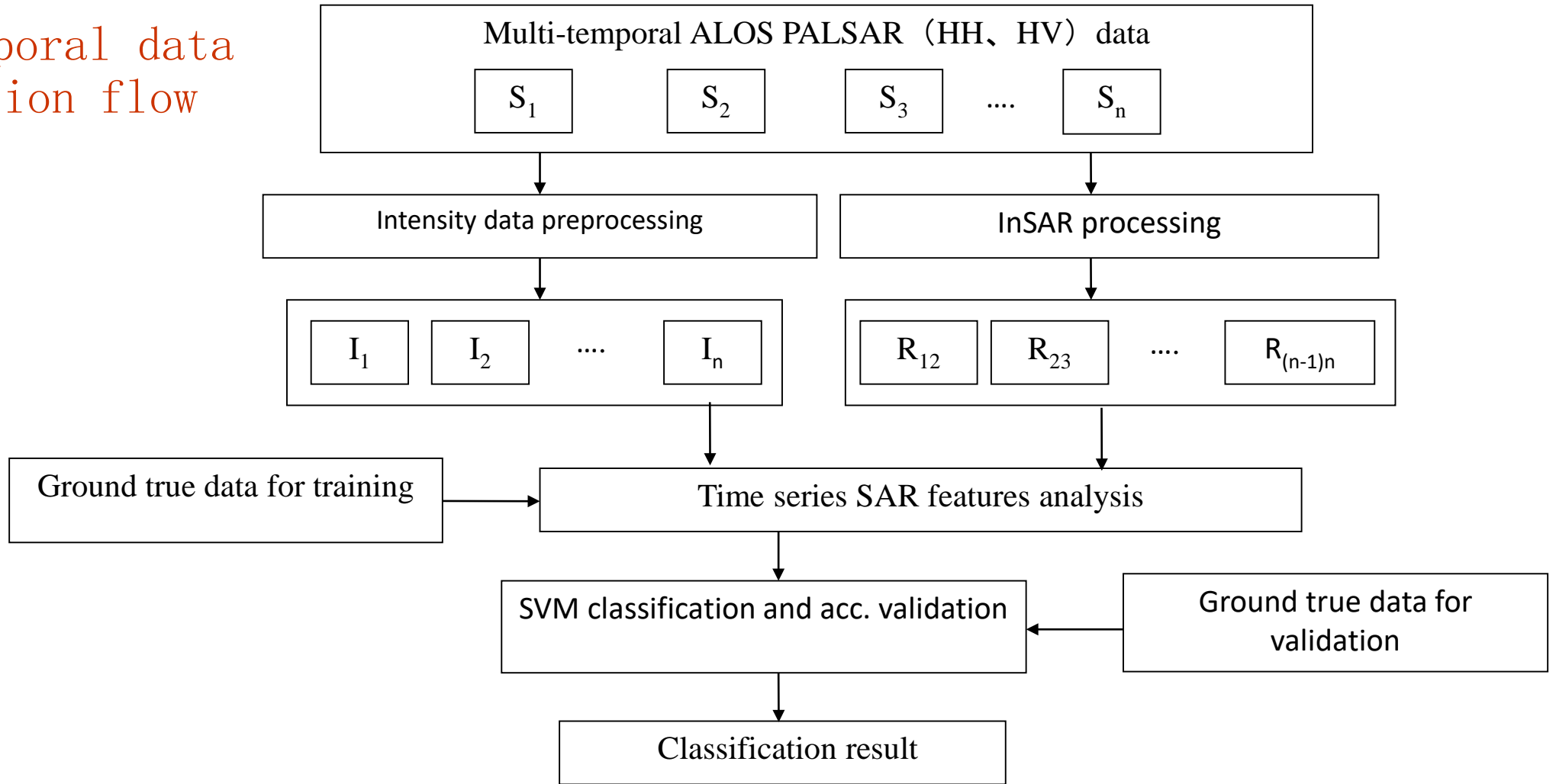
# 2.2 Forest land type classification using multi-temporal ALOS PALSAR Dual-polarization data

## Ground survey data

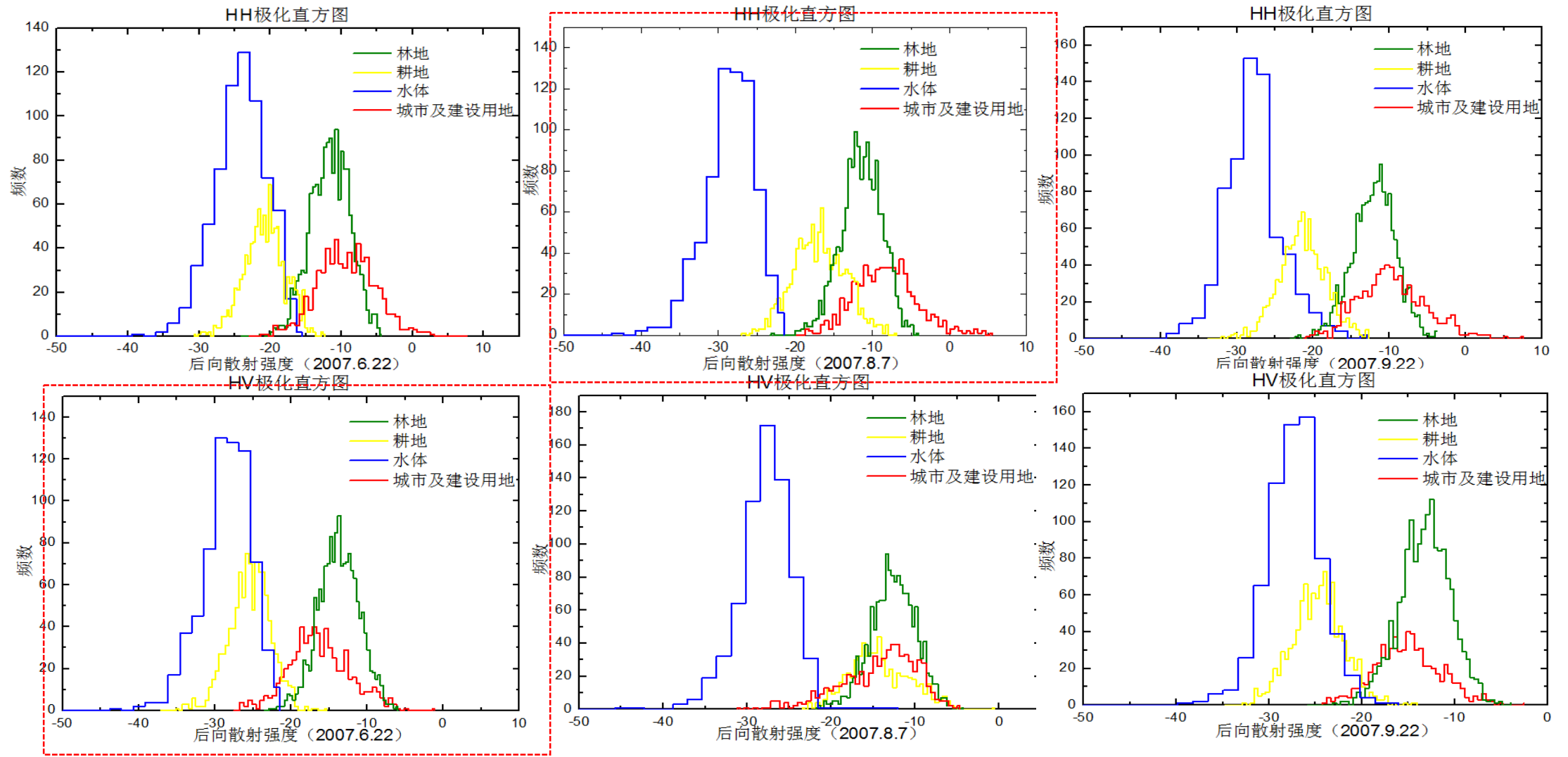


# 2.2 Forest land type classification using multi-temporal ALOS PALSAR Dual-polarization data

Multi-temporal data classification flow chart

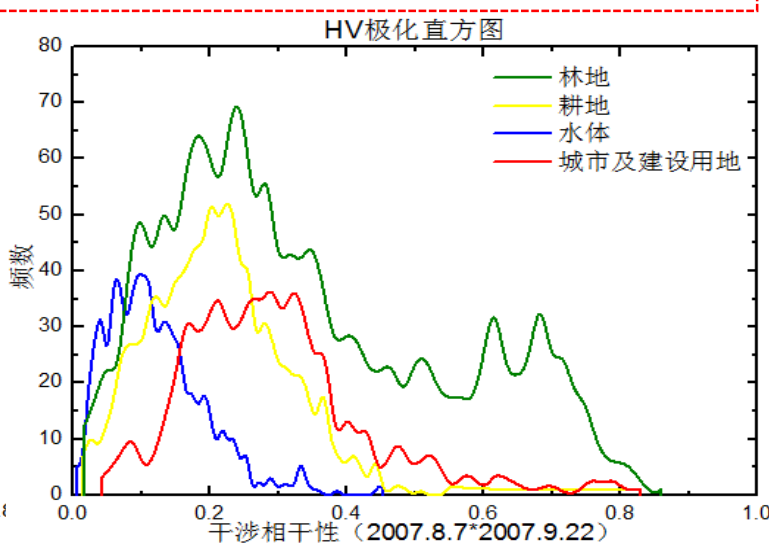
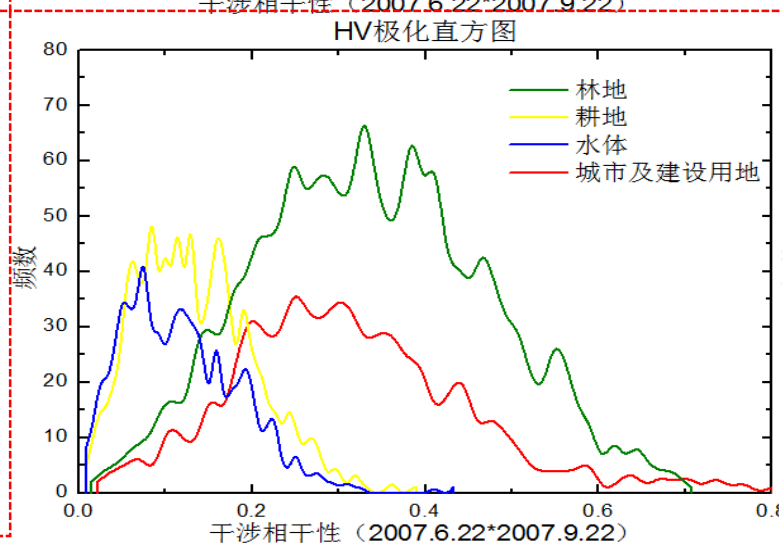
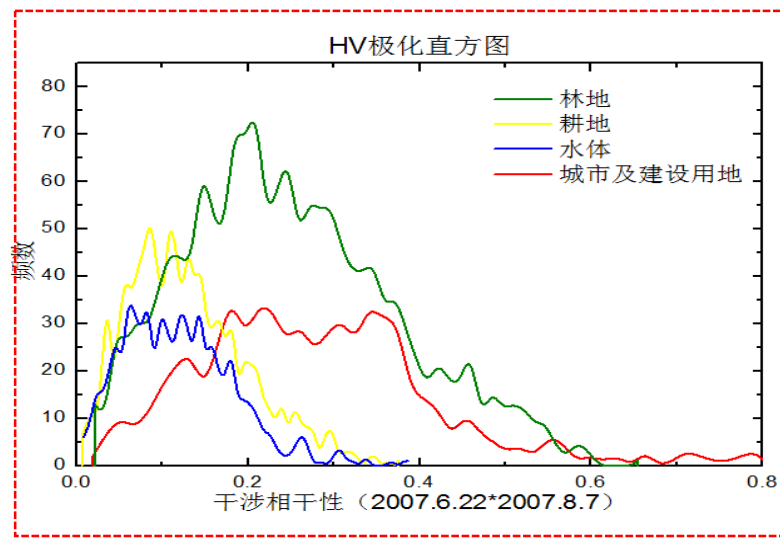
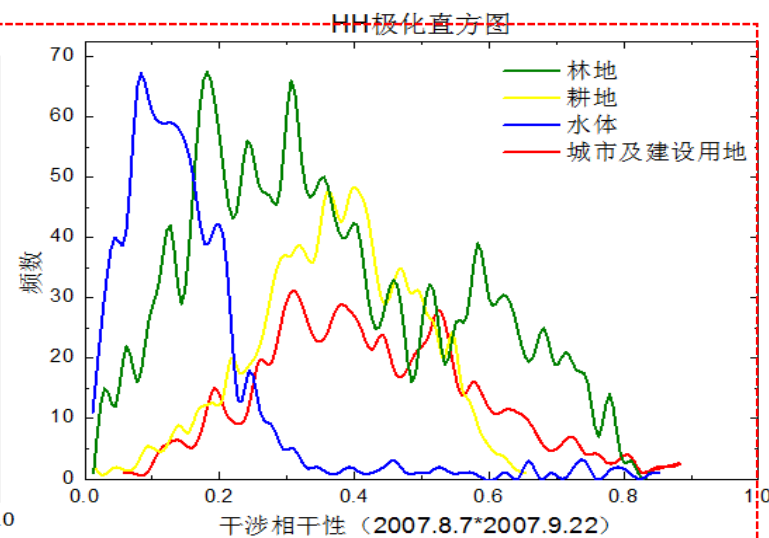
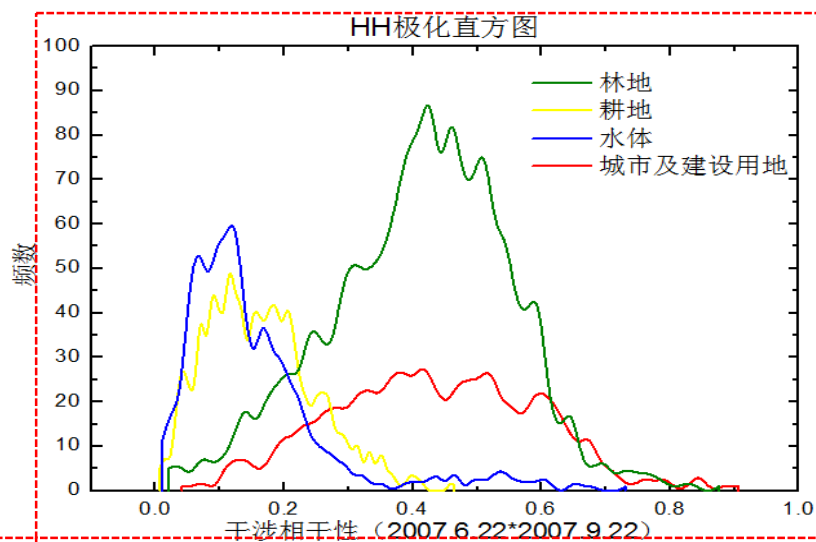
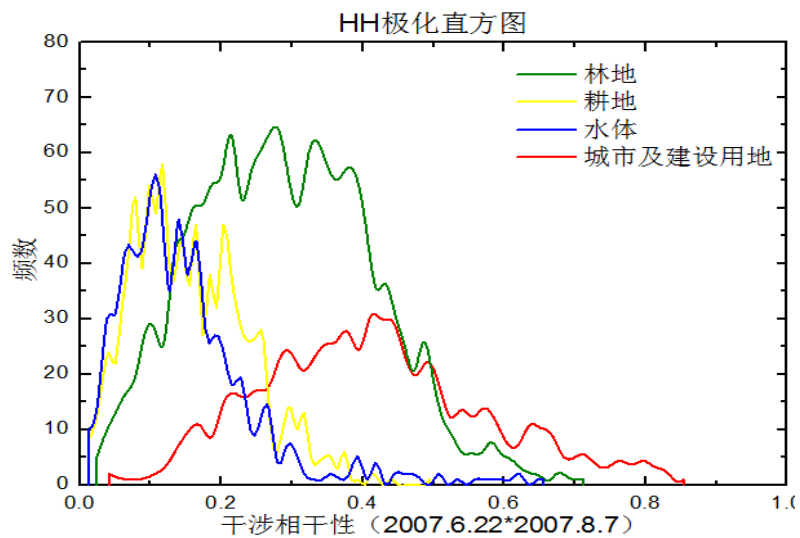


# Land cover classification: time series of intensity feature analysis





# Land cover classification: time series of InSAR coefficient analysis

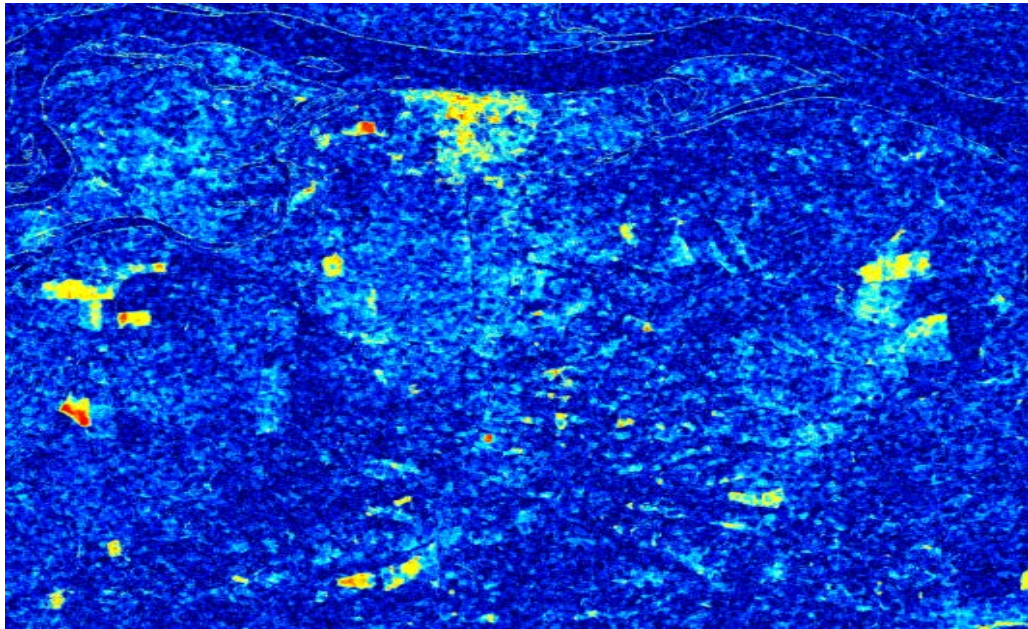


# Land cover classification: need new feature

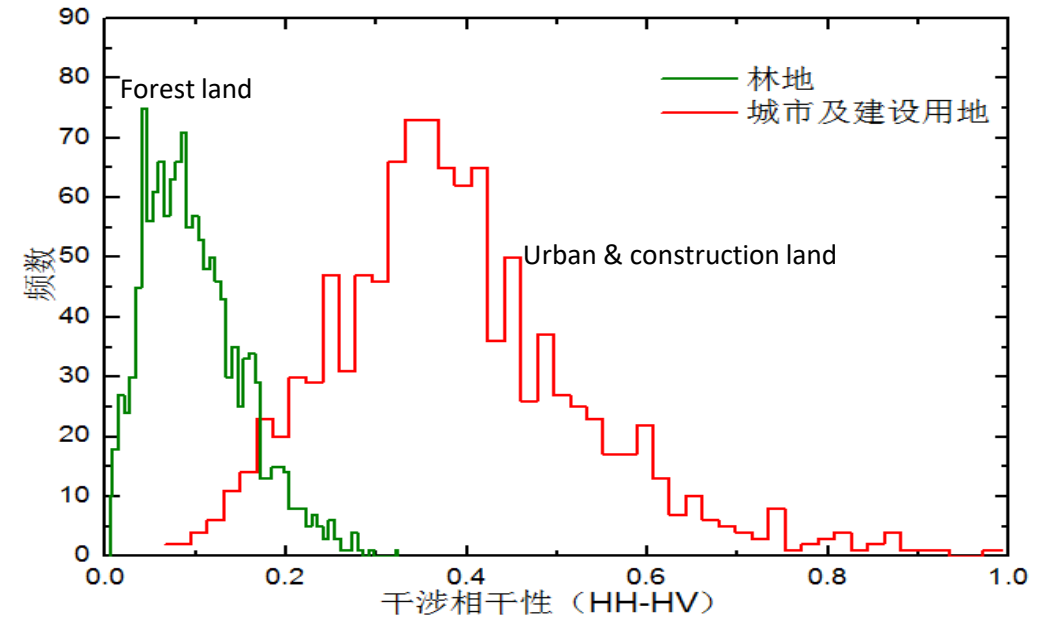
With the 5 features selected above, it is still difficult to classify **forest land from urban & construction land**

$$\rho_{ij} = \frac{\langle C_{ij} \rangle}{\sqrt{\langle C_{ii} \rangle \langle C_{jj} \rangle}}$$

Correlation coefficient between HH-HV



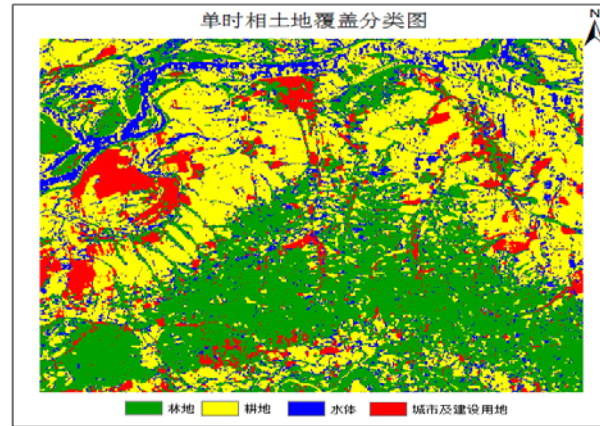
Correlation coefficient between HH and HV of Aug.



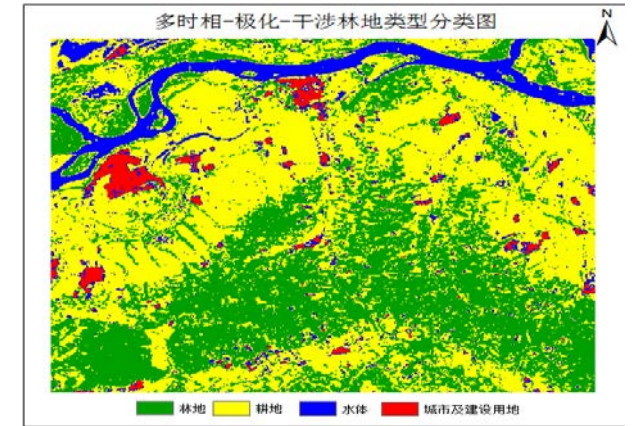
Histogram of HH-HV correlation coefficient

Land cover classification: input all the features selected to **SVM classifier**

- ❖ June-HV Intensity
- ❖ Aug.-HH Intensity
- ❖ June-Sept. HH-HH InSAR coefficient
- ❖ Aug.-Sept. HH-HH InSAR coefficient
- ❖ June-Aug. HV-HV InSAR coefficient
- ❖ Aug. HH-HV correlation coefficient



Classification result-single data



Classification result-multi-temporal data

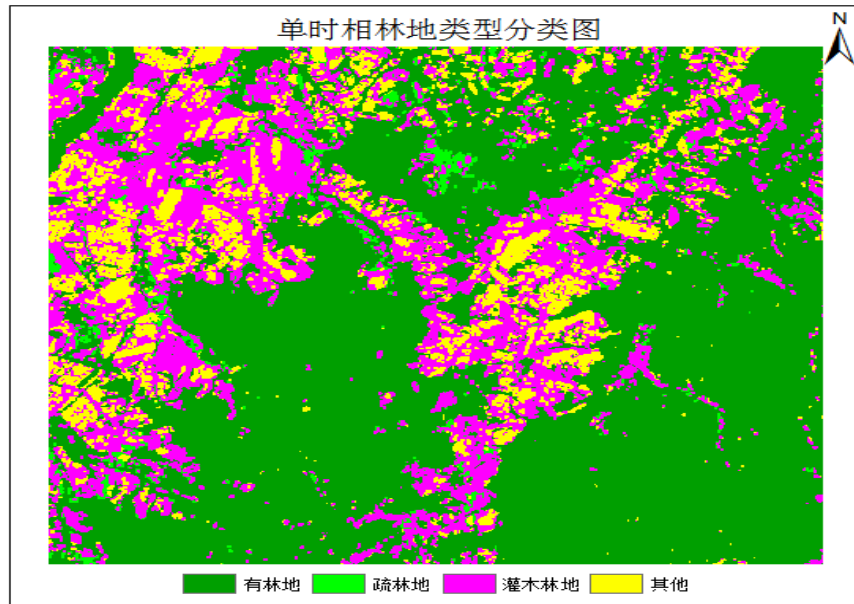
Land cover types	Acc. Single data	Acc. Multi-temporal data
Forest land (%)	96.34	97.82
Corp land (%)	92.96	93.87
Water body (%)	51.39	85.55
Urban & construction (%)	81.88	92.15
Total acc. (%)	83.72	91.37
Kappa	0.74	0.87



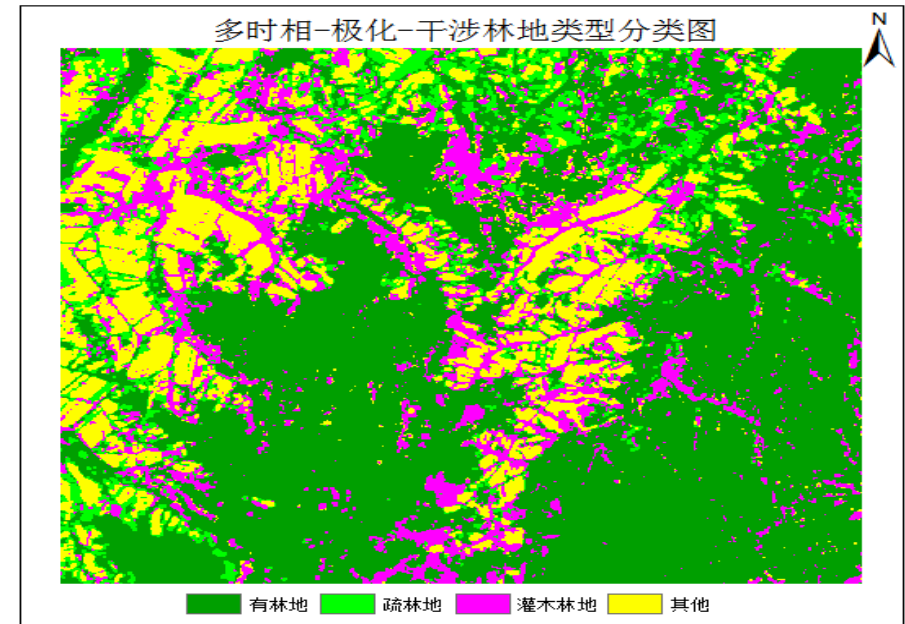
# Forest land type classification: features selected and results

- ❖ Mean HV intensity of three dates
- ❖ Mean HH-HH InSAR coefficient of three InSAR pairs
- ❖ The intensity ratio (8-HH/9-HV)

Forest land types	Acc. Single date	Acc. Multi-temporal date
Forested land (%)	96.76	99.00
Sparse forest land (%)	55.51	83.99
Shrub land (%)	60.01	82.43
Total acc. (%)	78.19	92.25
Kappa	0.69	0.90



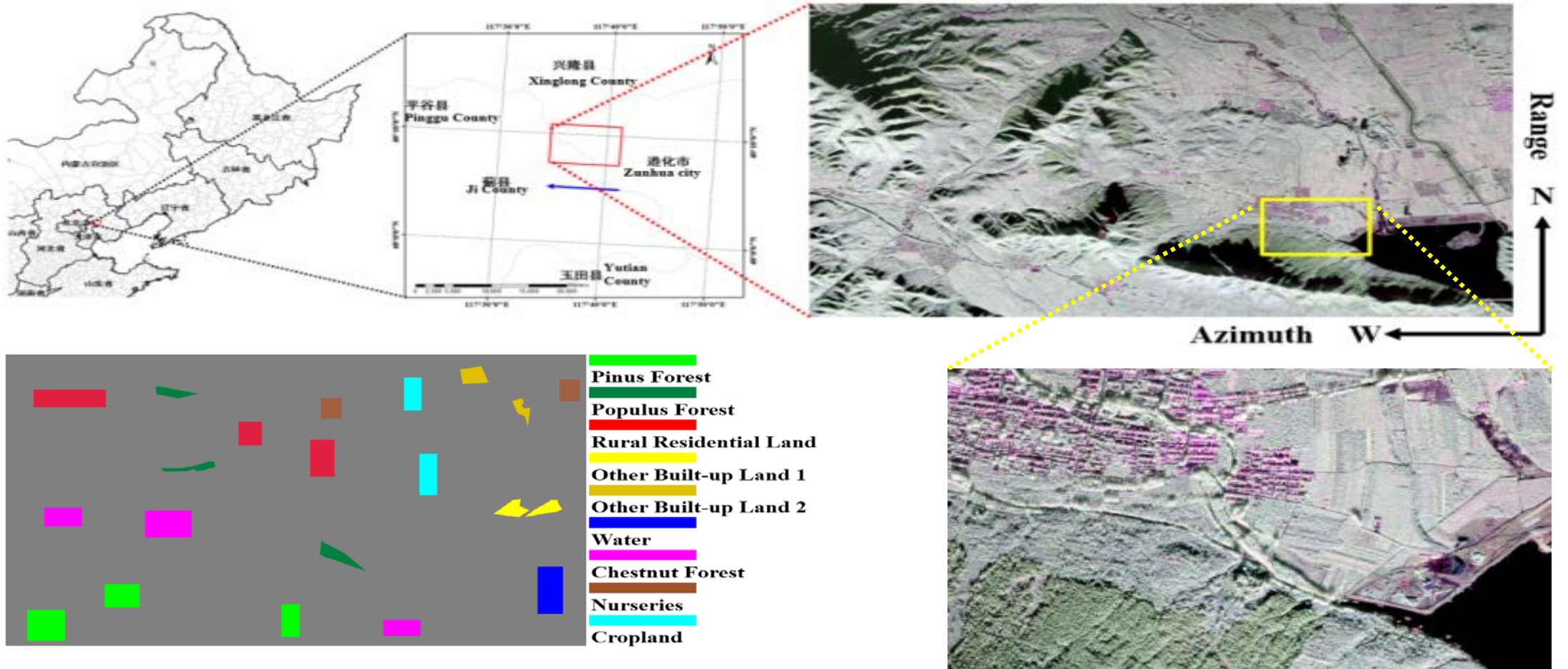
Forest type classification result using single data



Forest type classification result using multi-temporal data

### 2.3 Forest types classification using high resolution airborne PolSAR data

PauliRGB

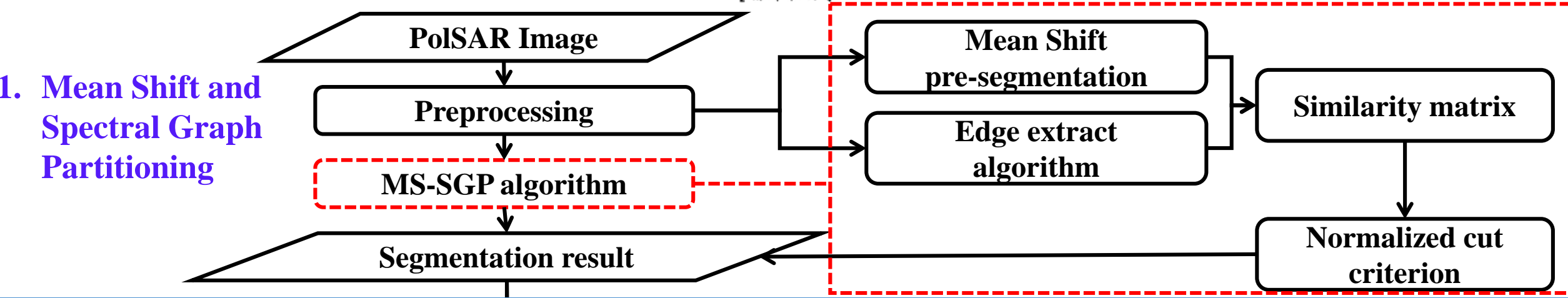


The ground true data and Classification system

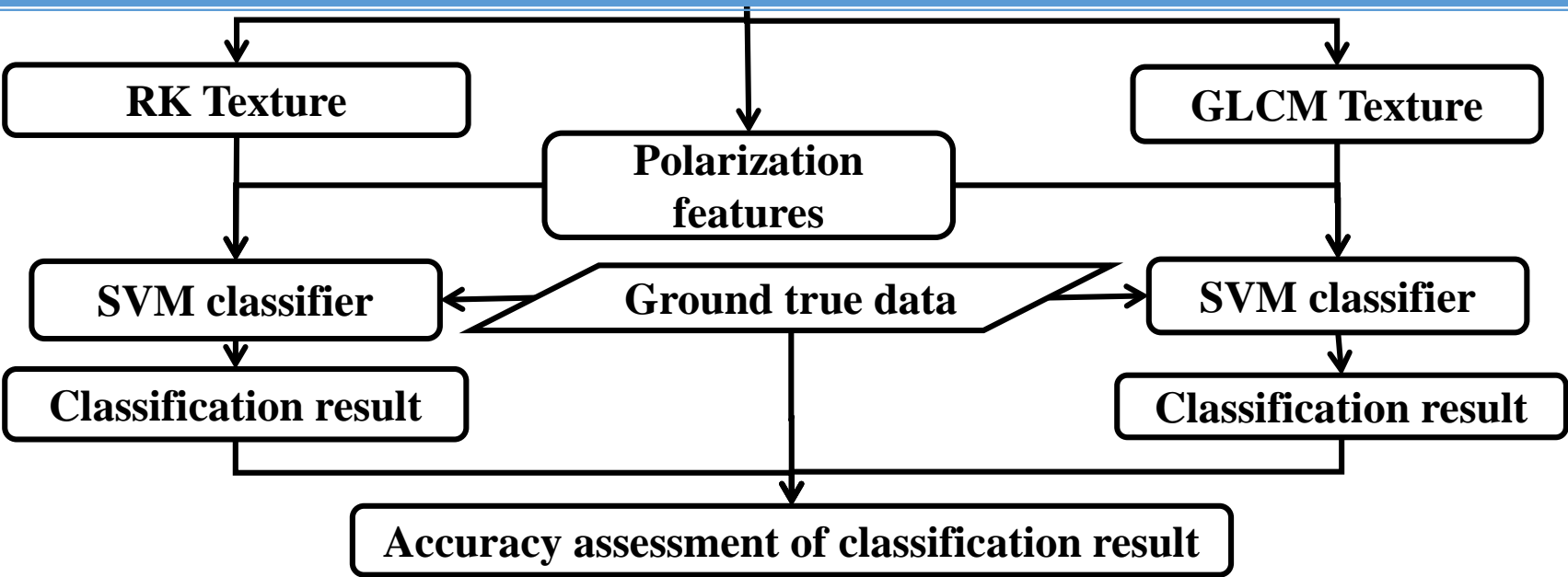


云南师范大学

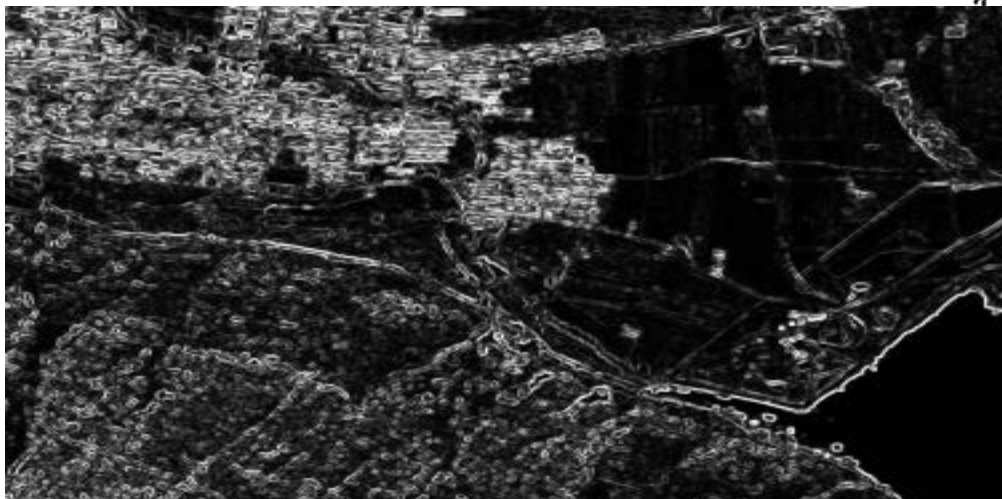
## 1. Mean Shift and Spectral Graph Partitioning



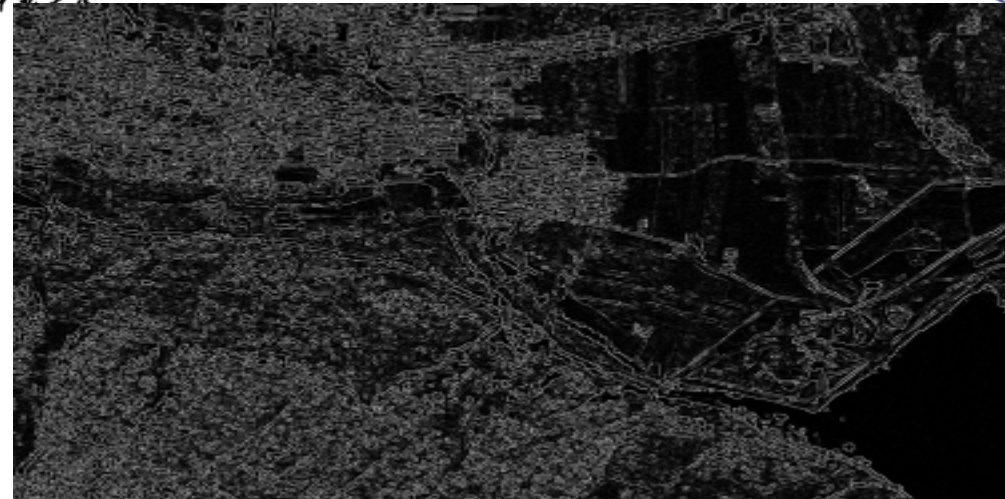
## 2. RK texture classification capability validation



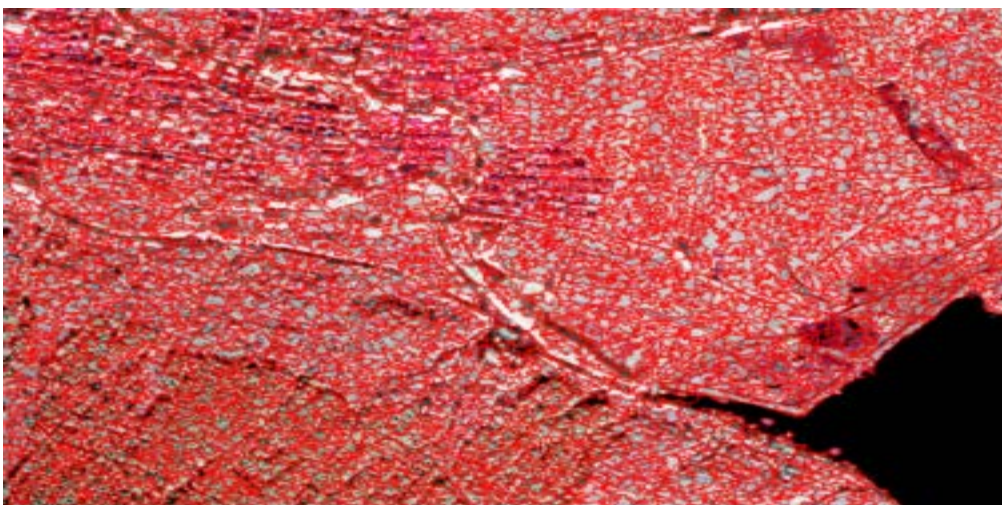
云南师范大学



**a. Raw result of edge map**



**b. Optimized result of edge map**



**c. Mean-shift Pre-segmentation result**



**d. Segmentation result based on MS-SGP**

# ● Features extraction

	Classification Features	Description	Number
Polarization features	$P_s, P_d, P_v$	Freeman-Durden Decomposition parameters	19
	$f_s, f_d, f_v, f_h$	Four-Component Decomposition parameters	
	$H, A, \alpha$	Cloud-Pottier Decomposition parameters	
	$T_{ij} (i, j=1, 2, 3)$	Elements of Polarimetric Coherence Matrix	
Textural features	U0/U45/U 90/U135, E0/E45/E90/E135, D0/D45/D90/D135, H0/H45/H90/H135, C0/C45/C90/C135, M0/M45/M90/M135	GLCM textural features : Uniformity、Entropy、Dissimilarity、 Homogeneity、Contrast、Mean (0°, 45°, 90°, 135° four direction)	24
	RK	Relative Kurtosis	1

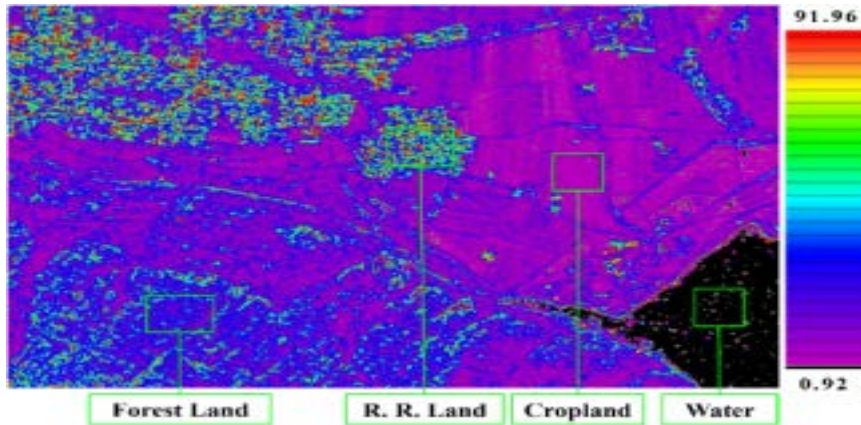


## ● RK textural feature

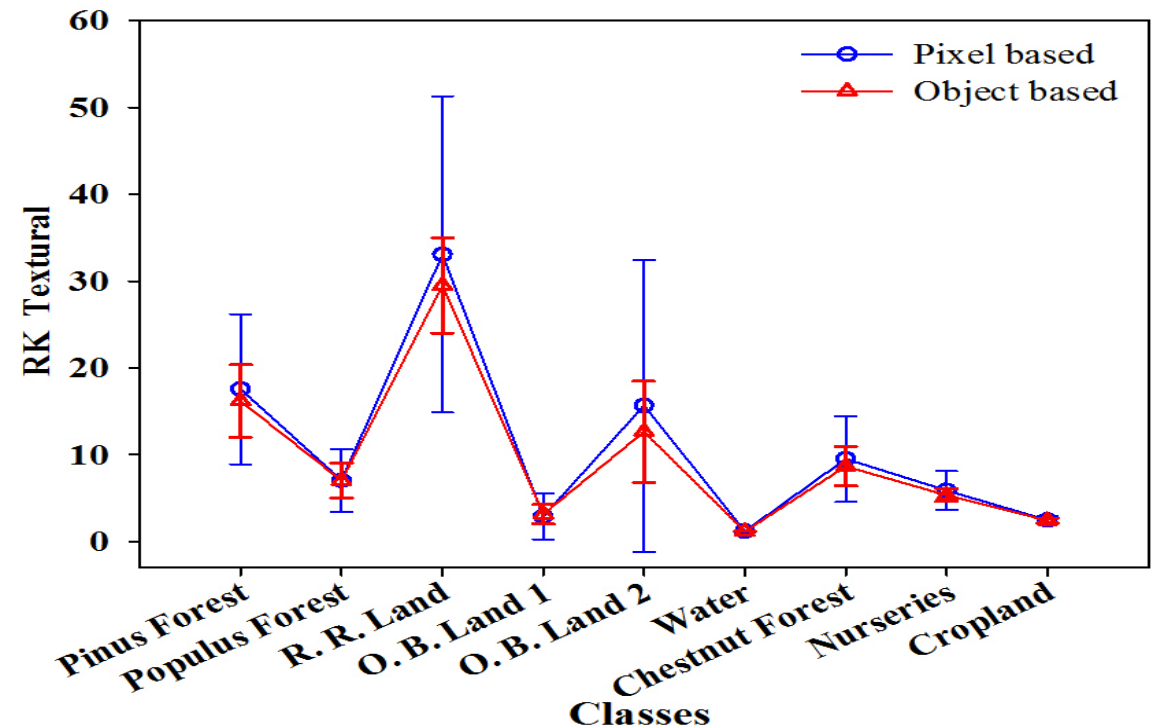
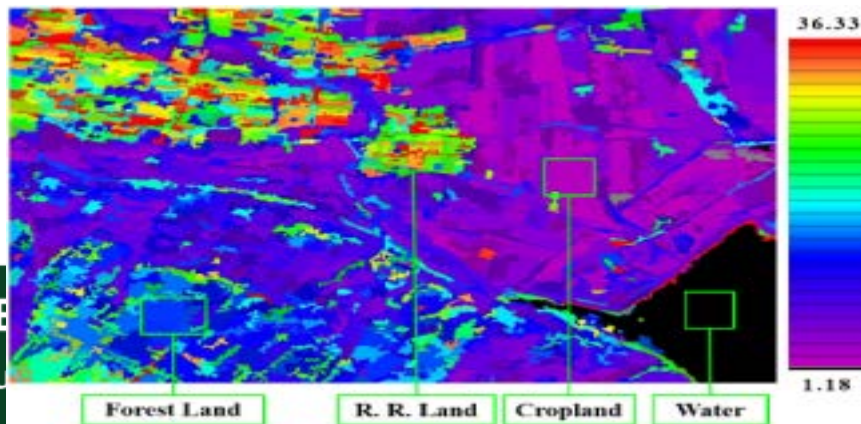
The relative kurtosis (RK) is the sample multivariate kurtosis relative to that of the standard multivariate Gaussian and is a common measure of non-Gaussianity(Anthony *et al.*,2010):

$$RK = \frac{\text{mean}[(y^T \hat{\Sigma}^{-1} y)^2]}{d(d+1)} = \frac{E\{z^2\}}{(E\{z\})^2} = \frac{L \cdot \text{var}\{\text{tr}(\hat{\Sigma}^{-1} C)\} + d^2}{d(d+1)}$$

Pixel based

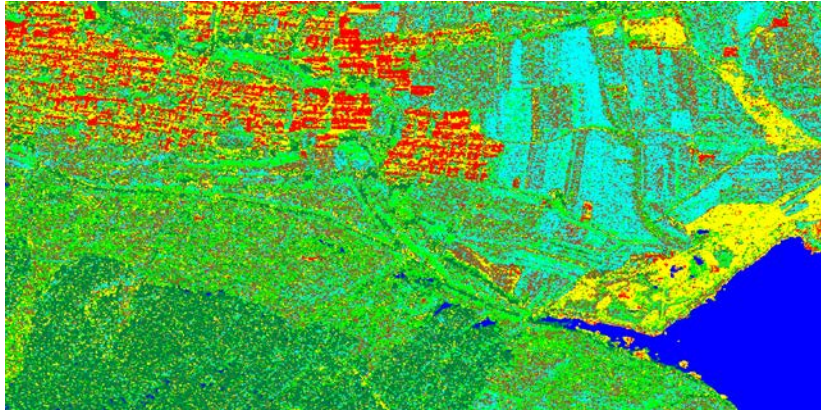


Object based

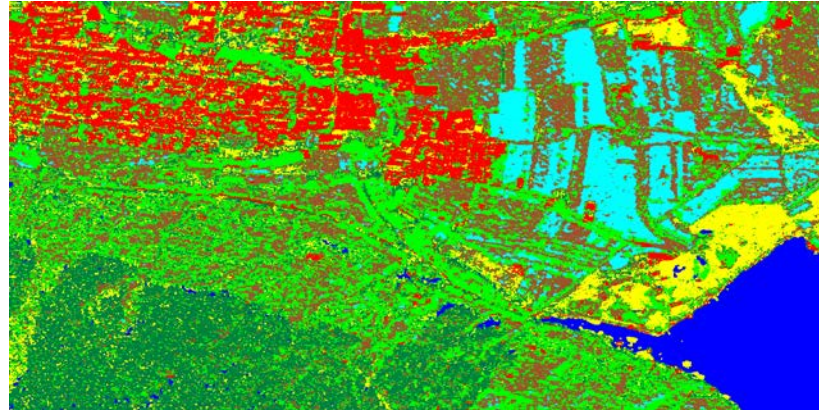




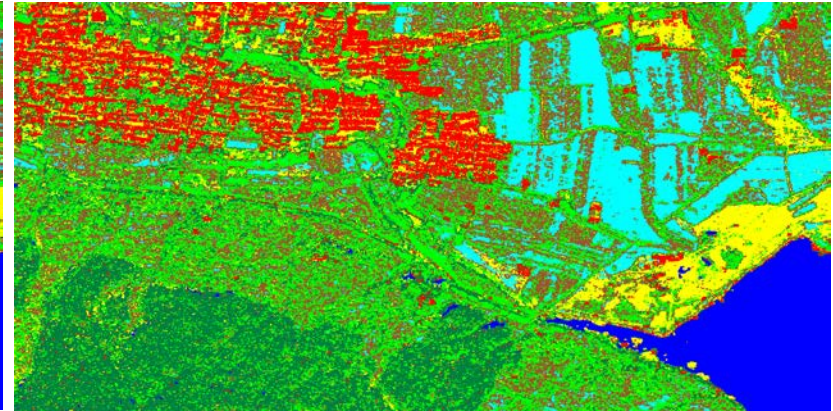
● Classification results



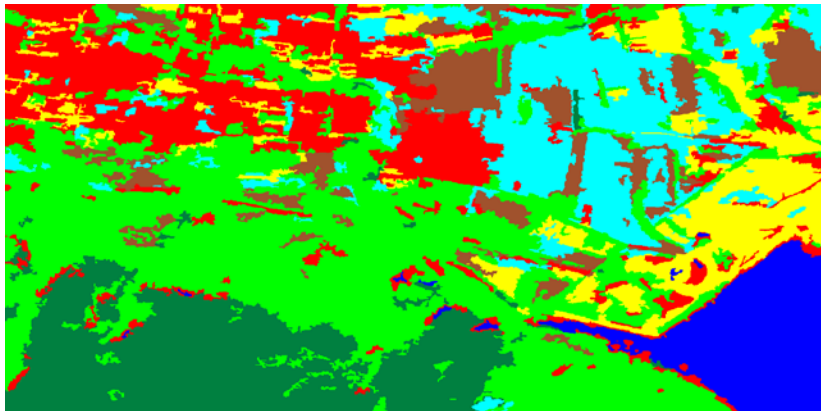
a. Pixel based Pol



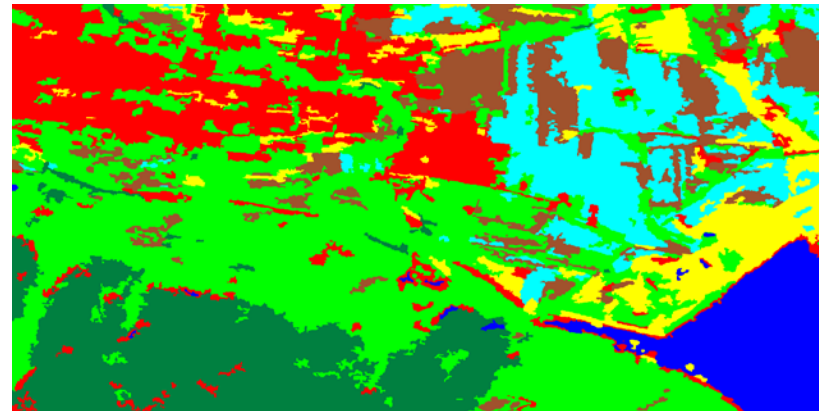
b. Pixel based Pol + GLCM



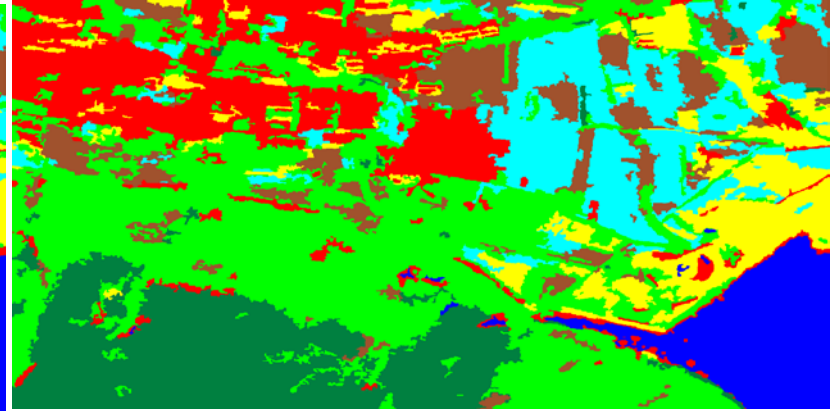
c. Pixel based Pol + RK



d. Object based Pol



e. Object based Pol + GLCM

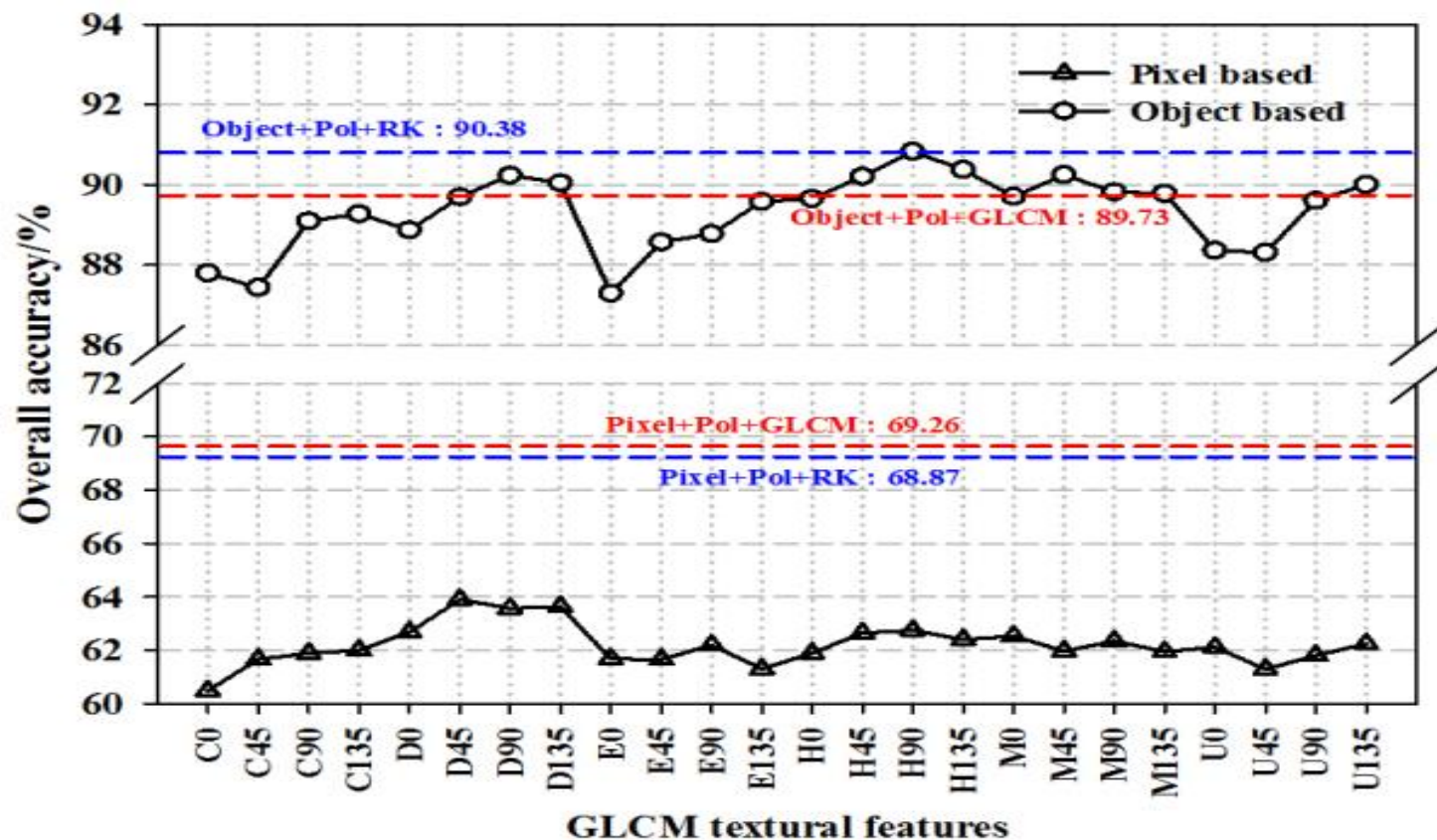


f. Object based Pol + RK



## ● Classification results - Accuracy assessment

Classification Overall accuracy with different GLCM textural features:



Overall accuracy:

**RK**  $\approx$  **GLCM**

Complexity:

**RK**  $<$  **GLCM**

Suitable for PolSAR:

**RK**  $>$  **GLCM**



## II. Applying PolSAR/PolInSAR to forest vertical structure information retrievals

# Outlines

## 1. Introduction

1.1 Forest application requirement and some concepts

1.2 Quantitative remote sensing inversion model for Bio-physical parameters

1.3 Model training and accuracy validation

## 2. PolSAR/PolinSAR forest structure parameter inversion model and its application

2.1 PolSAR forest biomass estimation with empirical model considering topography problem

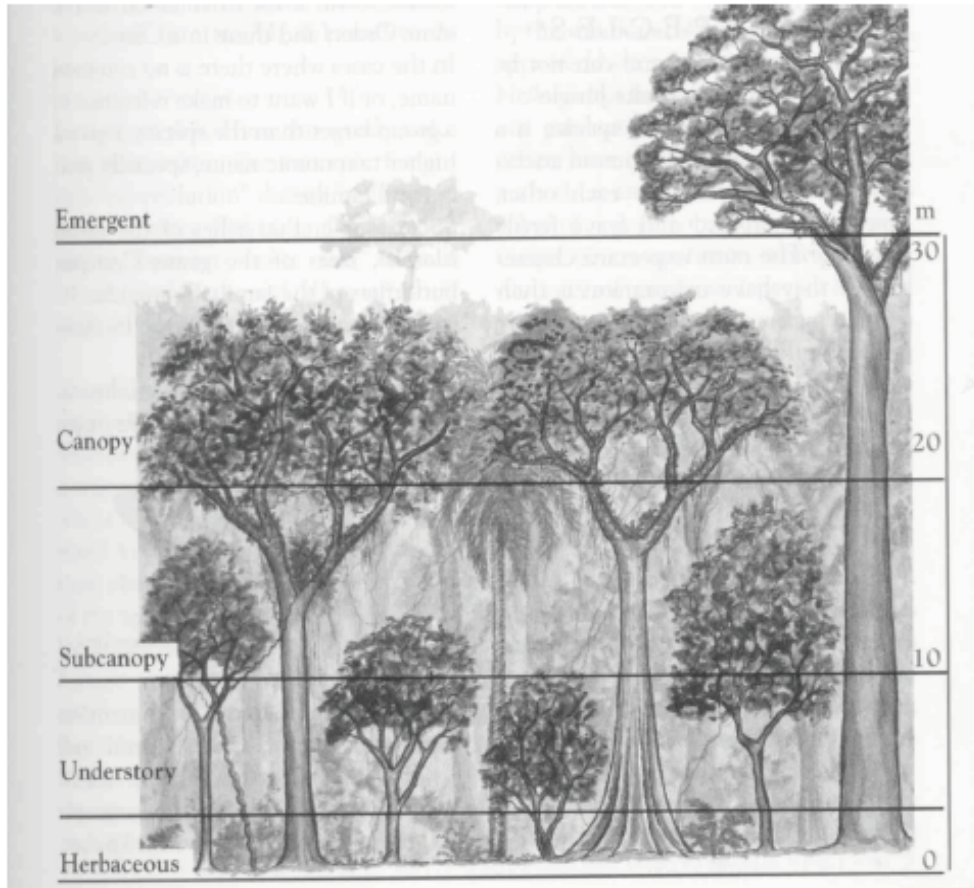
2.2 Single baseline PolinSAR for forest height inversion

2.3 Multi-baseline PolinSAR tomography for forest vertical structure information extraction

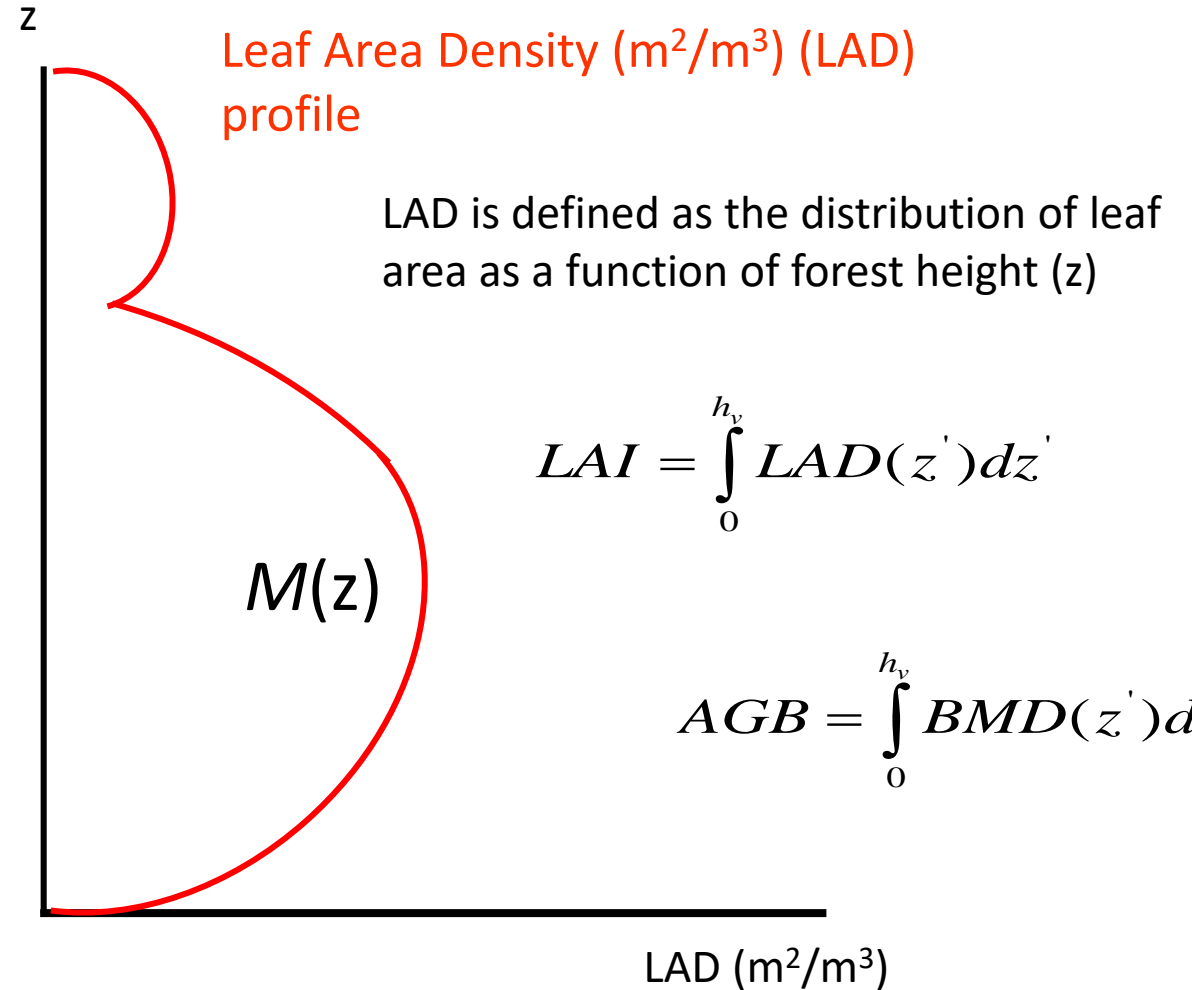
## 1.1 Forest application requirement and some concepts

- “Forest vertical structure” refers to the characteristics of forest vegetation as a function of vertical height above the ground
- The vertical structure of vegetated land surfaces is an important component of the description of ecosystems
- Quantitative measurements of vegetation characteristics as a function of vertical height are very useful for determinations of **biomass, leaf area index, and vegetation type** [*Waring et al.*, 1995].





Description (Santiago de la Vega, *The Laws of the Jungle*: Iguazu, Contacto Silvester, ediciones, Buenos Aires, Argentina August 1999, p. 17)



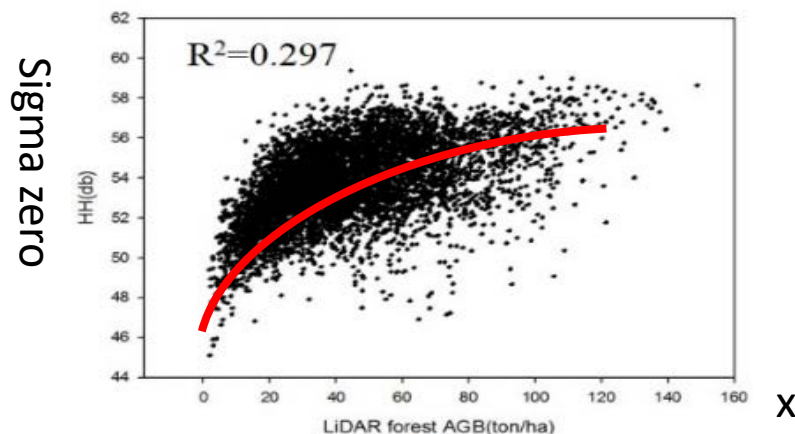
Other forest structure parameters: canopy height, volume, aboveground biomass, LAI...

# 1.2 Quantitative remote sensing inversion model for Bio-physical parameters

- **Incoherence and coherence radar models**
  - Empirical model
  - Semi-physical model & simplified physical model
  - Complex physical model
- **Forward vs backward(inversion) model**
  - **Model is simple, the forward model can be inversed**
    - Empirical model
    - Semi-physical model
    - Simple physical model
  - **Model is very complex, difficult to be inversed**
    - Complex physical model, only forward model
    - Used for SAR image simulation, physical understanding of the forest microwave backscattering mechanism

# • Empirical model

- If we go to the field to measure N forest plots;
- Compute the AGB of each plots, we have N samples of known AGB;
- From the SAR image we can extract the sigma zero corresponding to each plots, so we have N sigma zero values
- We plot the N points (X<sub>i</sub>, Sigma zero<sub>i</sub>), here X is the AGB, i is the plot index



- The forest AGB and sigma zero relationship can be described by one function:

$$\sigma^0 = a_0 + a_1 X + a_2 X^2 + \dots + a_n X^n$$

Forward model

- Or inversion model for AGB estimation

$$X = b_0 + b_1 \sigma^0 + b_2 \sigma^{0^2} + \dots + b_n \sigma^{0^n}$$

Inversion model



- **Semi-physical model & simplified physical model**

### Intensity model

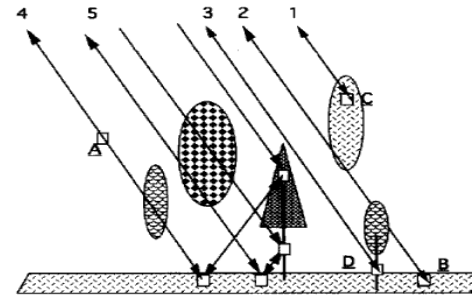
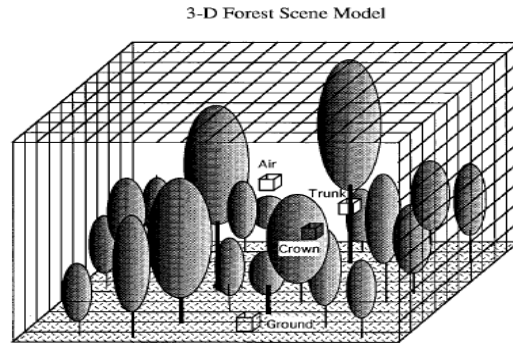
- Water cloud model (Attema, 1978; Ulaby, 1986)
- PolSAR intensity model (Sasan S. Saatchi, 2000)
- PolSAR intensity empirical model
  - Taking topography parameters as inputs (Sasan S. Saatchi, 2007)
  - Topography correction before applying model

### InSAR/PolInSAR model

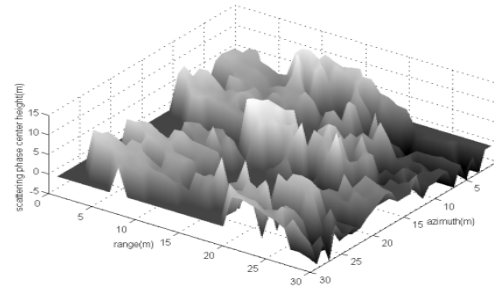
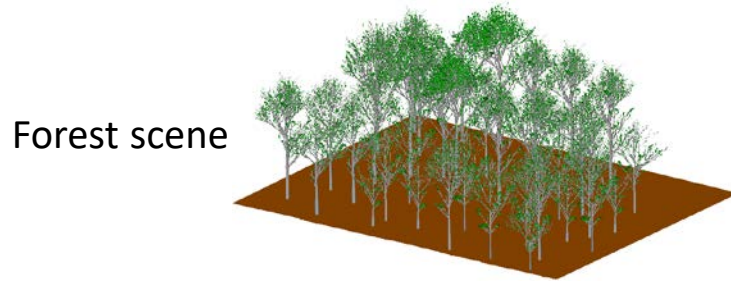
- InSAR water cloud model
- RVoG model
- Simplified model from RVoG
  - Phase difference
  - SINC
  - Phase diff plus SINC (Hybrid)
- Tomography model
  - Polarization Coherence Tomography (PCT)
  - Spectral analysis based tomography
  - AS based tomography

# • Complex physical model

- Ulaby incoherent forest microwave simulation
  - Polarimetric Intensity simulation for specific forest scene
  - Can not simulate SAR image
- 3D incoherent forest radar image simulation model (G. Sun & Ranson, 1995)



- 3D coherent forest radar image simulation model (G. Sun et al, 2005)



Simulated InSAR phase center

- PolSARProSim coherent simulation model
  - PolSAR image simulation of forest vegetation, low vegetation, bare soil
  - PolInSAR image simulation of forest vegetation

# 1.3 Model training and accuracy validation

- Just like classification, inversion also need model training (or model calibration) and model validation (accuracy estimation) ground truth data
  - Empirical model & Semi-empirical—**unknown model parameters, est.**
  - Physical model—**much more model parameters, most of them should be setup according to our knowledge, need truth**
  - Inversion result validation: **no validation, no application**
- How to get ground true data, eg. forest height , biomass
  - Field plots: big enough(slant to ground range, slope, enough looks)
  - LiDAR product: 2-4 points/m<sup>2</sup>, aided with field plots data
  - Samples should distribute evenly over the whole test site
  - Samples should cover big enough height or biomass range
- How to use the samples
  - Training and validation samples should be independent
  - If mixed together, model training and validation can be carried out by cross validation, one statistic method



# Outlines

## 1. Introduction

1.1 Forest application requirement and some concepts

1.2 Quantitative remote sensing inversion model for Bio-physical parameters

1.3 Model training and accuracy validation

## 2. PolSAR/PolinSAR forest structure parameter inversion model and its application

### **2.1 PolSAR forest biomass estimation with empirical model considering the topography effects**

2.2 Single baseline PolinSAR forest height and above ground biomass inversion

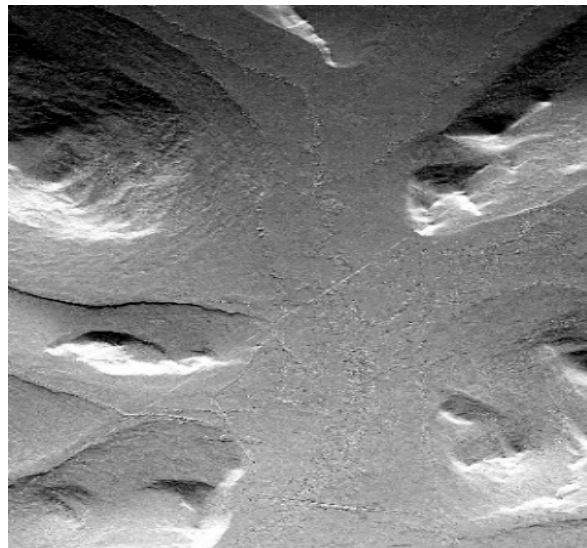
2.3 Multi-baseline PolinSAR tomography for forest vertical structure information extraction

# (1) Taking the topography parameters into the inversion model

## •Data used



Airborne P-band PolSAR acquired in the Northeast forest region, Genhe test site



The local incidence angle image computed from RD geo-location model and one DEM derived from LiDAR

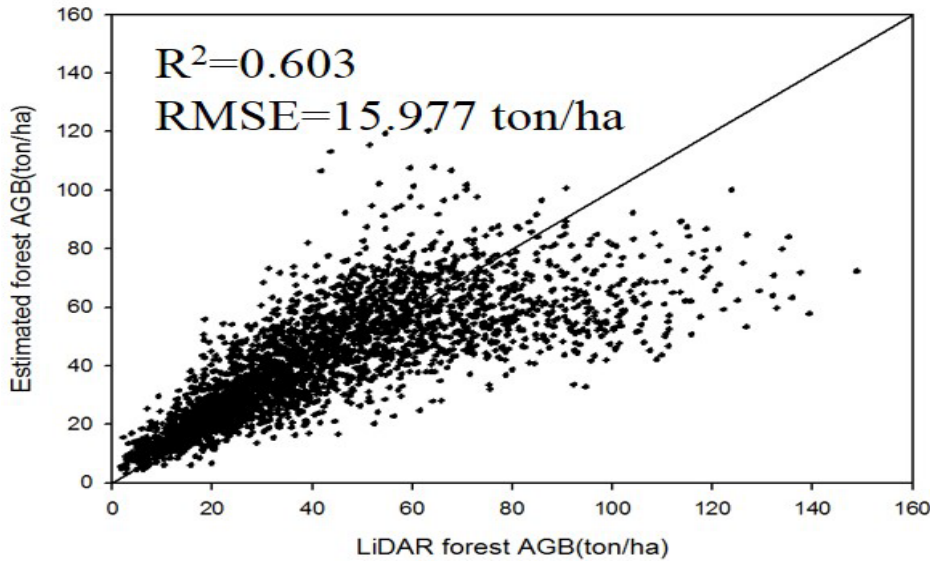
## •Model applied

$$\begin{aligned} \log(W) = & a_0 + a_1 \sigma_{HV}^0 \cos(\theta_0 - \theta_l) + \\ & a_2 (\sigma_{HV}^0 \cos(\theta_0 - \theta_l))^2 + \\ & a_3 \sigma_{HH}^0 \cos(\theta_0 - \theta_l) + \\ & a_4 (\sigma_{HH}^0 \cos(\theta_0 - \theta_l))^2 + \\ & a_5 \sigma_{VV}^0 \cos(\theta_0 - \theta_l) + \\ & a_6 (\sigma_{VV}^0 \cos(\theta_0 - \theta_l))^2 \dots \end{aligned}$$

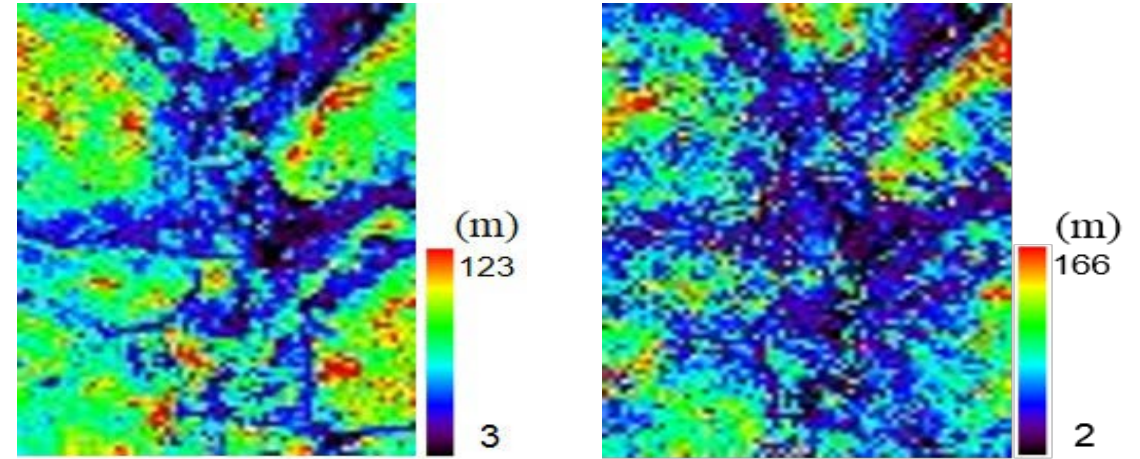
The empirical model for AGB estimation (Sassan Saatchi, 2007)

- Ground truth AGB: LiDAR derived AGB plot, size of 50m\*50m, N=5982
- Model training and validation: N/2 for training, N/2 for validation

## •Forest AGB estimation and validation results



*Correlation between estimated forest AGB and LiDAR AGB (2991 points).*



*Estimated forest AGB based on P-band PolSAR (left) and LiDAR AGB (pixel size is 50m\*50m)*





# (2) Applying terrain correction to PolSAR data before inversion

- Three-Stage Terrain Correction Method

$$\sigma_{rtc}^0 = \sigma_{POC}^0 \cdot \cos \psi \cdot \left( \frac{\cos \theta_{ref}}{\cos \theta_{loc}} \right)^n$$

## Stage①:POA Correction

- Circular polarization method

## Stage②:ESA Correction

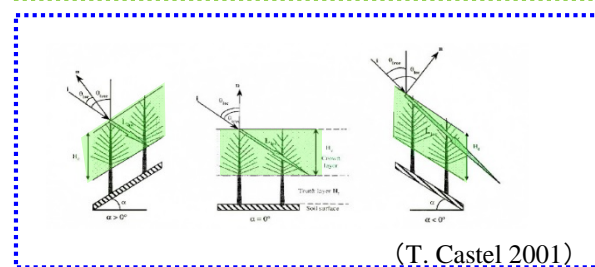
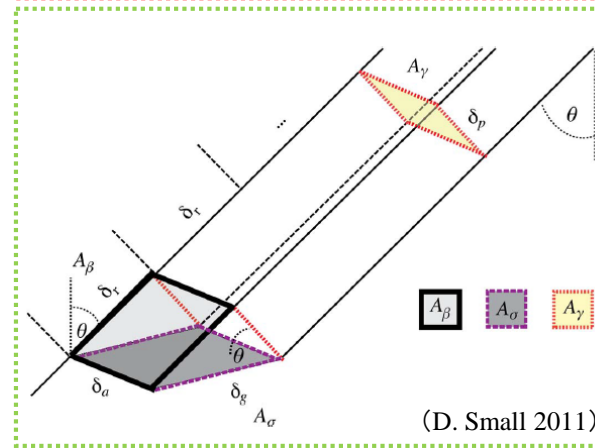
- Projection angle method

## Stage③:AVE Correction

- Minimum correlation coefficient method

$$C_{POC} = VC V^T$$

$$V = \frac{1}{2} \begin{bmatrix} 1 + \cos 2\theta & \sqrt{2} \sin 2\theta & 1 - \cos 2\theta \\ -\sqrt{2} \sin 2\theta & 2 \cos 2\theta & \sqrt{2} \sin 2\theta \\ 1 - \cos 2\theta & -\sqrt{2} \sin 2\theta & 1 + \cos 2\theta \end{bmatrix}$$



## (2) Applying terrain correction to PolSAR data before inversion

- Minimum correlation coefficient method

- We can evaluate the correction result by the correlation between corrected backscatter value and the local incident angle.

$$\sigma_{\theta_{loc}} = \sigma \cdot \left( \frac{\cos \theta_{ref}}{\cos \theta_{loc}} \right)^n \quad \Rightarrow \quad \begin{aligned} f(n) &= \rho(\theta_{loc}, \sigma_{\theta_{loc}}) \\ n &= \arg \min \{ \text{abs}[f(n)] \} \end{aligned}$$

- The value of  $n$  for each polarization channel:  $n(hh)=N_1, n(hv)=N_2, n(vv)=N_3$
- So, we get the correction coefficient for each polarization channel :

$$k_{hh} = \left( \frac{\cos \theta_{ref}}{\cos \theta_{loc}} \right)^{N_1} \quad k_{hv} = \left( \frac{\cos \theta_{ref}}{\cos \theta_{loc}} \right)^{N_2} \quad k_{vv} = \left( \frac{\cos \theta_{ref}}{\cos \theta_{loc}} \right)^{N_3}$$

- Finally, the correction coefficient matrix  $K$  for polarization covariance matrix  $C$  is:

$$K = \begin{bmatrix} k_{hh} & \sqrt{k_{hh}k_{hv}} & \sqrt{k_{hh}k_{vv}} \\ \sqrt{k_{hh}k_{hv}} & k_{hv} & \sqrt{k_{hv}k_{vv}} \\ \sqrt{k_{hh}k_{vv}} & \sqrt{k_{hv}k_{vv}} & k_{vv} \end{bmatrix} \quad C_{out} = C \odot K$$

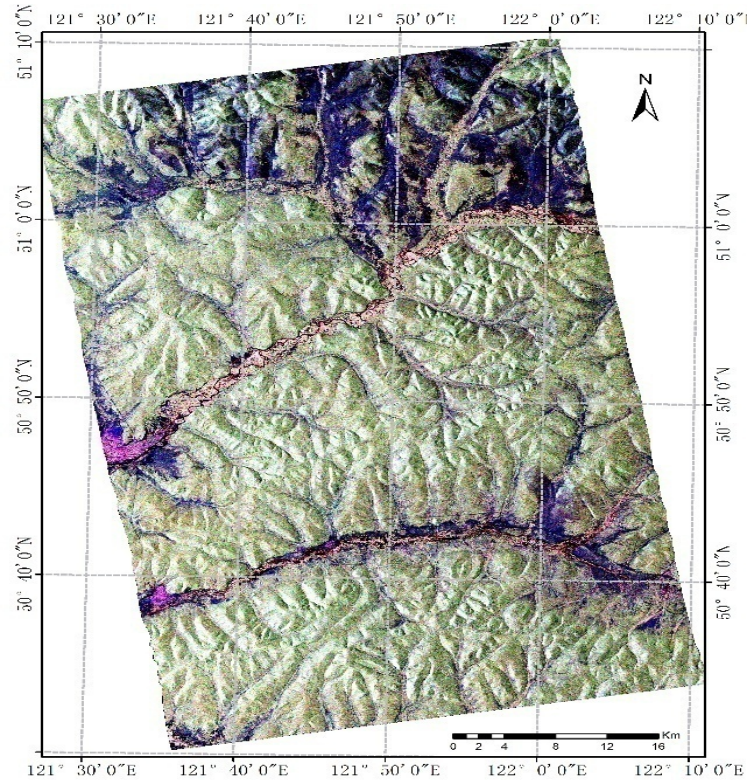
Note :  $\odot$  is the Hadamard product.



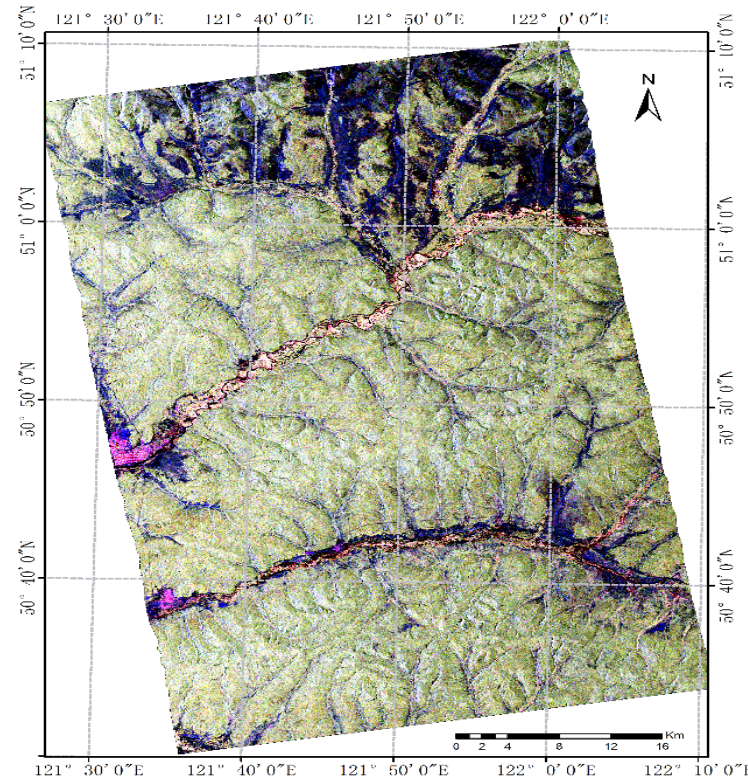
## (2) Applying terrain correction to PolSAR data before inversion

### • Result and Analysis

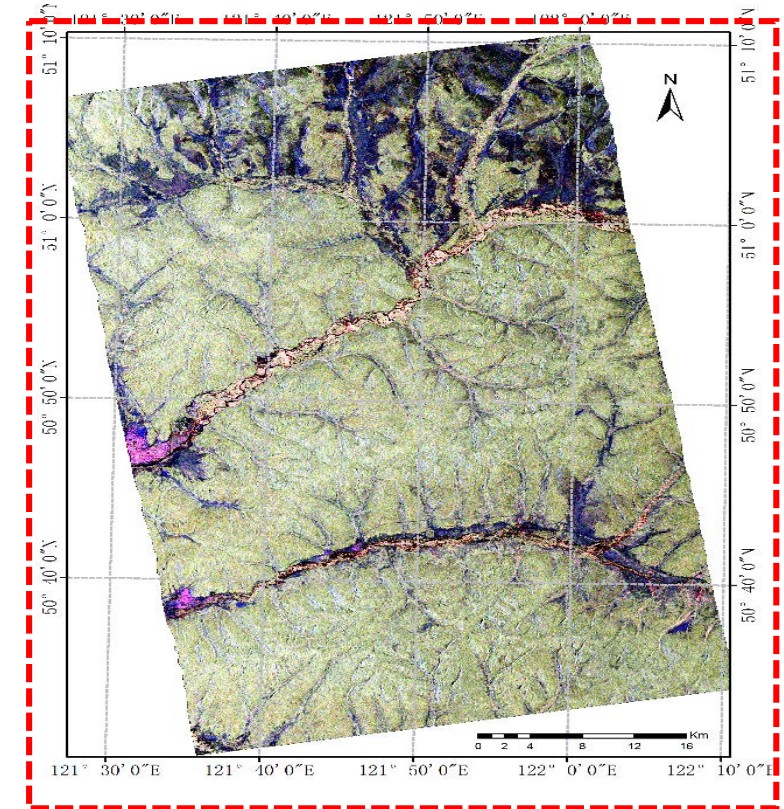
- Angular variation effect correction result (AVEc)



GTC Pauli RGB



POAc+ESAc Pauli RGB

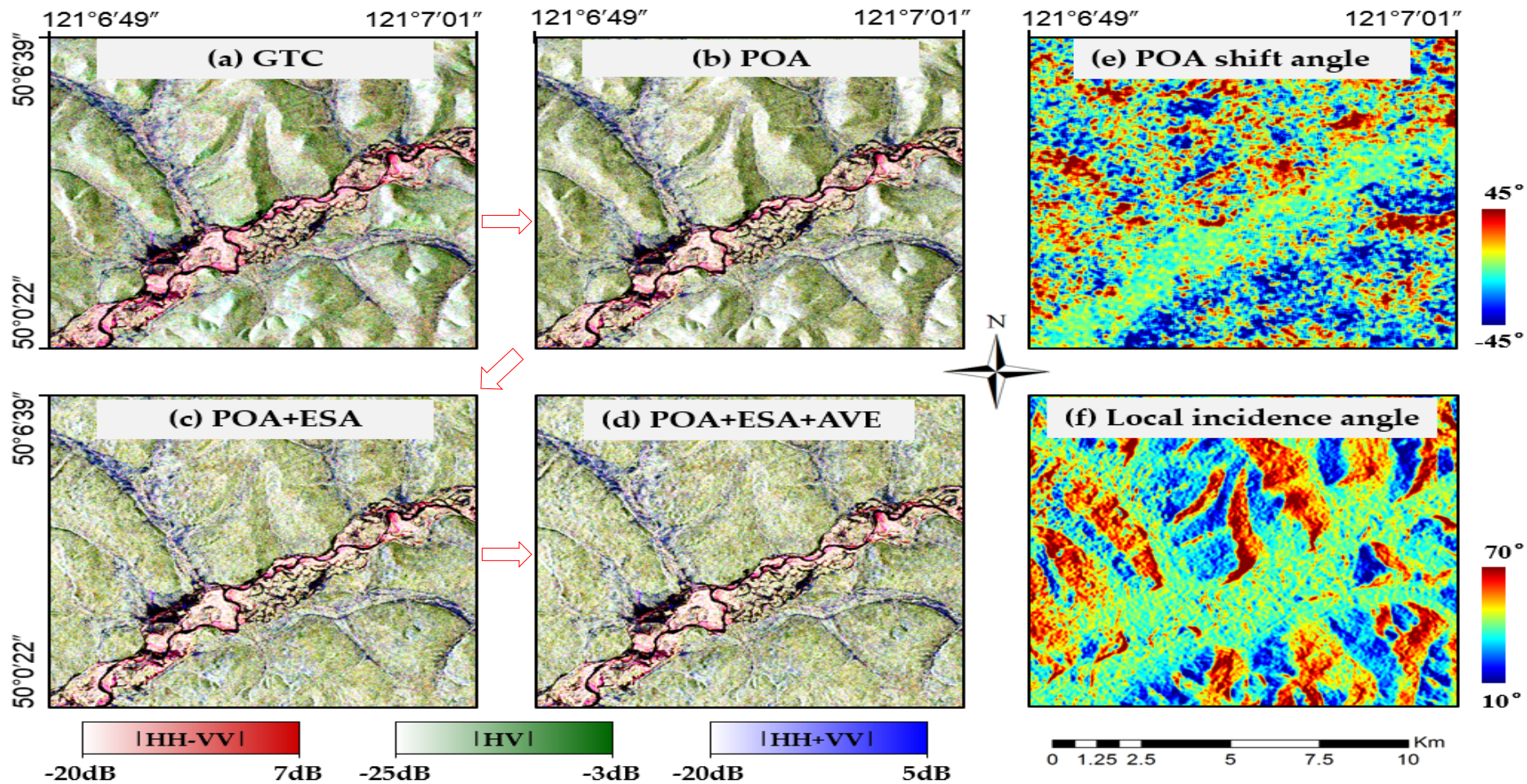


POAc+ESAc+AVEc Pauli RGB

- *The remaining terrain effects in PolSAR image has been effectively removed, there is no significant difference between front slope and back slope.*

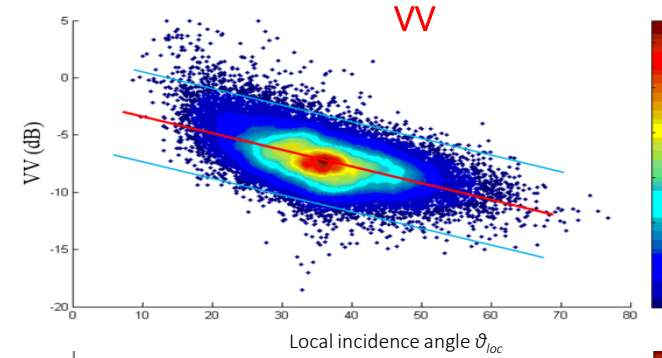
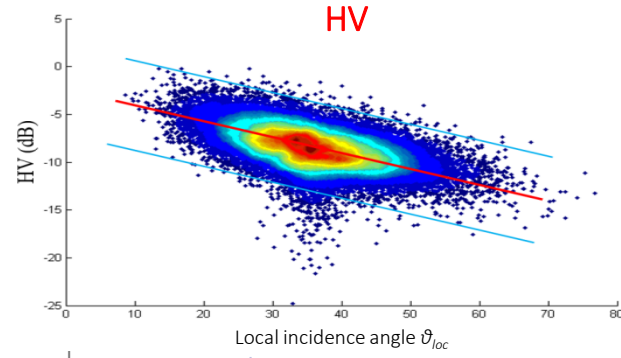
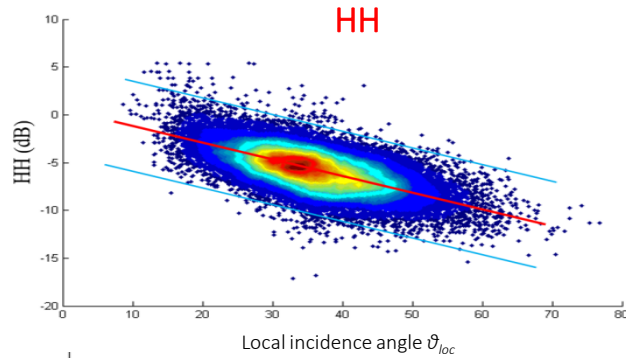


- Different stage Terrain Correction result (Enlarged)

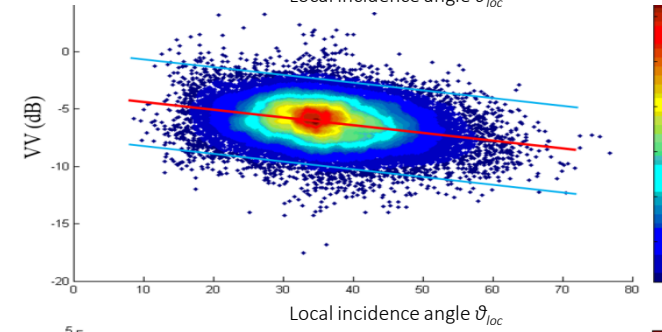
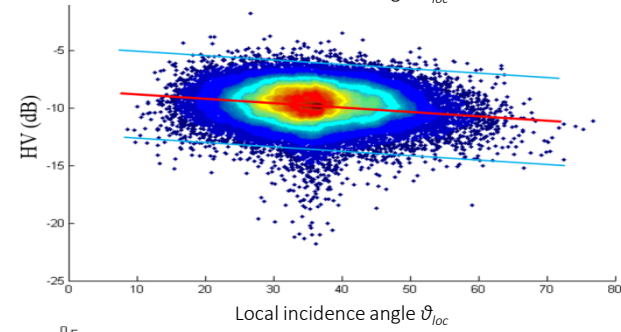
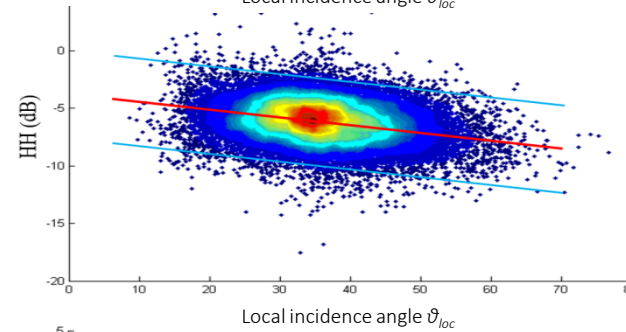




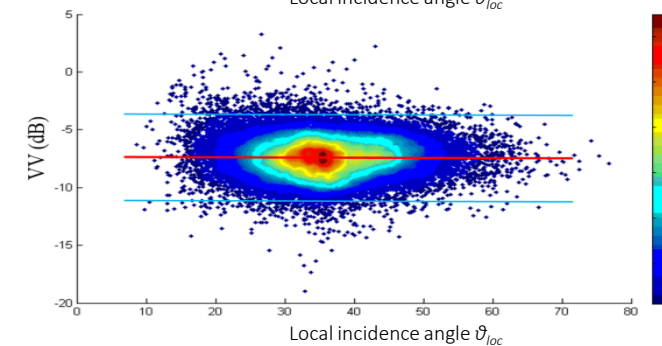
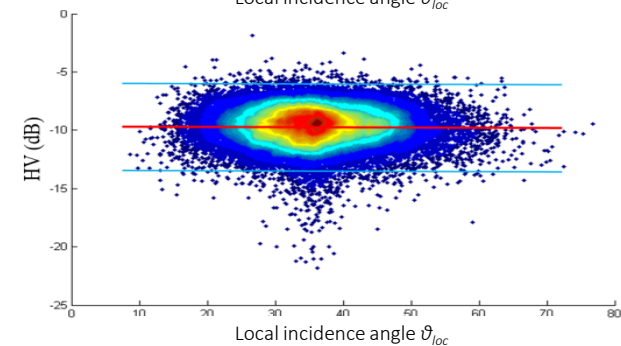
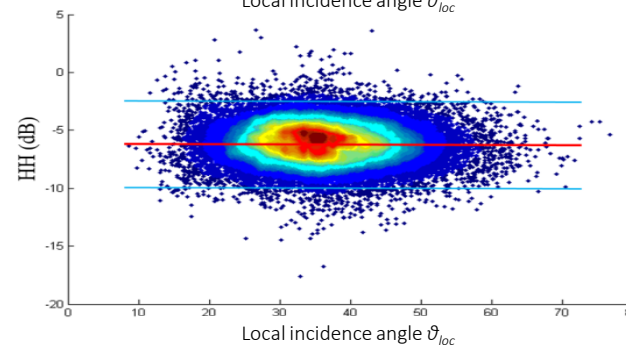
GTC



POAc  
+  
ESAc



POAc  
+  
ESAc  
+  
AVEc

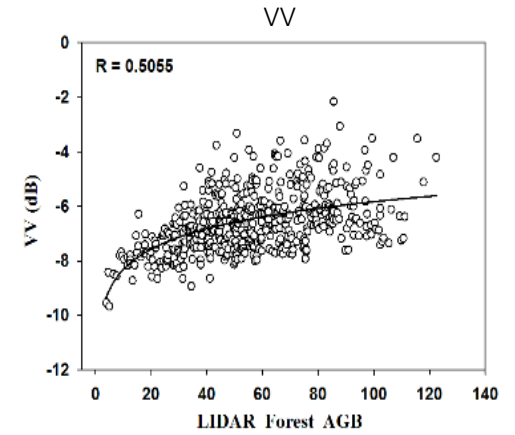
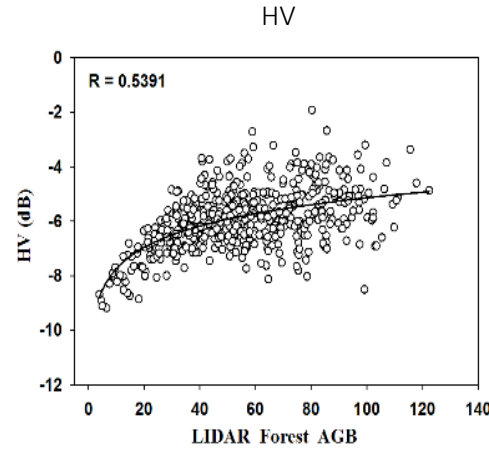
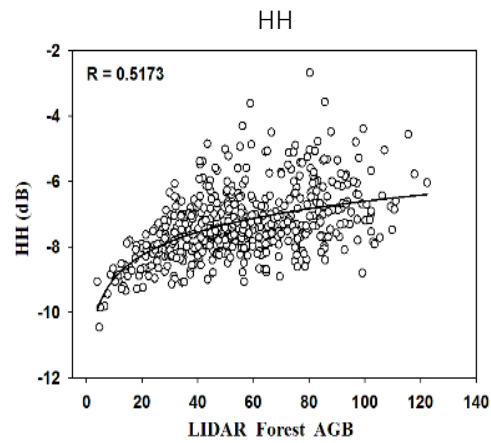


*Compare scatter plots of different correction stage, along with the correction stages performed, the correction result is getting better and better.*

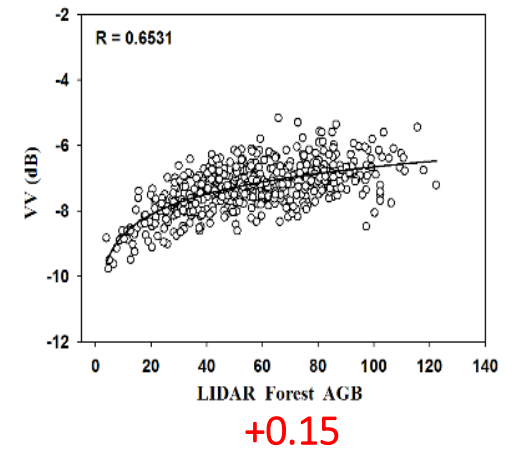
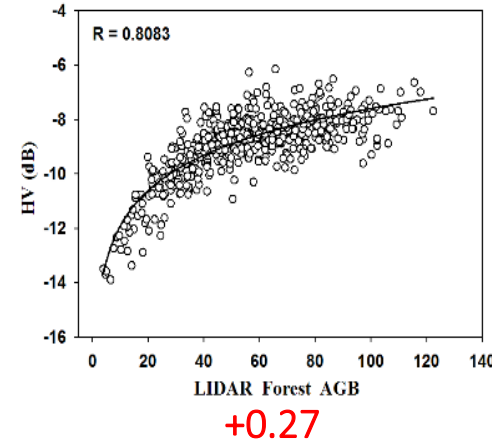
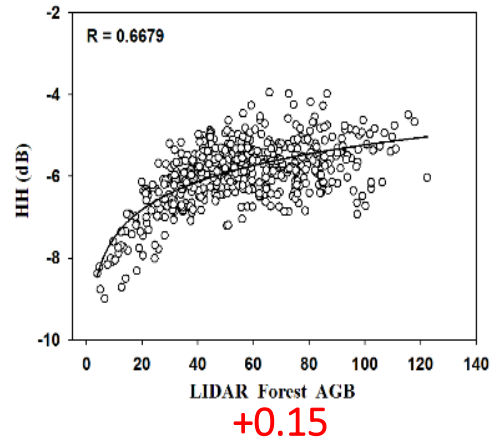


- The correlation between backscatter coefficient and forest AGB

Before correction



After correction



- Obviously, the corrected backscatter coefficients have the better correlation with forest AGB than uncorrected case.

# Outlines

## 1. Introduction

1.1 Forest application requirement and some concepts

1.2 Quantitative remote sensing inversion model for Bio-physical parameters

1.3 Model training and accuracy validation

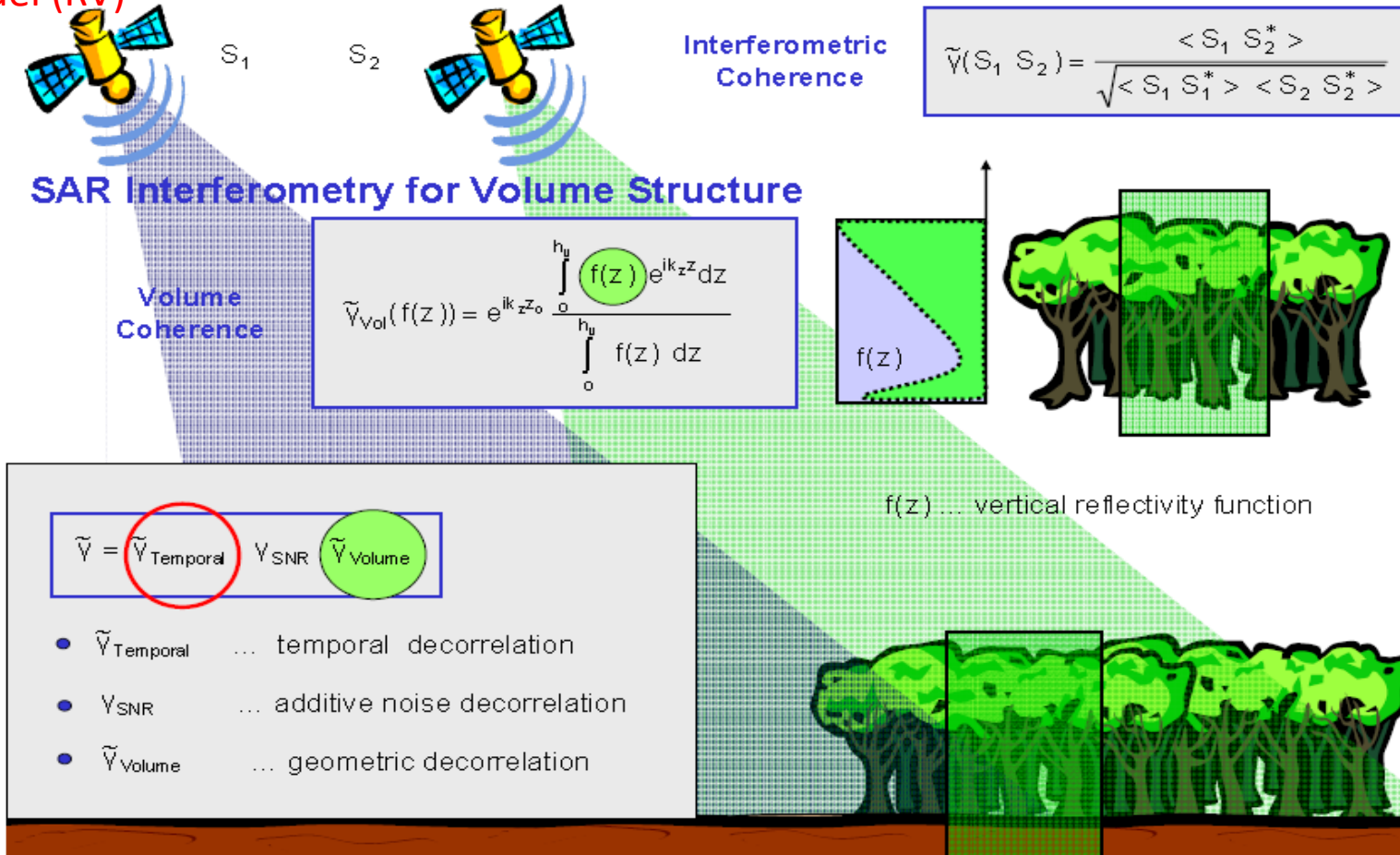
## 2. PolSAR/PolinSAR forest structure parameter inversion model and its application

2.1 PolSAR forest biomass estimation with an empirical model

**2.2 Single baseline PolInSAR forest height inversion**

2.3 Multi-baseline PolinSAR tomography for forest vertical structure information extraction

## Radom Volume Model (RV)



K. Papathanassiou, S-K. Lee, F. Kugler, et al. Estimation of Forest Vertical Structure by means of Multi-Baseline Pol-InSAR. POLInSAR 2009





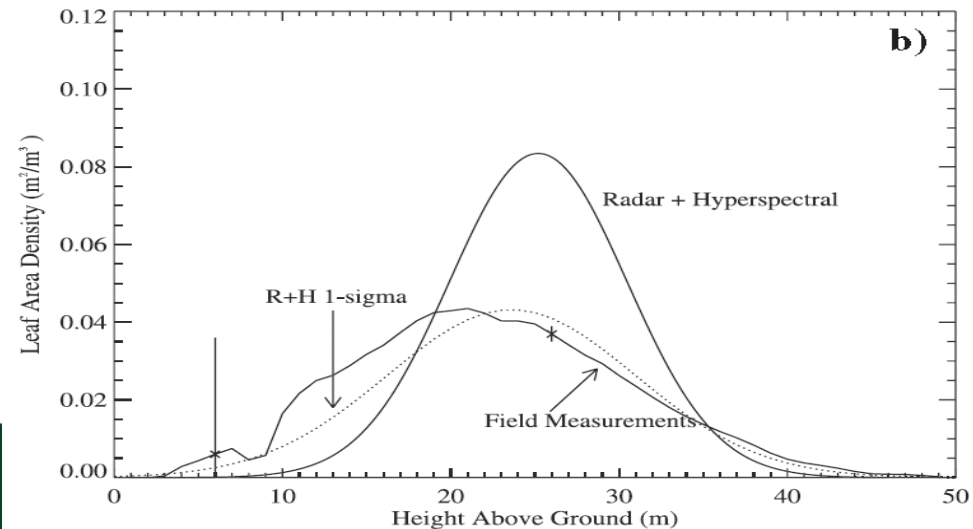
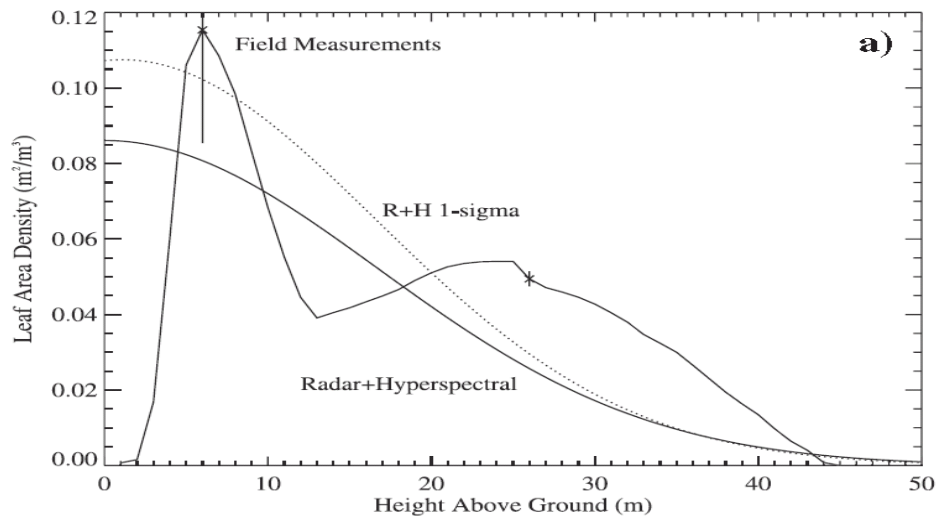
- Treuhaft R. N. (2002) define cross correlation as

$$\text{complex coherence} = \frac{e^{i\phi(z_0)} \int_0^\infty dz' e^{i\alpha_z(B, \lambda, \theta_0)z'} \rho(z') \langle f_b^2(z') \rangle \exp\left[\frac{-2}{\cos\theta_0} \int_0^\infty dz'' \sigma_x(z'')\right]}{\int_0^\infty dz' \rho(z') \langle f_b^2(z') \rangle \exp\left[\frac{-2}{\cos\theta_0} \int_0^\infty dz'' \sigma_x(z'')\right]}$$

$f(z)$

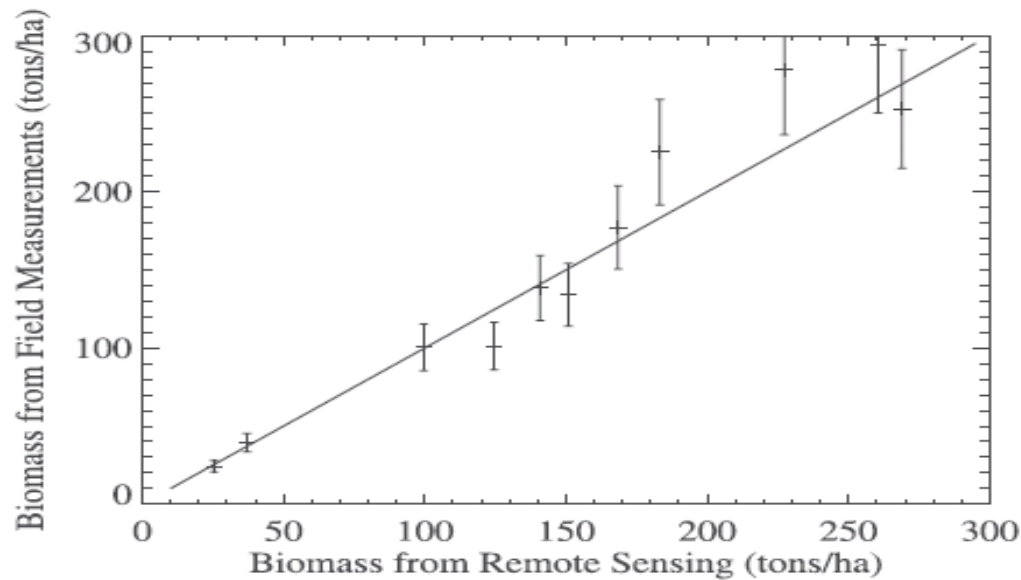
AIRSAR, single baseline, multi-altitudes

$$LAD(z) = LAI \times f(z; z_G, \sigma_G)$$



- Treuhaft R. N. (2003) developed one model to estimate forest above ground biomass from  $f(z)$  and LAI

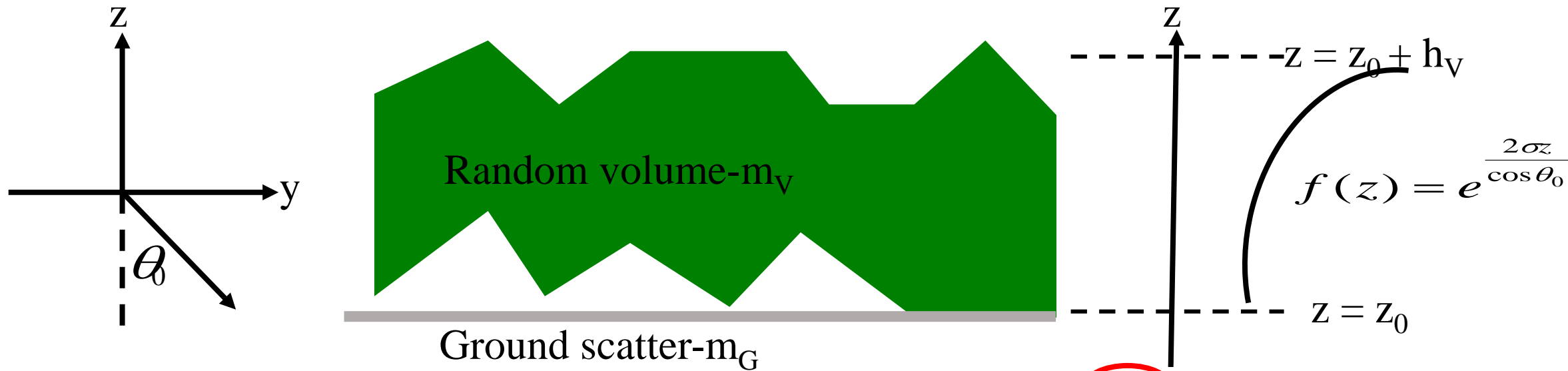
$$Biomass = a + b(LAI\sigma_G + z_G)$$



AIRSAR, single baseline,  
multi-altitudes

RMSE: 25ton/ha

- Konstantinos P. P. & Shane R. C. simplified the correlation definition using RVoG model.



$$\gamma = \exp(i\phi_0) \frac{\gamma_V + m}{1 + m}$$

$\gamma_V$  - complex coherence of volume alone

$m$  - effective ground-to-volume amplitude ratio

$$\gamma_V = \frac{I_2}{I_1} \begin{cases} I_2 = \int_0^{h_v} \exp\left(\frac{2\sigma z'}{\cos \theta_0}\right) \exp(ik_z z') dz' \\ I_1 = \int_0^{h_v} \exp\left(\frac{2\sigma z'}{\cos \theta_0}\right) dz' \end{cases}$$

$$k_z = \frac{4\pi\Delta\theta}{\lambda \sin \theta}$$



- Three stages full model inversion

## **Input: 11 coherence images:**

OPT1, OPT2, OPT3, HHHH, HVHV, VVVV, LLLL, LRLR, RRRR, PAULI-1, PAULI-2

## **Method:**

**Stage 1: Line fitting and find the intersection point P1 and P2;**

**Stage 2: Find out the ground phase point and the coherence for  $\underline{W}_v$ ;**

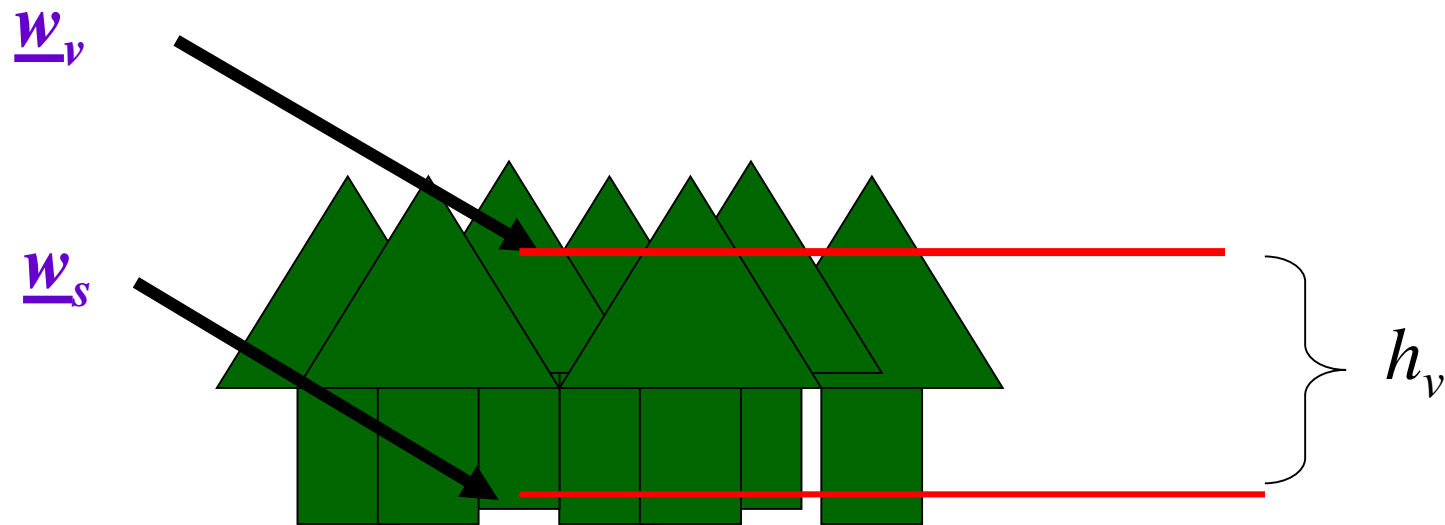
**Stage 3: From the 2D lookup table (LUT) to get the tree height  $h_v$ .**

- RVoG can be further simplified for forest height inversion
  - Coherence phase difference (CPD) inversion
  - Coherence amplitude SINC inversion (SINC)
  - Coherence PD and amplitude hybrid inversion (HYBRID)

Input: Coherence for  $\underline{w}_v$  and  $\underline{w}_s$

Method:

$$h_v = \frac{\arg(\gamma_{\underline{w}_v}) - \arg(\gamma_{\underline{w}_s})}{k_z}$$



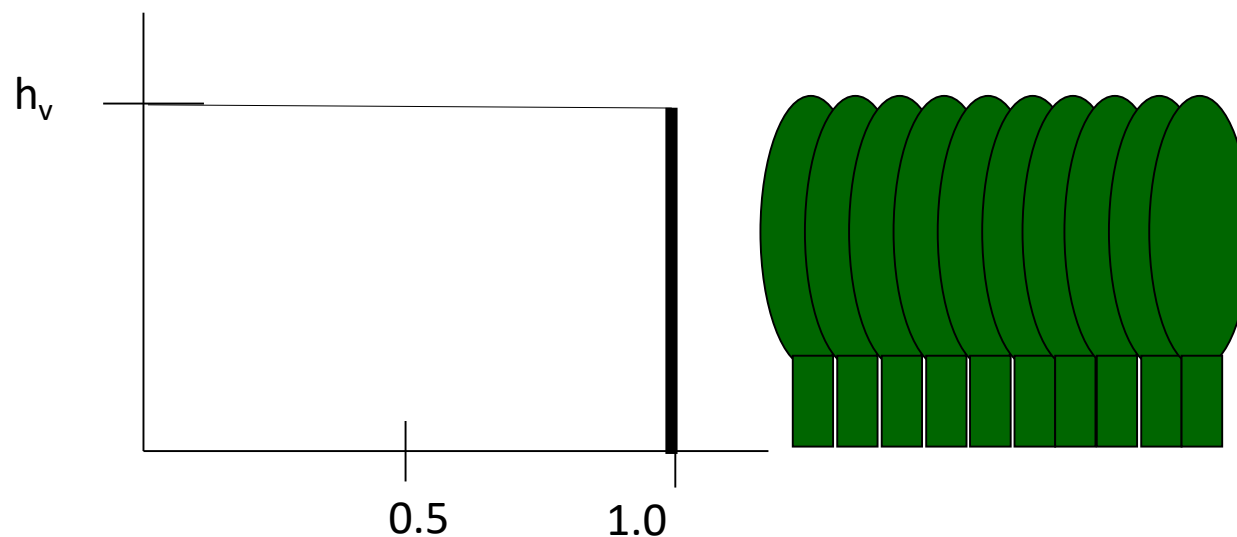


Input: Coherence image for  $\underline{w}_v$

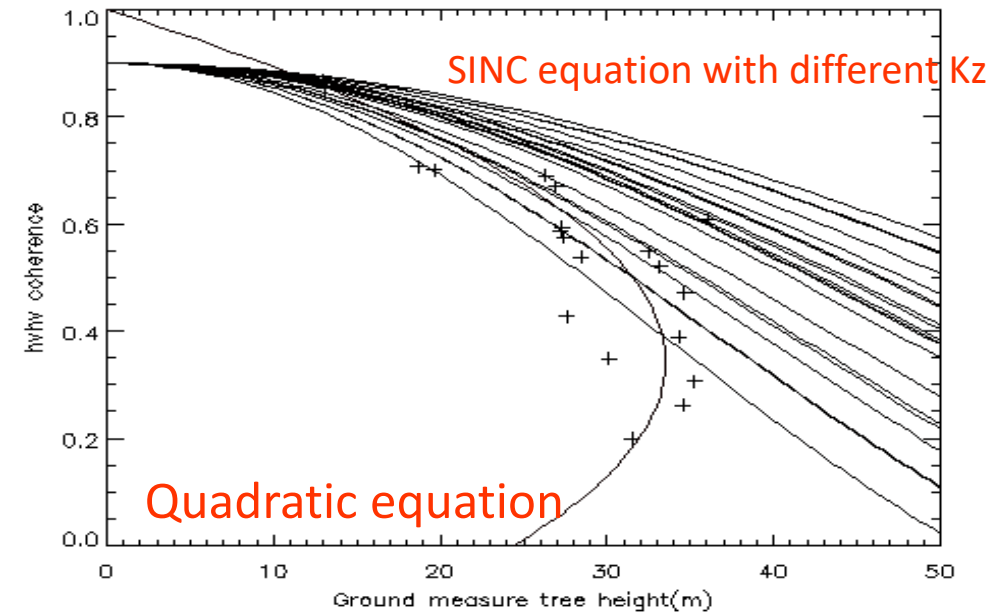
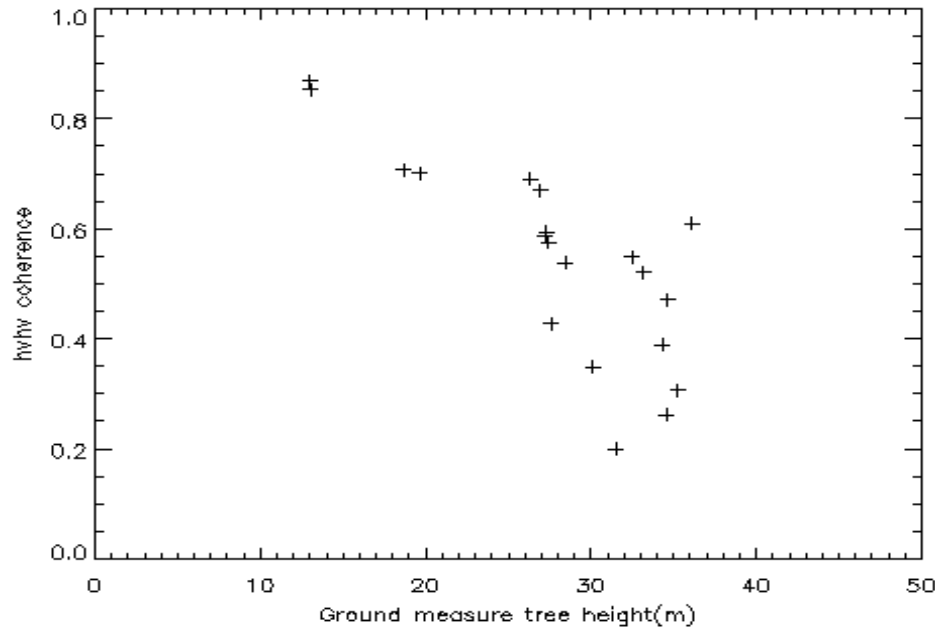
Method: Assuming uniform vertical distribution of scatterers with height  $h_v$

$$\gamma_{\underline{w}_v} = \lim_{\sigma \rightarrow 0} \left( \frac{\int_0^{h_v} e^{2\sigma z' / \cos \theta} e^{-ik_z z'} dz'}{\int_0^h e^{2\sigma z' / \cos \theta} dz'} \right) = e^{i\frac{1}{2}k_z h} \frac{\sin\left(\frac{1}{2}k_z h\right)}{\frac{1}{2}k_z h} \quad \Rightarrow \quad h_v = \frac{2 \cdot \text{sinc}^{-1}\left(|\gamma_{\underline{w}_v}|\right)}{k_z}$$

$$f(z) = \text{rect}\left(\frac{z}{h_v}\right)$$



# Understanding SINC inversion



The relationship between HV-HV coherence and tree height is really very good!

The relationship can be modeled by a clusters of SINC functions with different  $K_z$  value and a certain non-volumetric de-correlation factor

$$|\gamma| = 0.9 \cdot |\gamma_{w_v}|$$

$$h_v = \frac{2 \cdot \text{sinc}^{-1}(|\gamma_{w_v}|)}{k_z}$$

Input: Coherence image for  $\underline{w}_v$  and  $\underline{w}_s$

Method:

$$\mathbf{h}_v = \frac{\arg(\gamma_{\underline{w}_v}) - \hat{\phi}}{\mathbf{k}_z} + \varepsilon \frac{2 \cdot \text{sinc}^{-1}(|\gamma_{\underline{w}_v}|)}{\mathbf{k}_z}$$

where,

$$\hat{\phi} = \arg(\gamma_{\underline{w}_v} - \gamma_{\underline{w}_s} (1 - L_{\underline{w}_s})) \quad 0 \leq L_{\underline{w}_s} \leq 1$$

$$AL_{\underline{w}_s}^2 + BL_{\underline{w}_s} + C = 0 \Rightarrow L_{\underline{w}_s} = \frac{-B - \sqrt{B^2 - 4AC}}{2A}$$

$$A = |\gamma_{\underline{w}_s}|^2 - 1 \quad B = 2\text{Re}((\gamma_{\underline{w}_v} - \gamma_{\underline{w}_s}) \cdot \gamma_{\underline{w}_s}) \quad C = |\gamma_{\underline{w}_v} - \gamma_{\underline{w}_s}|^2$$



- Three stages SINC inversion

**Input: 11 coherence images:**

OPT1, OPT2, OPT3, HHHH, HVHV, VVVV, LLLL, LRLR, RRRR, PAULI-1, PAULI-2

**Method:**

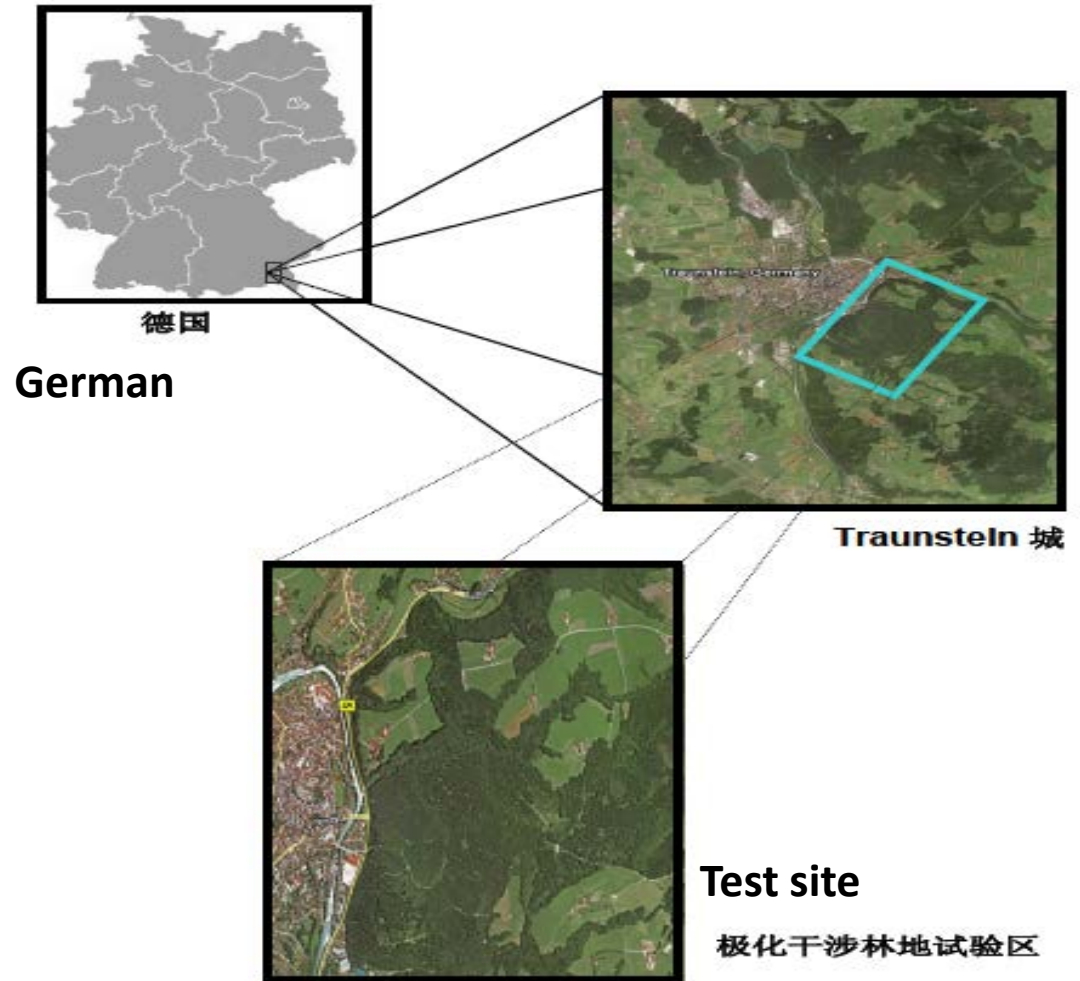
Stage 1: Line fitting and find the intersection point P1 and P2;

Stage 2: Find out the ground phase point and the coherence for  $\underline{w}_v$ ;

Stage 3: Use SINC function to get the tree height  $h_v$ .

$$h_v = \frac{2 \cdot \text{sinc}^{-1} \left( \left| \gamma_{\underline{w}_v} \right| \right)}{k_z}$$

- TREESAR Campaign Site: TRAUNSTEIN
  - Topography 600~650m;
  - Spruce, beech and fir.
- E-SAR POLinSAR data:
  - L-band repeat pass InSAR;
  - 3000m above ground;
  - Incidence angle: 25~60deg;
  - SLC resolution: 1.5m\*3m;
  - 5m spatial baseline;
  - 20 minutes temporal baseline.



Master



20031011, 9:00

Slave



20031011, 8:40

©DLR

1414width\*4642lines



# Ground true data

Mean Forest height  
(h100)

36.1m

13.0m



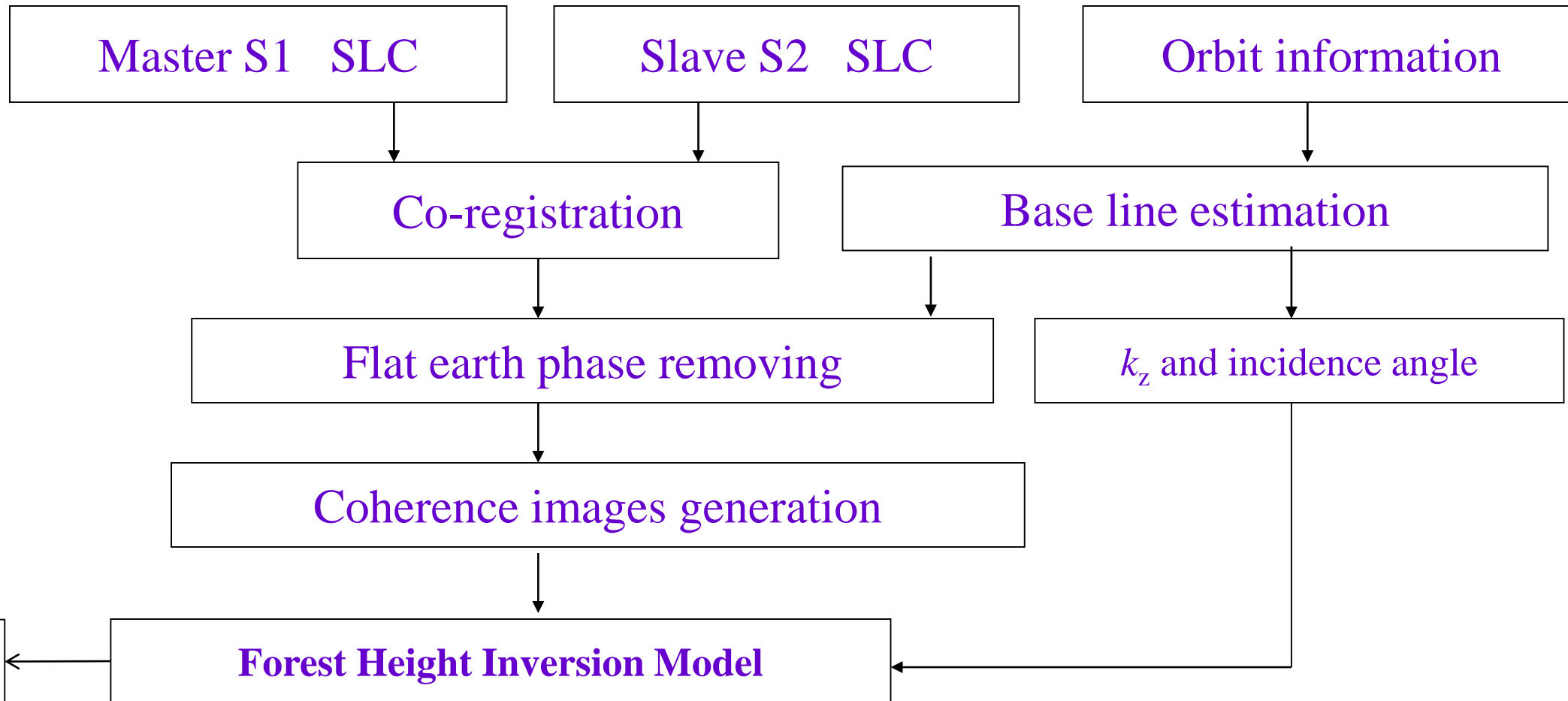
Biomass  
(ton/ha)

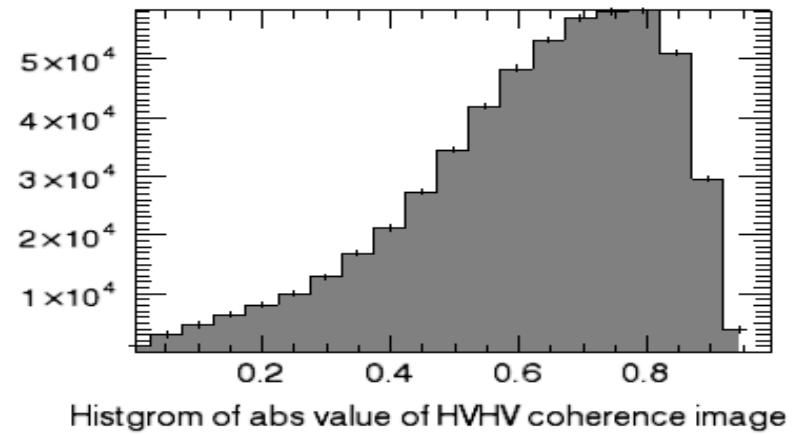
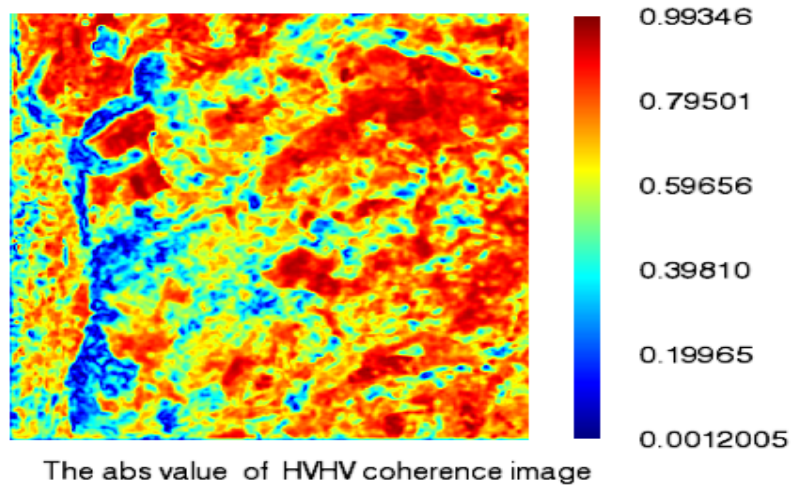
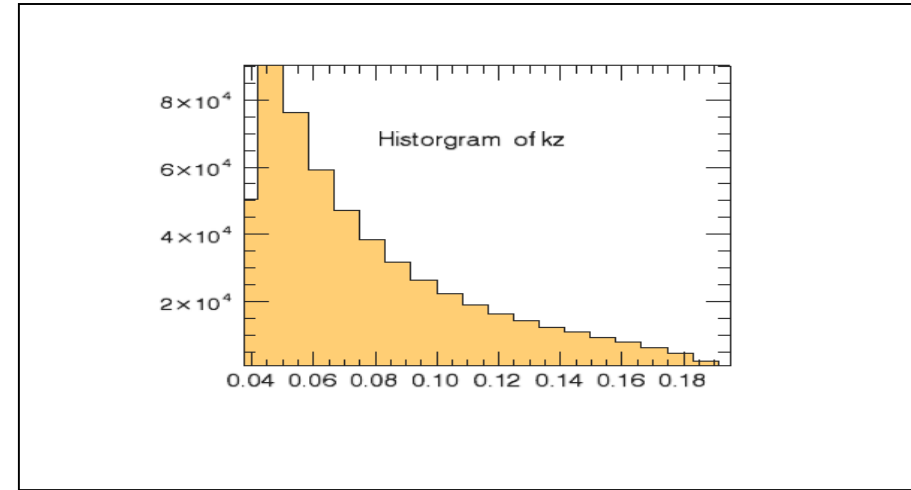
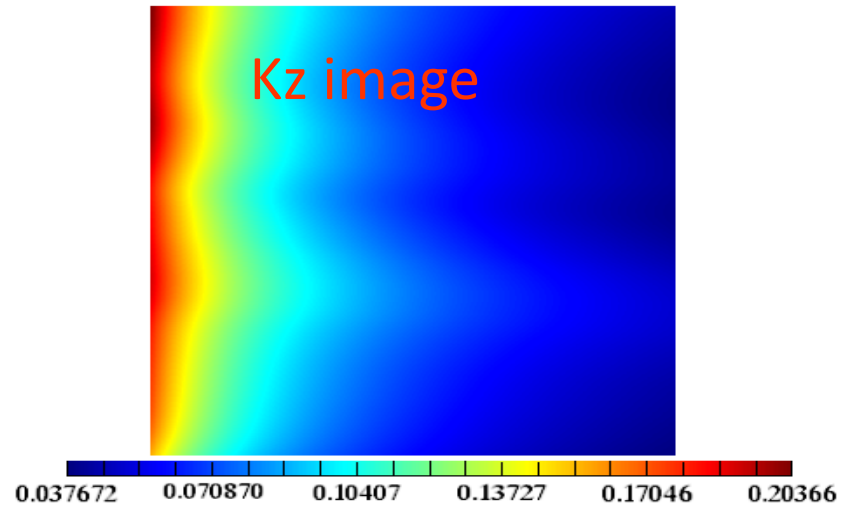
445.2

38.7

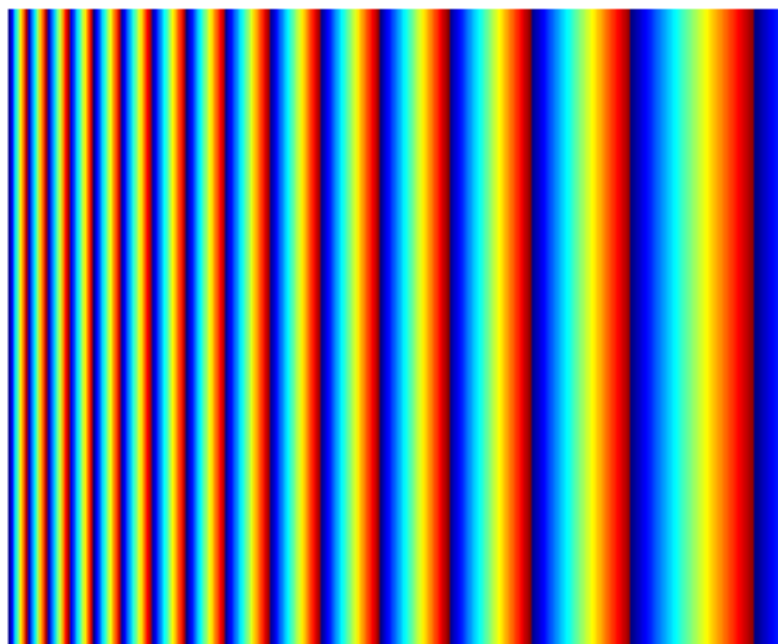


## •InSAR processing route

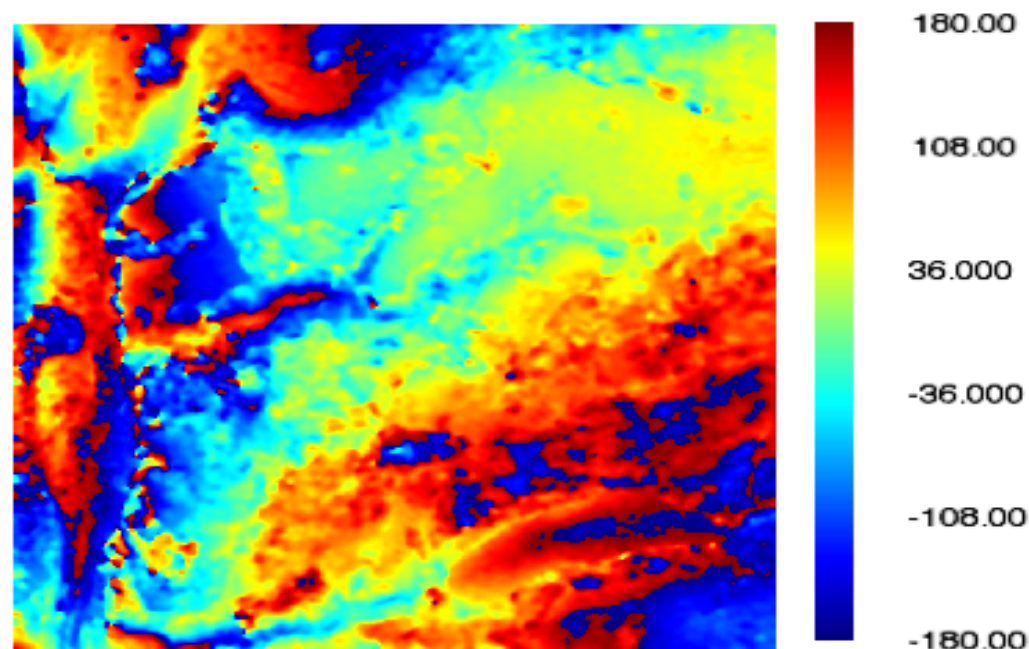
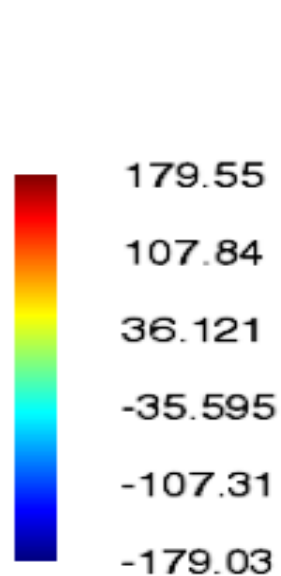




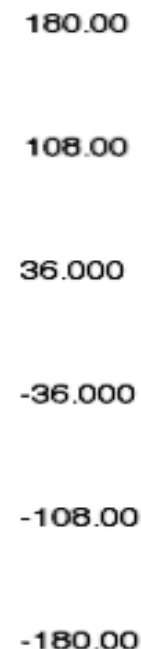


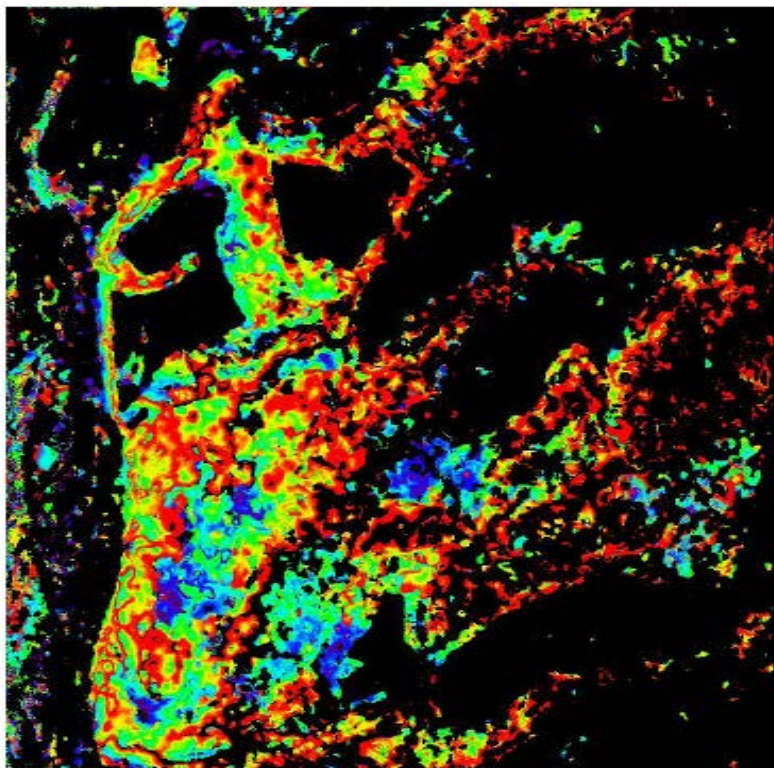


Flat earth phase (degree)

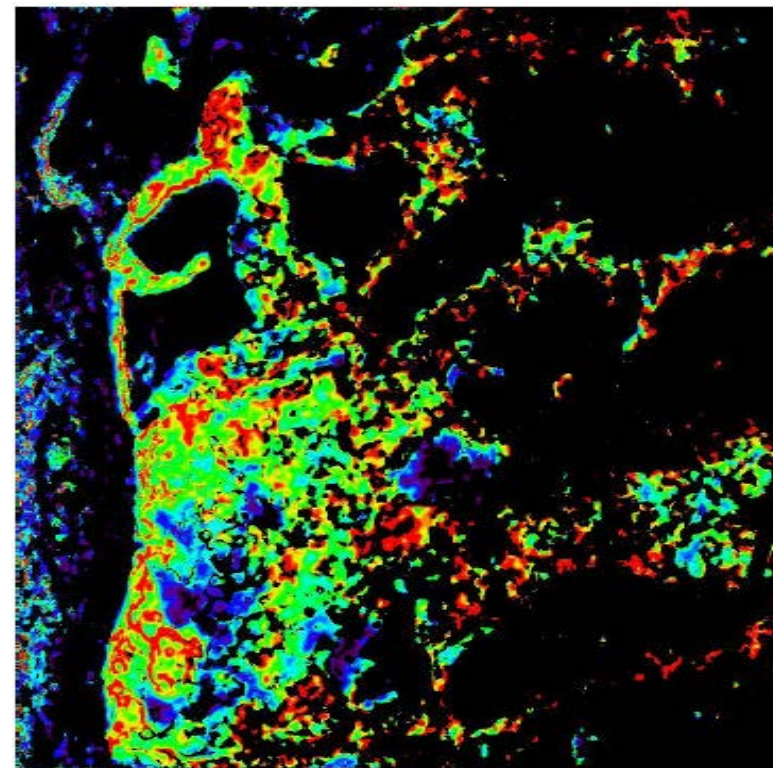


Phase of HVHV coherence image after earth phase flattening



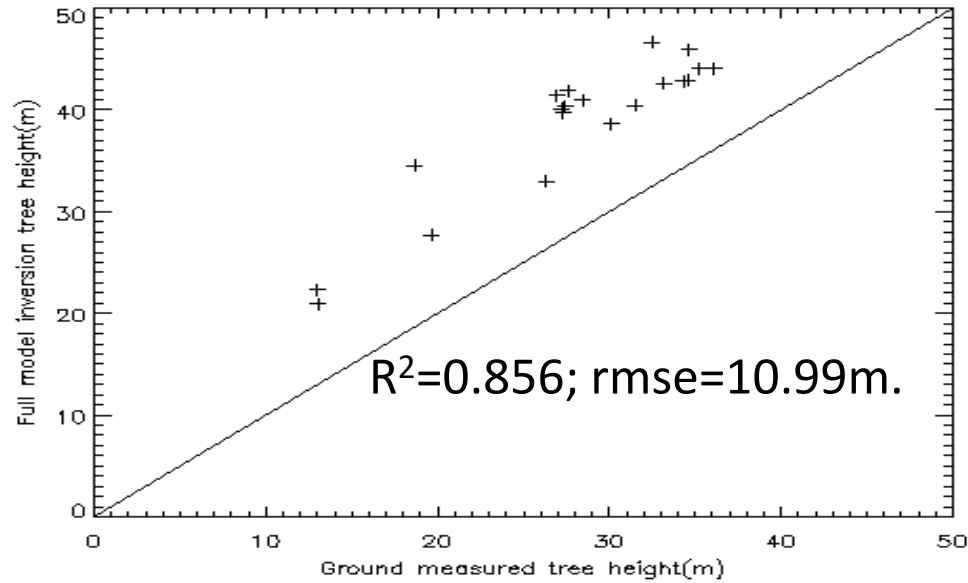


Forest height from three-stage full model inversion

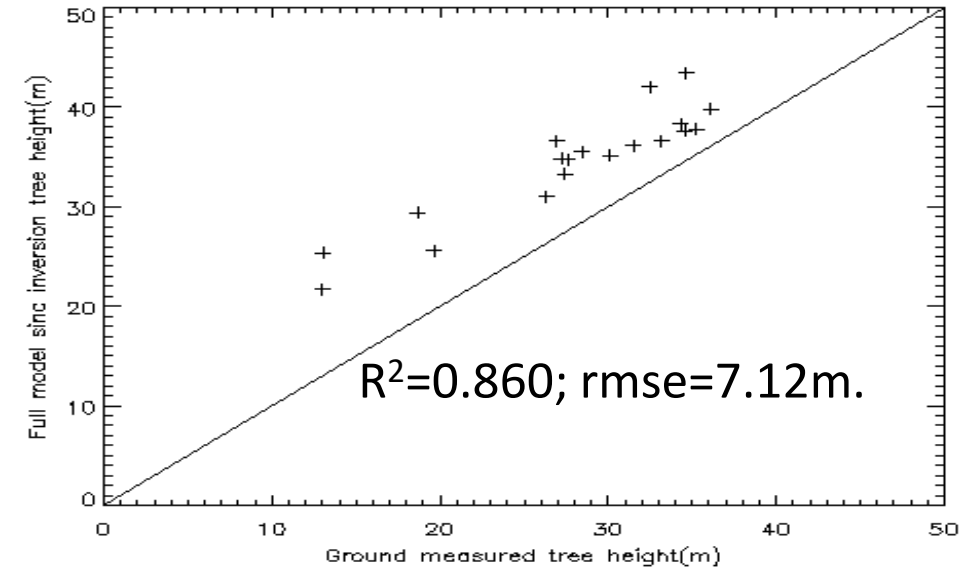


Forest height from three-stage SINC inversion

• Three stages 2D LUT inversion



• Three stages SINC inversion



The error/bias can be calibrated or corrected with some ground truth



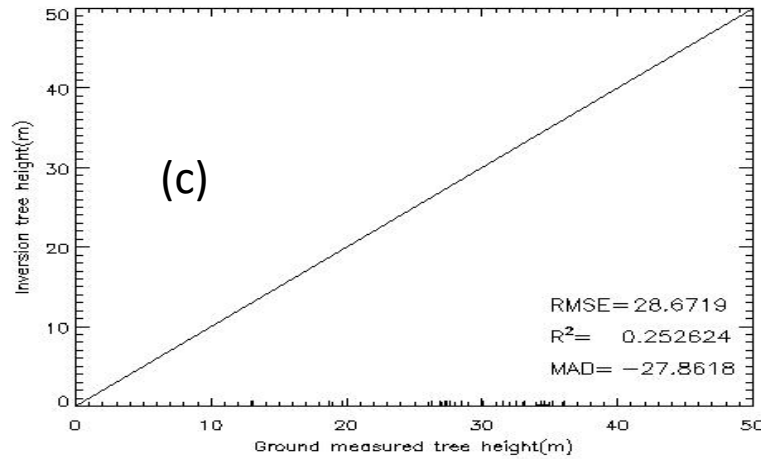
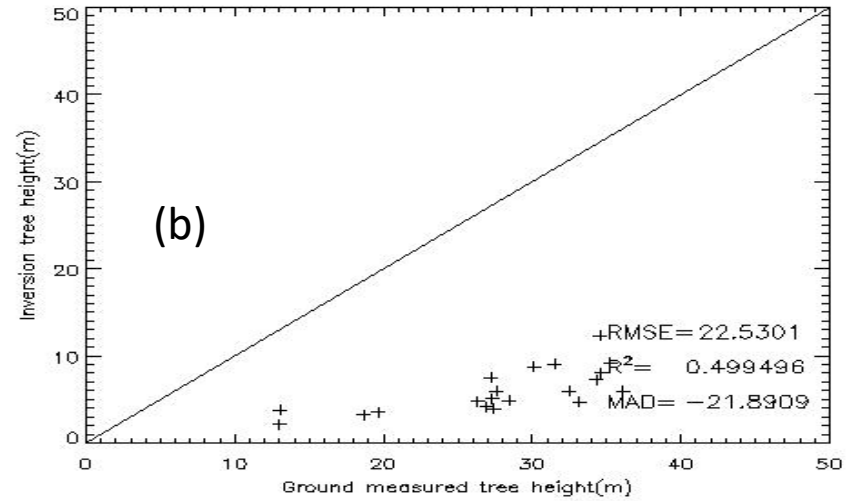
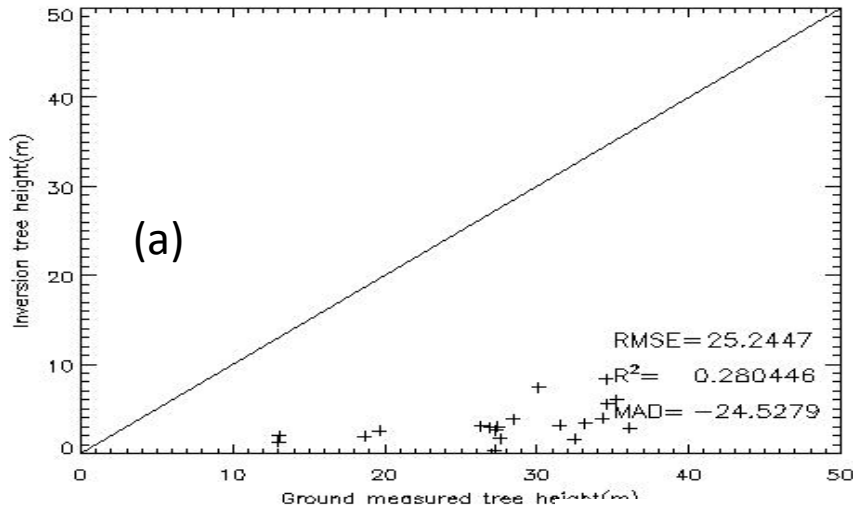
# Applying coherence optimization to forest height inversion

- **The following coherence optimization methods validated:**

- ✓ Phase diversity (PD) (M. Tabb, J. Orrey, et al., 2002)
- ✓ Maximization of the magnitude difference (BF-mag) (M. Lavalley, et al., 2007)

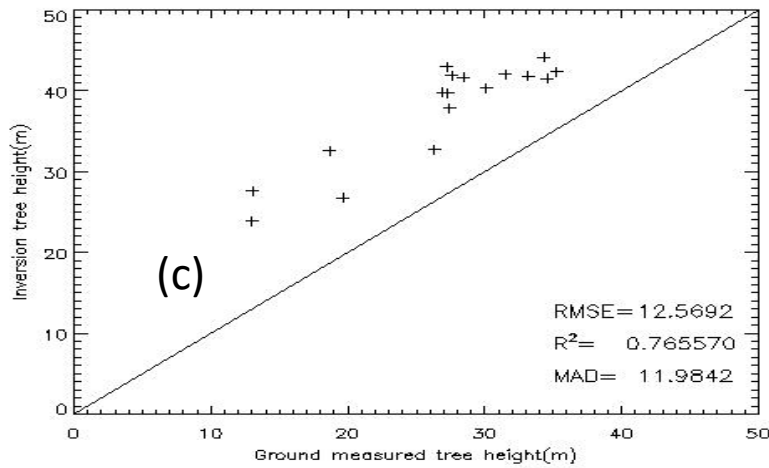
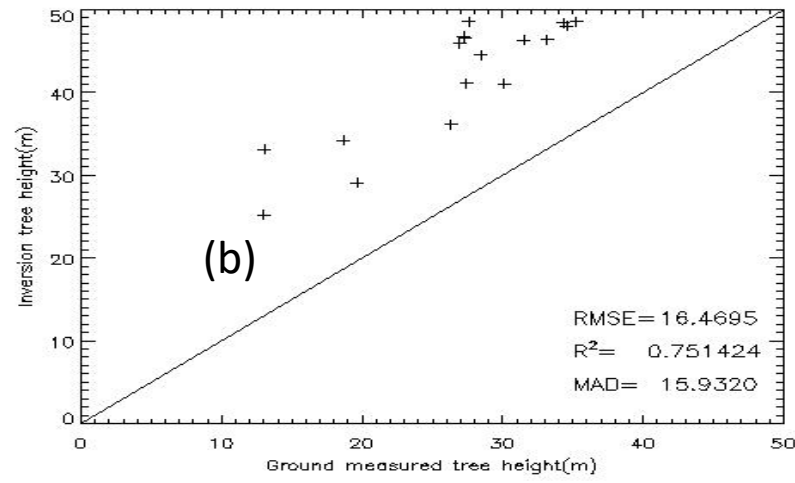
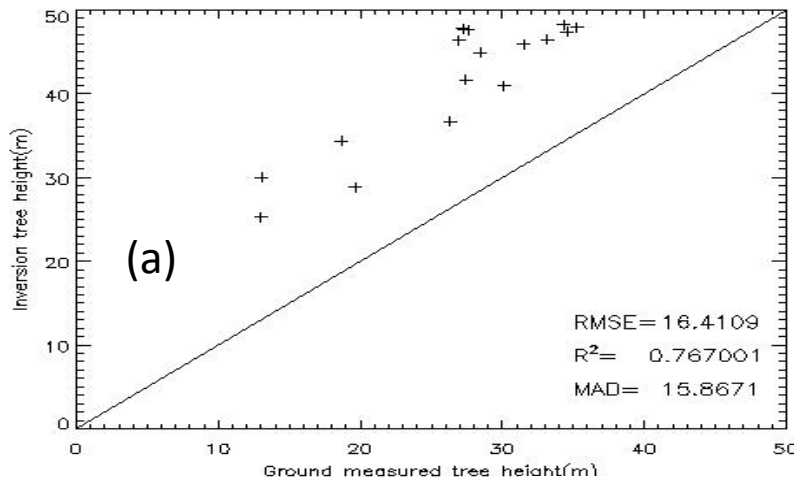
- **Three kinds of inversion methods compared:**

- ✓ Using phase difference only
- ✓ Applying SINC inversion to coherence amplitude
- ✓ Hybrid inversion with both phase difference and amplitude



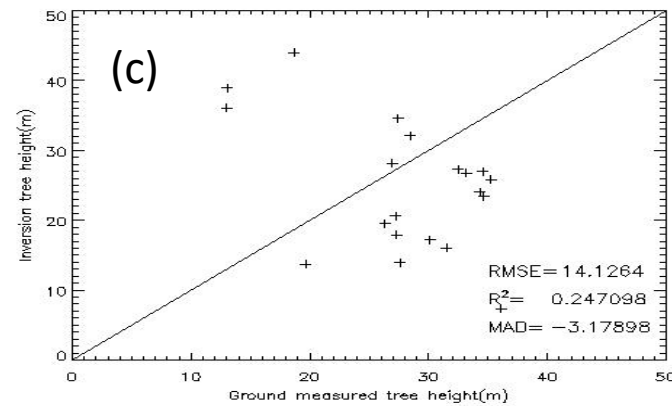
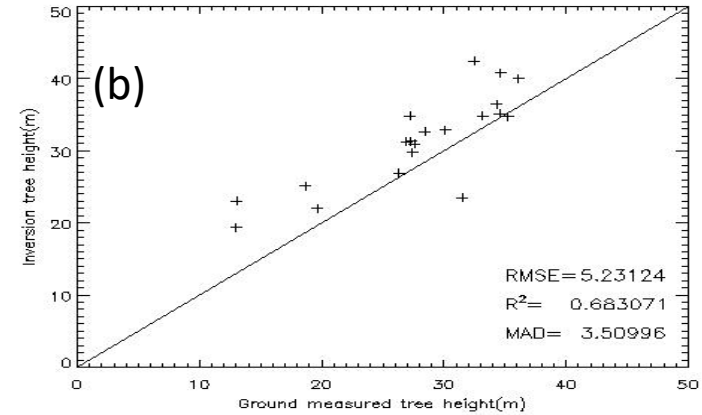
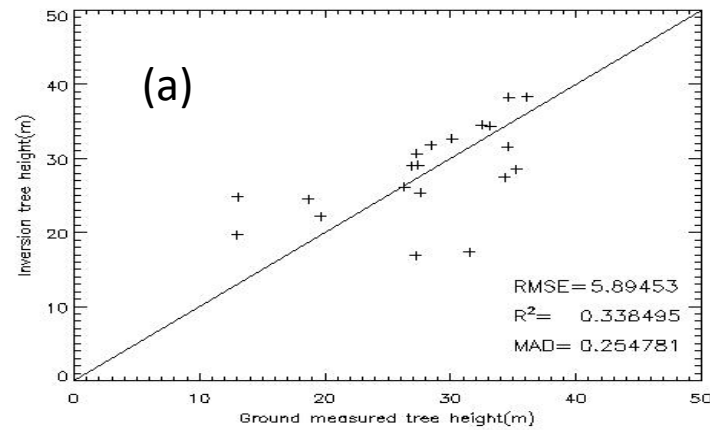
(a) HV, HH-VV channel    (b) PD channel    (c) BF-Mag channel

# Applying SINC inversion to coherence amplitude



(a) HV channel      (b) PD high phase center channel      (c) **BF-Mag maximum** coherence magnitude difference channel





(a) HV channel

(b) PD channel

(c) BF-Mag channel

# Outlines

## 1. Introduction

1.1 Forest application requirement and some concepts

1.2 Quantitative remote sensing inversion model for Bio-physical parameters

1.3 Model training and accuracy validation

## 2. PolSAR/PolinSAR forest structure parameter inversion model and its application

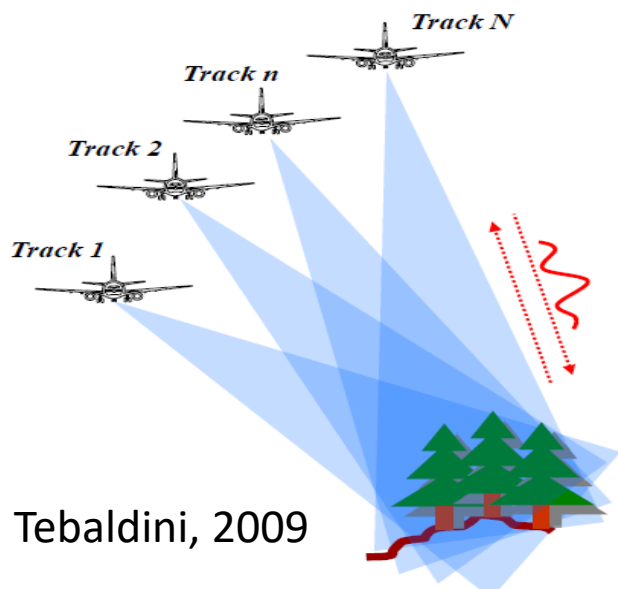
2.1 PolSAR forest biomass estimation with an empirical model

2.2 Single baseline PolinSAR forest height and above ground biomass inversion

**2.3 Multi-baseline PolinSAR tomography for forest vertical structure information extraction**

# Multi-baselines PolInSAR Tomography

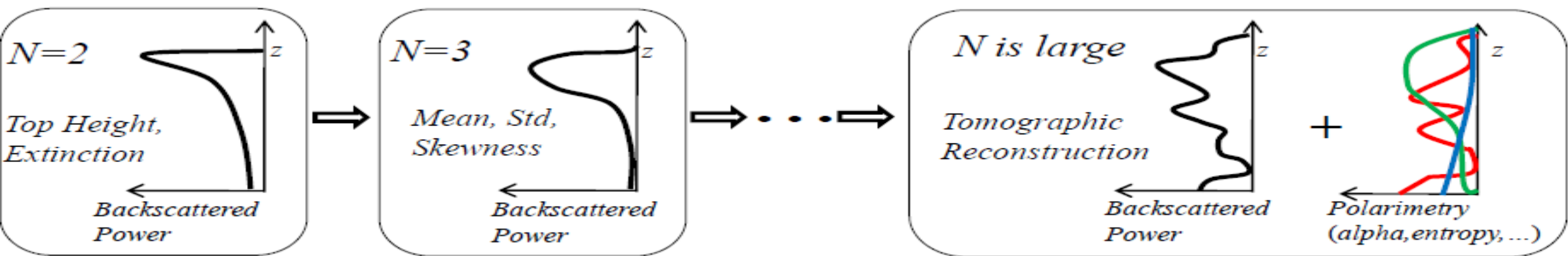
## 多基线极化干涉层析



### 相对于单基线的优势:

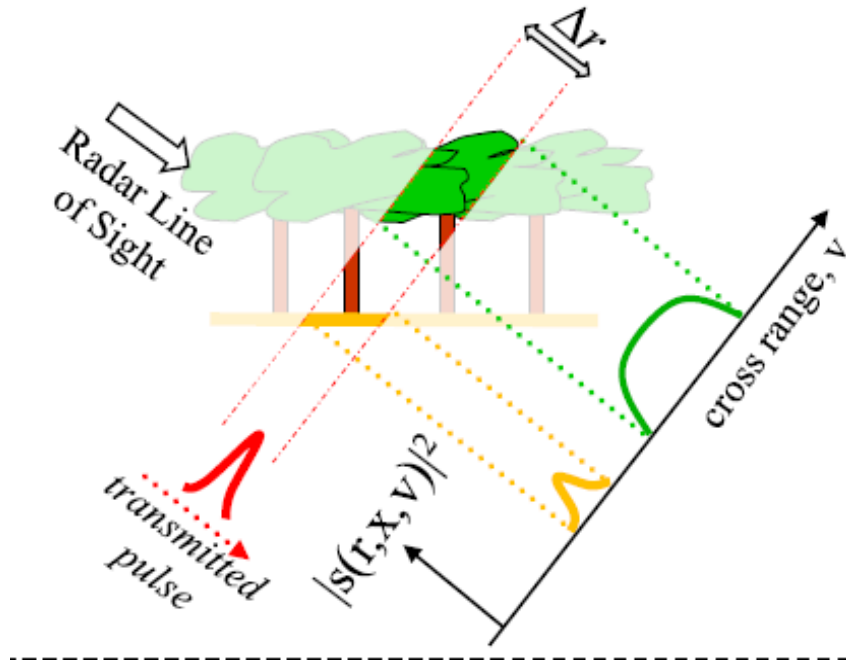
#### Advantage of multi-baselines

- ✓更多的观测，更多的方程 More observations, more functions can be solved
- ✓可解参数增多，用于刻画更精细的垂直结构 More Unknown parameters solved, more detailed structure information
- ✓可增强反演稳健性，如对时间去相干的抵抗增强 Increase the robust, eg. combat temporal decorr.
- ✓减少单基线所需的假设条件 Less assumptions





# (1) Spectral analysis based multi-baseline SAR tomography



每个聚焦的SLC SAR影像可认为是通过在垂直于斜距方向的复反射率函数的傅里叶变换得到的:

$$y_n(r, x) = \int s(r, x, v) \exp\left(-j \frac{4\pi}{\lambda r} b_n v\right) dv$$

$y_n(r, x)$  : SLC pixel in the  $n$ -th image

$s(r, x, v)$ : average complex reflectivity of the scene within the SAR 2D resolution cell at  $(r, x)$

$b_n$  : normal baseline for the  $n$ -th image

$\lambda$  : carrier wavelength

形成多基线观测矢量

$$\mathbf{y}_{MB} = \begin{bmatrix} y_1(r, x) \\ y_2(r, x) \\ \vdots \\ y_N(r, x) \end{bmatrix}$$

多视干涉相干矩阵

$$\hat{\mathbf{R}} = \langle \mathbf{y}_{MB} \mathbf{y}_{MB}^H \rangle_L$$

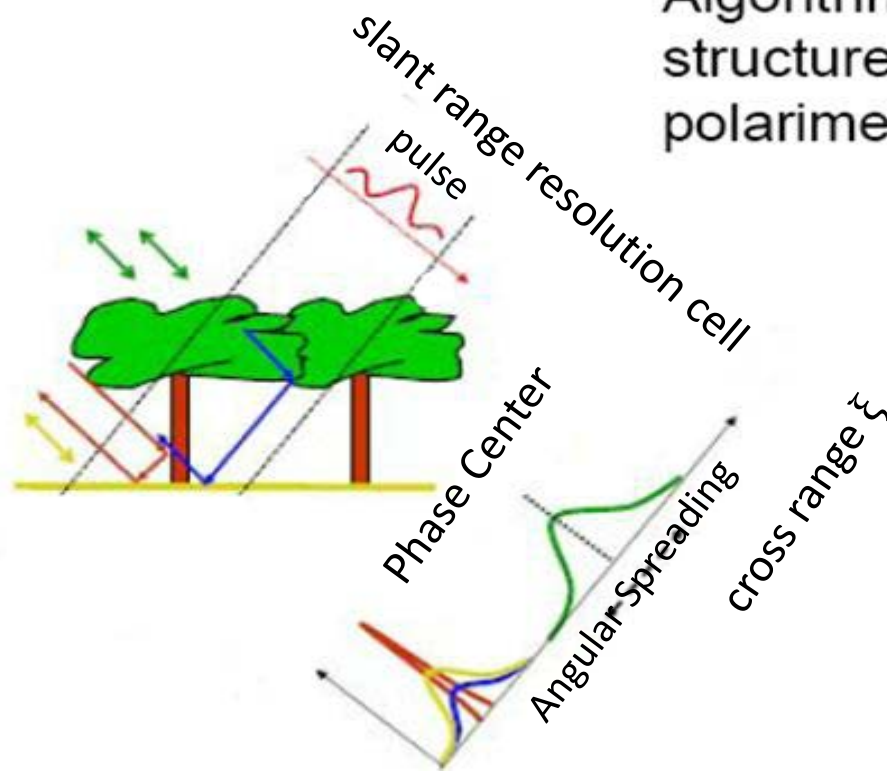
$$\{\mathbf{R}\}_{nm} = \frac{E[y_n y_m^*]}{\sqrt{E[|y_n|^2] E[|y_m|^2]}} = \gamma_{nm}$$

通过谱估计算法得到垂直于斜距向的后向散射能量分布

$$|\hat{s}(r, x, v)|^2 = \hat{S}(v)$$

Beam Forming, Capon, MUSIC

## AS: Algebraic Synthesis



## SAR Tomography (T-SAR)

Algorithm to characterise forest structure using multi-baseline, polarimetric SAR data

$$\text{SKP} : \mathbf{W} = E [\mathbf{y}\mathbf{y}^H] = \sum_k^{K_T} \mathbf{C}_k \otimes \mathbf{R}_k$$

Tomography processing steps :

- Covariance Estimation
- SKP Decomposition
- Algebraic Synthesis of Ground Structure
- Ground Phase Estimation
- Algebraic Synthesis of Volume Structure
- Tomographic Analysis

SKP: Sum of Kronecker product

representation of Fourier Spectra associated to four scattering mechanisms

Tebaldini, 2009

Tebaldini, S.; Rocca, F., Multibaseline Polarimetric SAR Tomography of a Boreal Forest at P- and L-Bands, IEEE. Geoscience & Remote Sensing, 2012, 50(1): 232-246

$$W = C_g \otimes R_g + C_v \otimes R_v$$

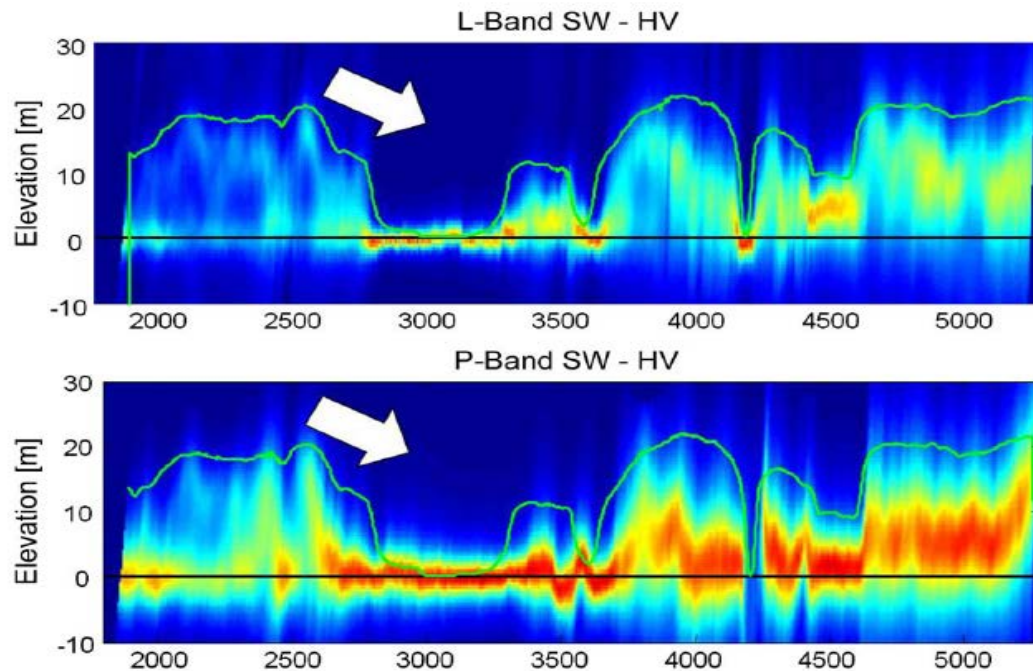
W: the n baseline polarimetric covariance matrix

$C_g$ : ground covariance matrix among different polarizations

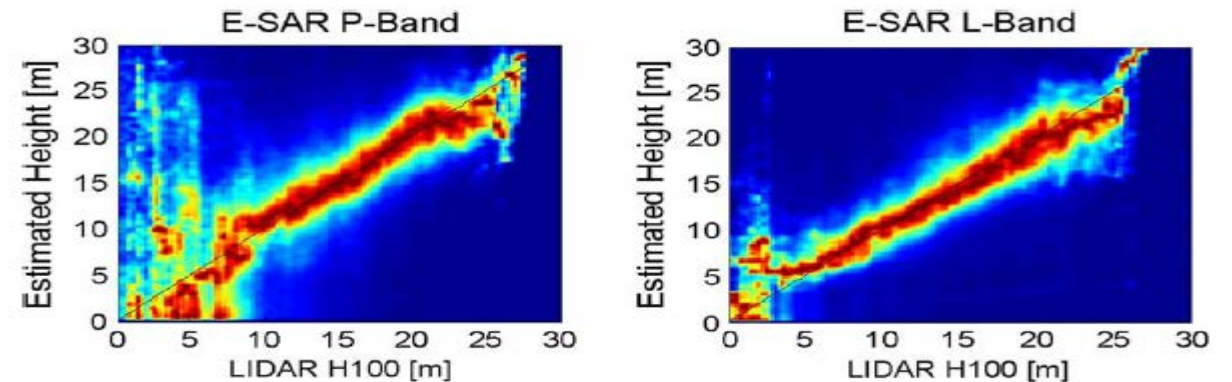
$R_g$ : ground InSAR coherence matrix among different tracks

$C_v$ : volumetric covariance matrix among different polarizations

$R_v$ : volumetric InSAR coherence matrix among different tracks



Forest height estimation accuracy validated with LiDAR forest height

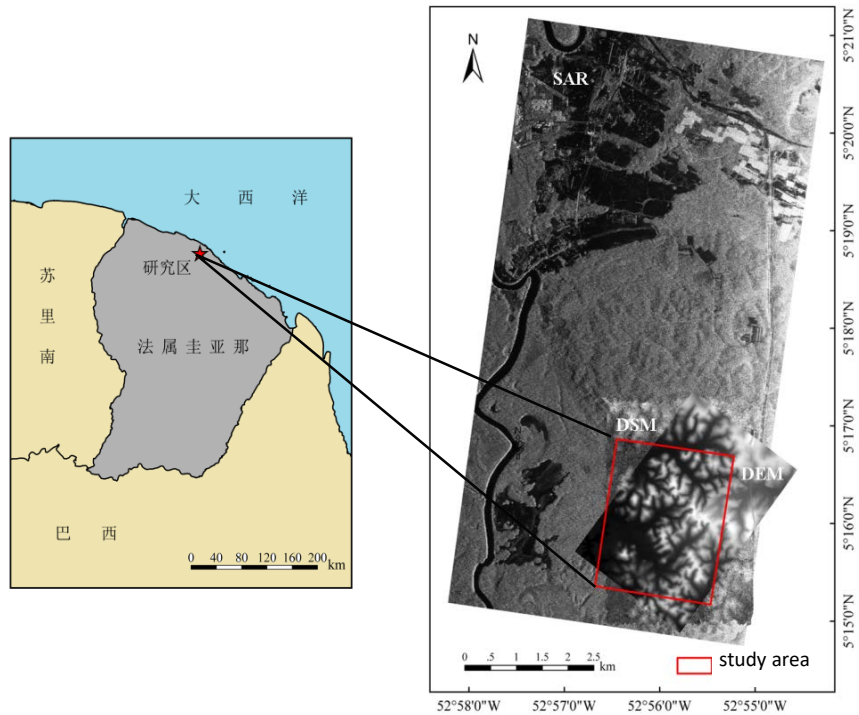


Airborne SAR data from BioSAR 2008



# Forest Above Ground Biomass Estimation from P-band Tomography Data

## Study area-Paracou, French Guyana



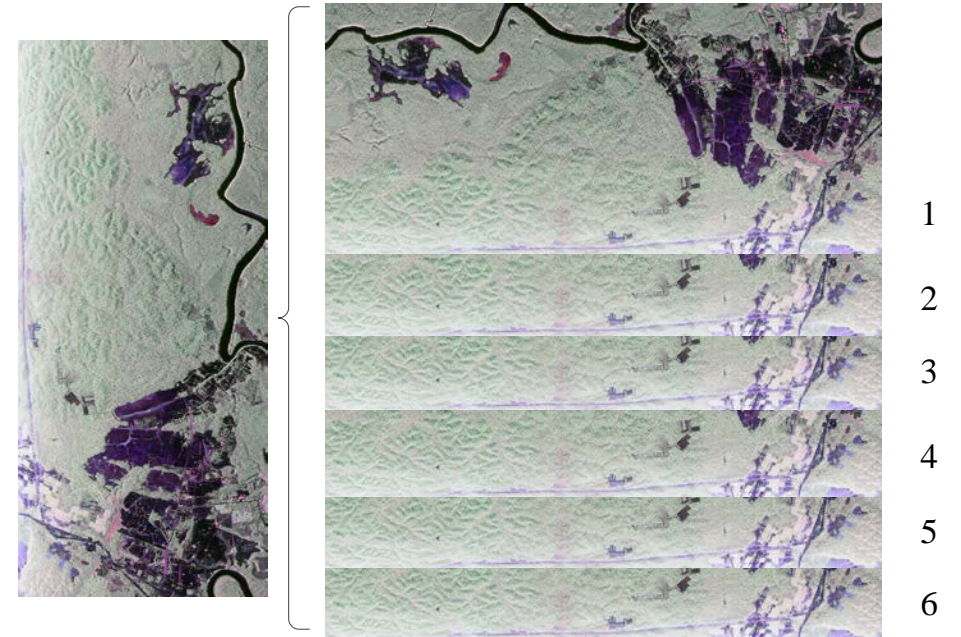
Location of the test site and the coverage area of SAR/LiDAR data

- ❖ Location: a lowland tropical rain forest
- ❖ Landscape: a patchwork of small hills
- ❖ Elevation: 5-50 m
- ❖ Forest canopy height: 20-45m
- ❖ Biomass: 200 -500 t·hm<sup>-2</sup>

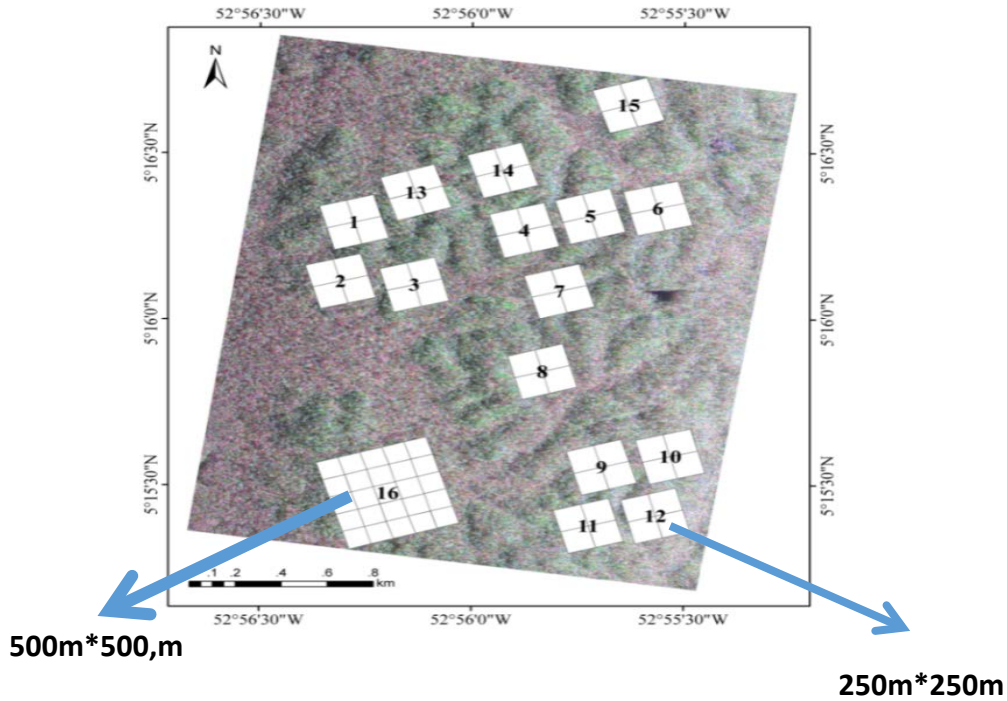
# Study data- TropiSAR 2009 airborne data

## ❖ Multi-baseline PolInSAR data:

- ✓ ONERA SETHI SAR system
- ✓ Flight height: 3962m
- ✓ P-band, fully polarizations
- ✓ Resolution is 1 m in slant range and 1.245 m in azimuth direction
- ✓ 6 tracks with average spatial baseline of 15 m
- ✓ Temporal baseline: 2h
- ✓ Date: Aug. 2009



# Study data- in situ forest AGB



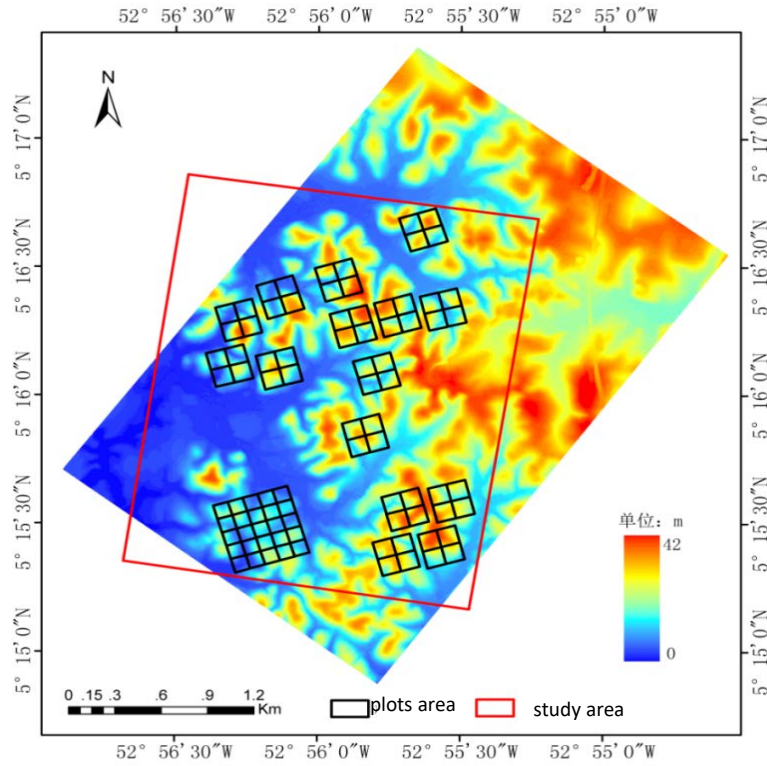
## ❖ Forest AGB data:

- ✓ 16 permanent forest plots
- ✓ 85 independent subplots

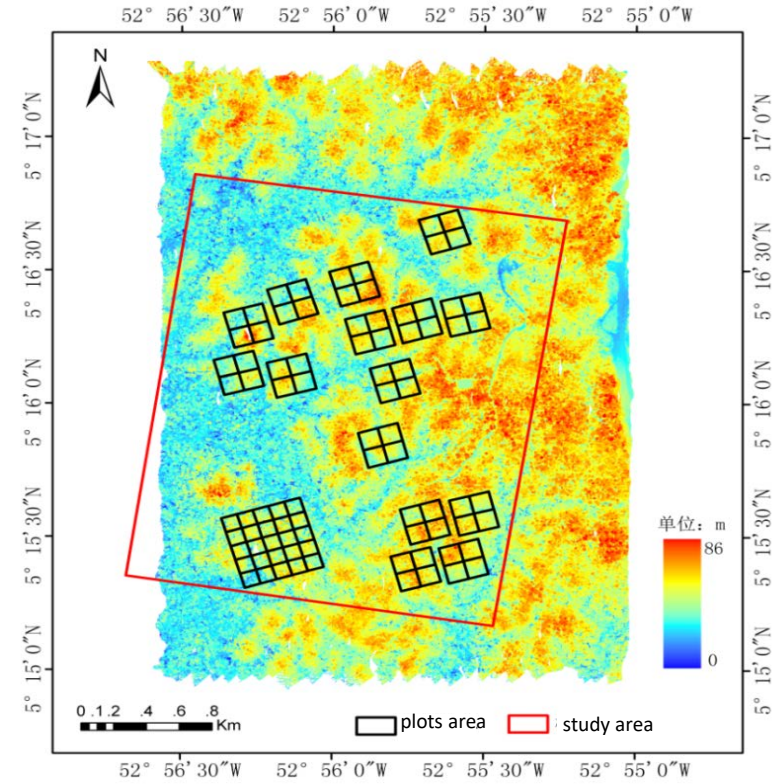
Plot No.	Forest AGB (t·hm <sup>-2</sup> )	Plot No.	Forest AGB (t·hm <sup>-2</sup> )	Plot No.	Forest AGB (t·hm <sup>-2</sup> )
1	315.23	30	257.24	59	434.35
2	341.52	31	265.99	60	430.95
3	372.59	32	256.70	61	359.84
4	449.15	33	327.13	62	424.98
5	334.66	34	337.86	63	392.67
6	310.92	35	365.02	64	407.41
7	318.69	36	320.09	65	419.96
8	421.61	37	277.15	66	390.67
9	304.49	38	297.58	67	455.83
10	285.31	39	333.78	68	372.16
11	358.88	40	321.43	69	435.19
12	287.34	41	405.47	70	402.44
13	297.81	42	385.09	71	473.52
14	305.31	43	407.40	72	342.81
15	270.79	44	412.93	73	424.14
16	264.79	45	312.17	74	406.25
17	318.51	46	315.63	75	371.43
18	300.01	47	298.85	76	433.59
19	305.21	48	290.73	77	365.39
20	278.46	49	400.48	78	382.44
21	495.42	50	385.71	79	371.51
22	463.65	51	384.36	80	442.23
23	395.89	52	450.56	81	453.50
24	372.69	53	445.56	82	391.43
25	369.41	54	400.37	83	381.65
26	426.96	55	423.16	84	386.99
27	386.24	56	361.57	85	464.37
28	386.87	57	388.68		
29	249.90	58	417.14		



# Study data- LiDAR DEM and DSM

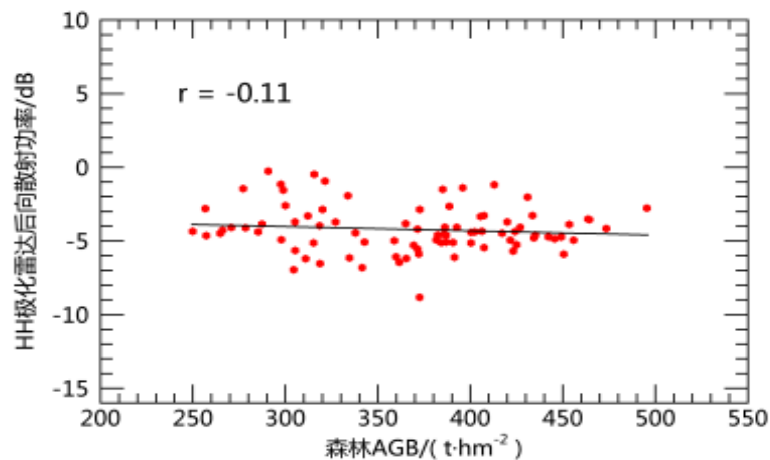


LiDAR DEM

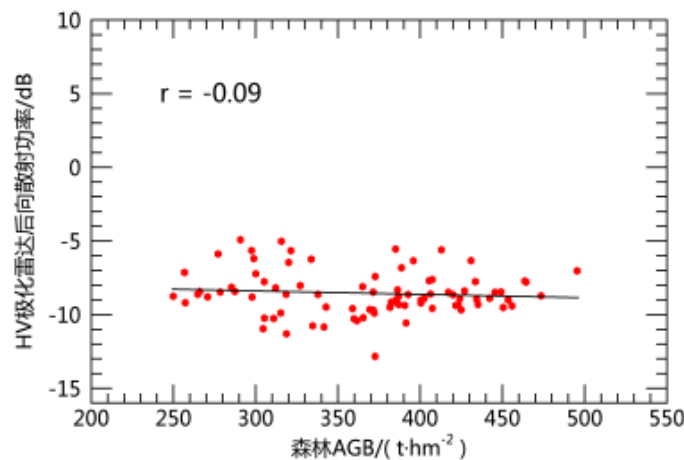


LiDAR DSM

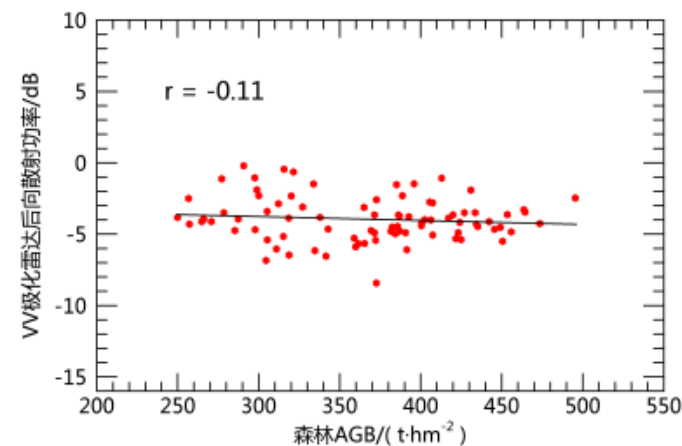
## P-band intensity of each polarization is not sensitive to forest AGB



HH

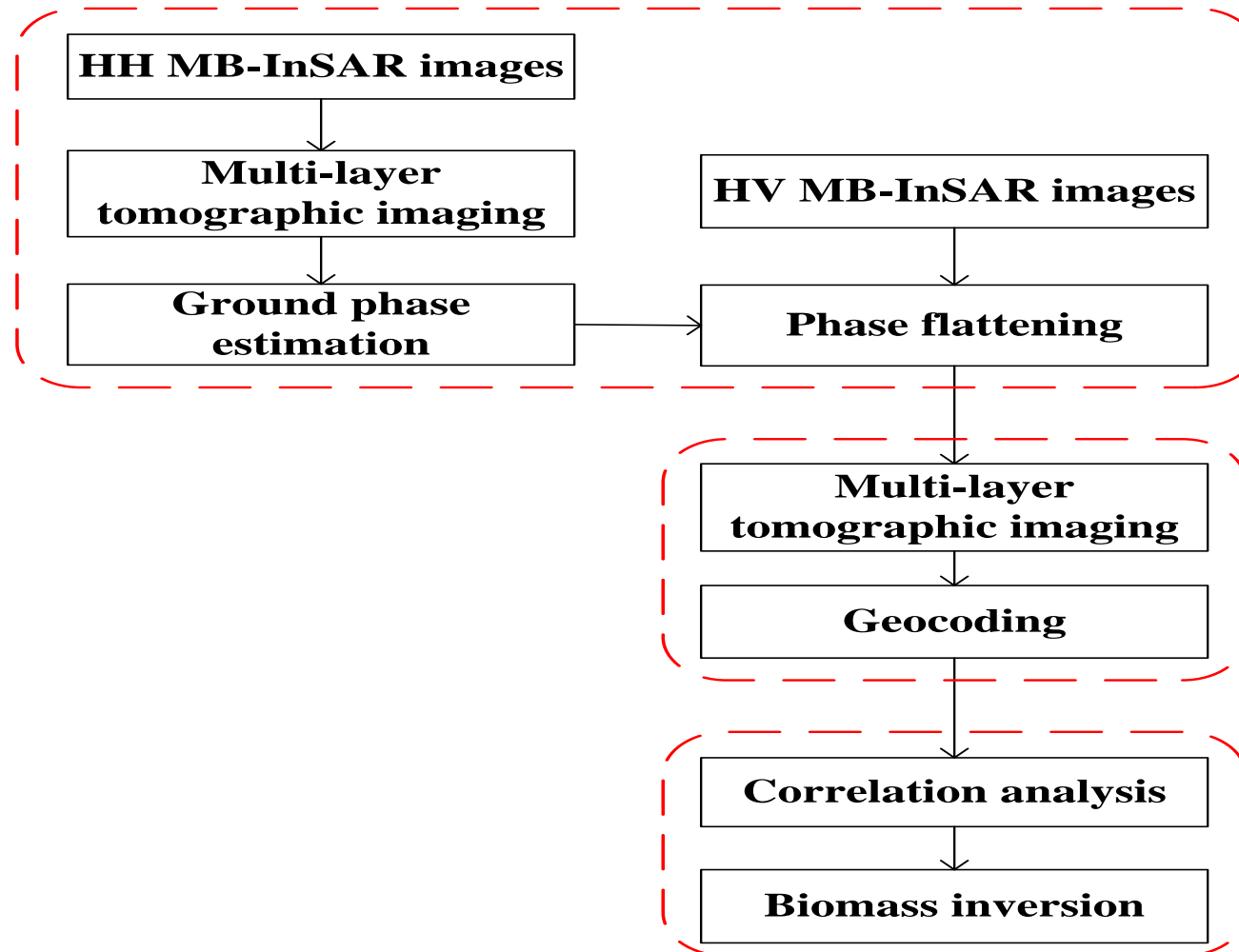


HV



VV

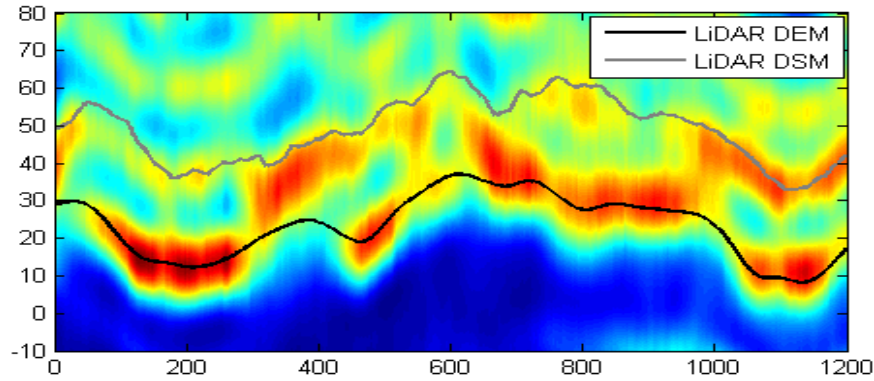
# Methodology - flow chart



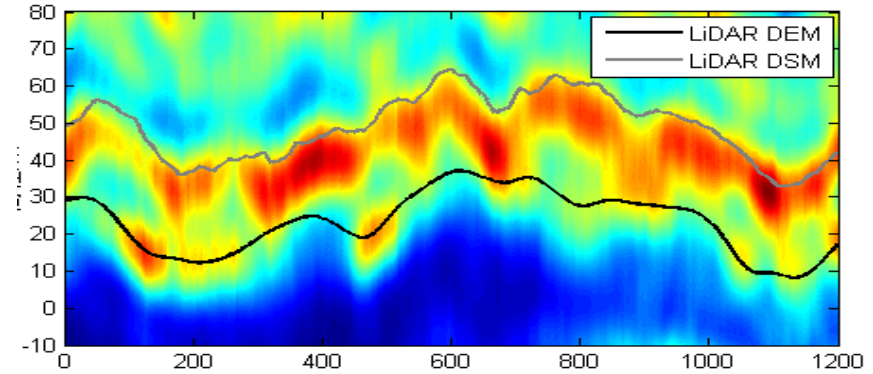
Beamforming spectral estimator



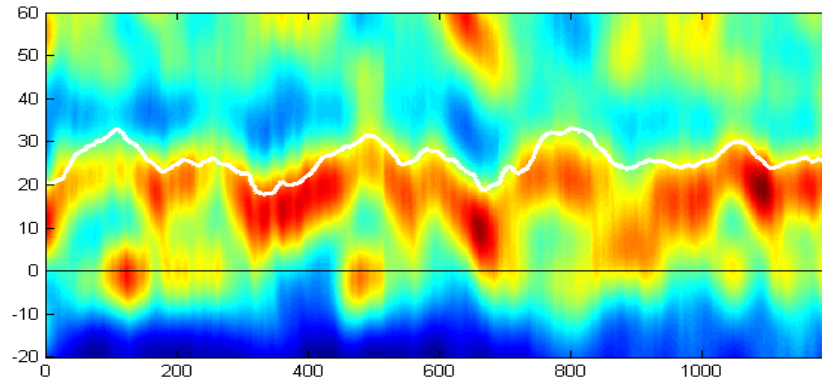
# Results - results from tomography



Backscatter profile of HH polarization before phase flattening

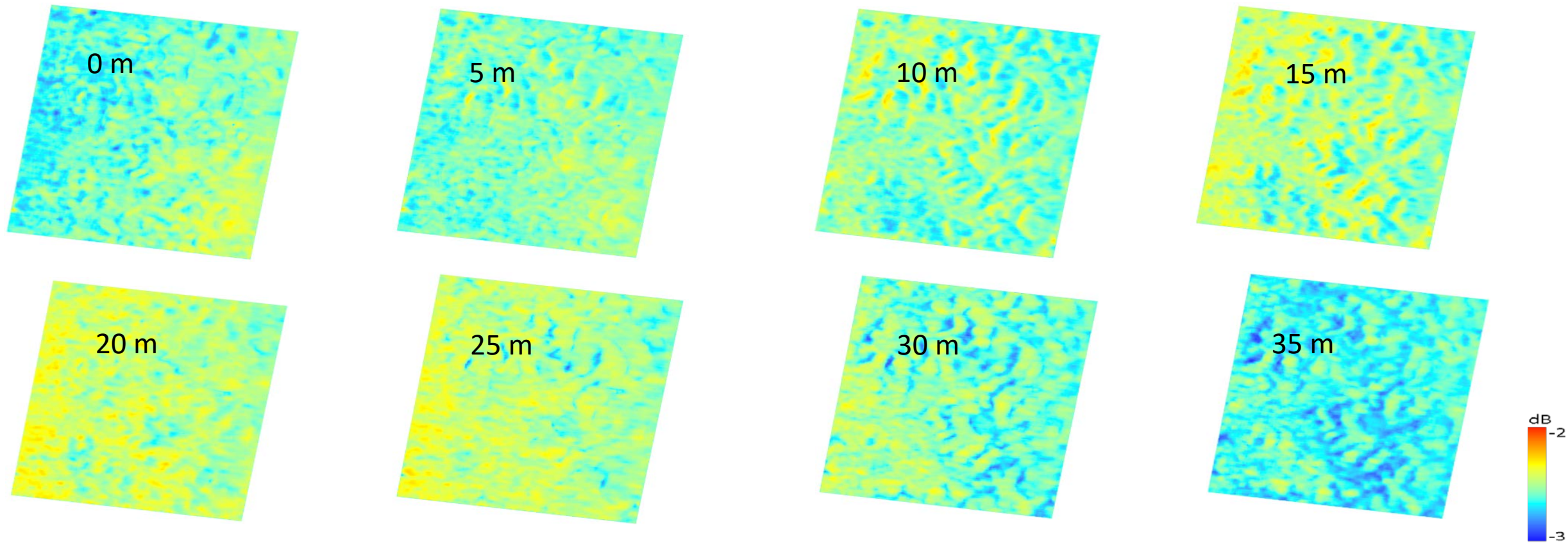


Backscatter profile of HV polarization before phase flattening

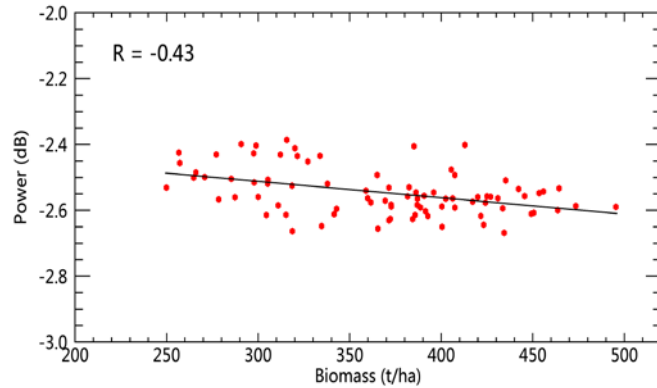


Backscatter profile of HV polarization after phase flattening

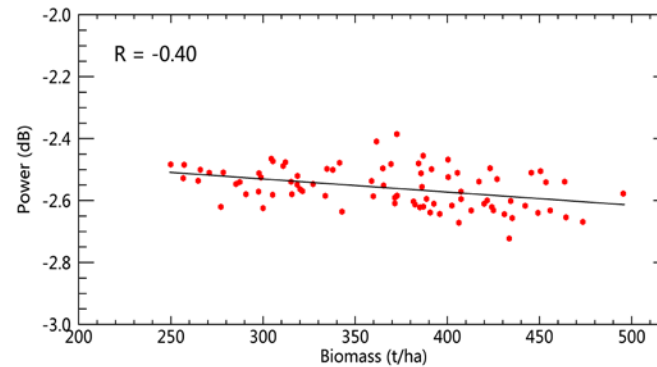
## Results - tomographic relative reflectivity at different heights after geocoding



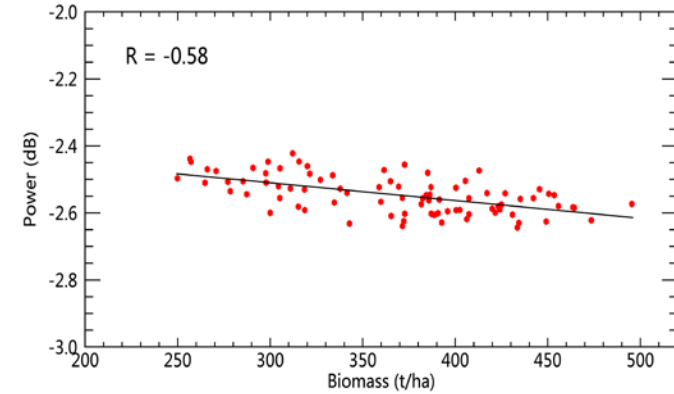
# Results - linear regression



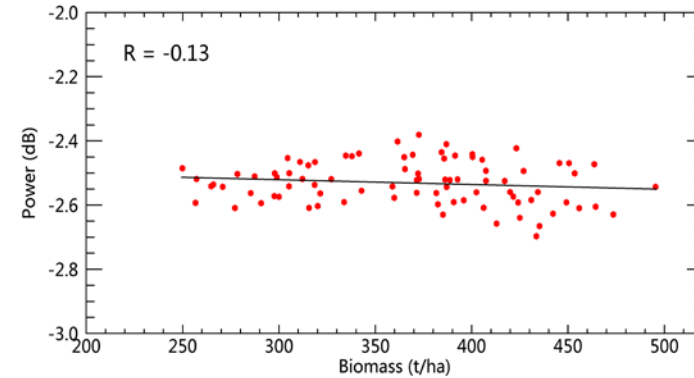
0 m



10 m



5 m

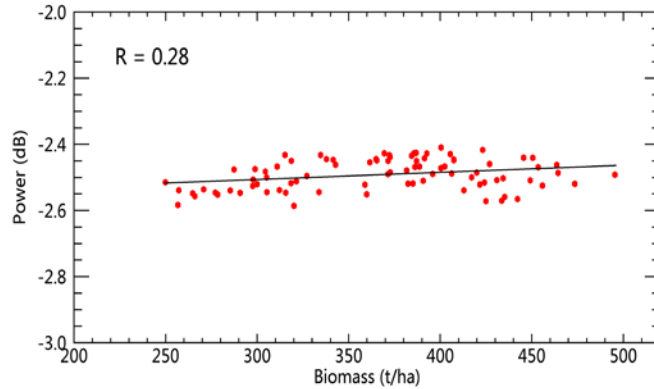


15 m

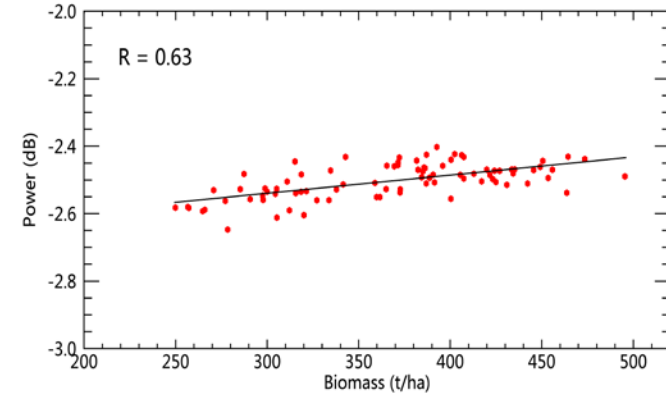
**Negative correlation for the layers below 20 m.**



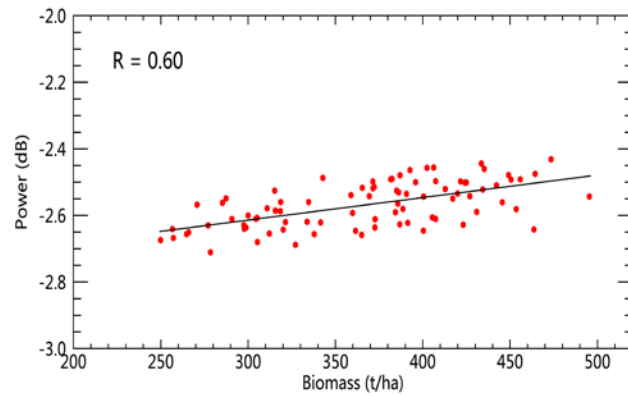
# Results - linear regression



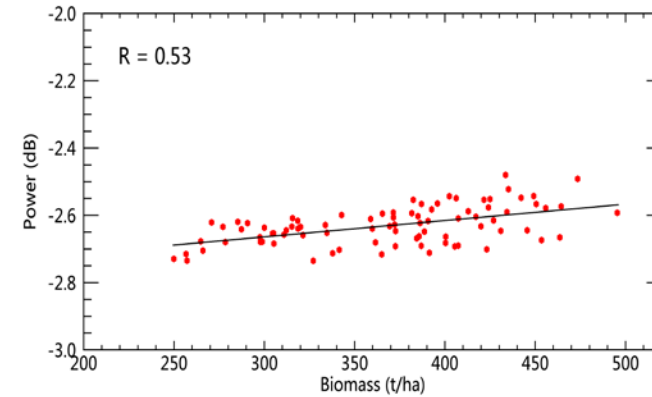
20 m



25 m



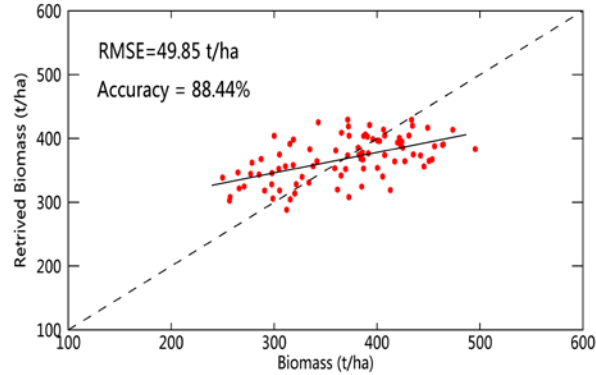
30 m



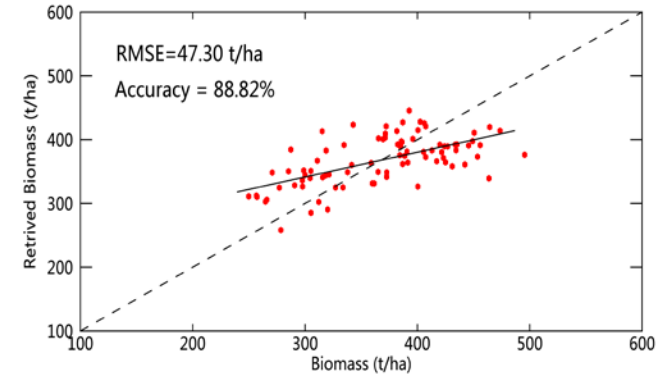
35 m

**Positive correlation for the layers between 20 m and 40 m.**

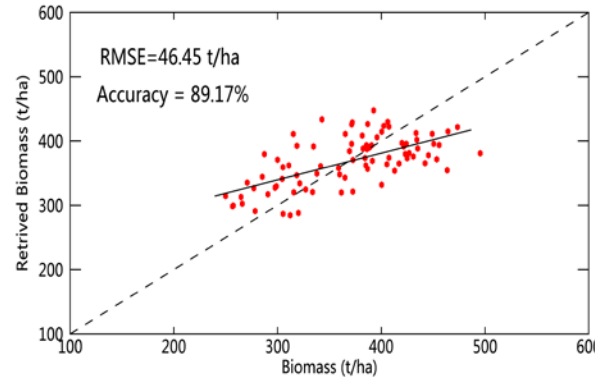
# Results - biomass inversion



Cross-validation for the layer at 5-m



Cross-validation for the layer at 25-m



Cross-validation for the combined layers with 5-m and 25-m



**The AGB estimation model was refined by combining 5-m and 25-m layers.**

## III. Current Limitation and developing trends



# Current limitations

- **Topography problems**

- Most of the wonderful PolSAR and PolInSAR demos for forest applications are in the test sites of relative flat topography;
- More work should be carried out for more complex forest regions, more rough topography and more complex forest structure.

# Current limitations

- **Vertical structure information accuracy**
  - We need multi-baseline InSAR observation of the same forest area
  - It is expensive for airborne system and very difficult for space-borne system currently
- **From “relative reflectivity profile” to forest parameters**
  - The SAR tomography profile is difficult for validation, few studies on it
  - How to link the profile information to real forest parameters: volume density, above ground biomass, LAI etc. needs to be further studied

# Developing trends

- Key Space-borne SAR system
  - TerraSAR-X(June, 2007)
  - Tandem-X(June, 2010)
  - Sentinel-1A (April 3, 2014)
  - ALOS-2 mission (JAXA) (May 24, 2014)
  - GF-3 PolSAR (Aug. 10, 2016)
  - R.C.M
  - SAOCOM
  - BIOMASS mission (ESA) (~2020)
- China PolSAR/PolInSAR System
  - CASM Airborne System (P-PoSAR & X-InSAR→X-PolInSAR)
  - Multi-modes Airborne SAR System

There will be more suitable PolSAR/PolInSAR data sources to support research activities and even operational applications, such as global forest height mapping, forest above ground biomass mapping in the near future.



Thanks for your attentions.